

Spring 5-15-2018

# Quantum Fields in Extreme Backgrounds

Leandro Medina de Oliveira  
*Washington University in St. Louis*

Follow this and additional works at: [https://openscholarship.wustl.edu/art\\_sci\\_etds](https://openscholarship.wustl.edu/art_sci_etds)

 Part of the [Condensed Matter Physics Commons](#), and the [Elementary Particles and Fields and String Theory Commons](#)

---

## Recommended Citation

Medina de Oliveira, Leandro, "Quantum Fields in Extreme Backgrounds" (2018). *Arts & Sciences Electronic Theses and Dissertations*. 1561.  
[https://openscholarship.wustl.edu/art\\_sci\\_etds/1561](https://openscholarship.wustl.edu/art_sci_etds/1561)

This Dissertation is brought to you for free and open access by the Arts & Sciences at Washington University Open Scholarship. It has been accepted for inclusion in Arts & Sciences Electronic Theses and Dissertations by an authorized administrator of Washington University Open Scholarship. For more information, please contact [digital@wumail.wustl.edu](mailto:digital@wumail.wustl.edu).

WASHINGTON UNIVERSITY IN ST. LOUIS

Department of Physics

Dissertation Examination Committee:

Michael C. Ogilvie, Chair

Mark G. Alford

P. S. Bhupal Dev

Willem H. Dickhoff

Renato Feres

Quantum Fields in Extreme Backgrounds

by

Leandro Medina de Oliveira

A dissertation presented to  
The Graduate School  
of Washington University in  
partial fulfillment of the  
requirements for the degree  
of Doctor of Philosophy

May 2018  
St. Louis, Missouri

© 2018, Leandro Medina de Oliveira

# TABLE OF CONTENTS

LIST OF FIGURES .....	v
ACKNOWLEDGEMENTS .....	vii
ABSTRACT .....	ix
1 INTRODUCTION .....	1
2 QUANTUM THEORY IN EXTERNAL FIELDS .....	7
2.1 Magnetic fields in quantum mechanics.....	10
2.2 The Klein paradox .....	12
2.3 WKB calculation .....	13
2.4 Euler–Heisenberg effective Lagrangian .....	15
2.4.1 Vacuum decay.....	23
2.4.2 Nikishov’s virial representation.....	25
2.4.3 Borel summability .....	26
2.4.4 Constant magnetic field .....	28
2.4.5 Constant electric field .....	29
2.5 Schwinger’s proper time method.....	30
3 THE WORLDLINE FORMALISM .....	36
3.1 Preliminaries .....	37
3.2 Zero-temperature effective action .....	38
3.2.1 Worldline instantons.....	40
3.2.2 Fluctuation prefactors .....	42
3.3 Spinors .....	48
3.4 Virial representation.....	49
4 FINITE TEMPERATURE FIELD THEORY .....	52



4.1	Gauge theories at finite temperature .....	54
4.2	Effective action in the presence of a Polyakov loop .....	57
4.2.1	Low temperature expansions .....	59
4.2.2	High temperature expansions .....	60
4.3	Recovering confinement .....	62
4.3.1	Model A.....	63
4.3.2	Model B.....	63
5	MAGNETIC FIELDS AT FINITE TEMPERATURE .....	65
5.1	Effective action for spinors in a magnetic field .....	66
5.1.1	Strong field expansion.....	69
5.2	High temperature expansion .....	70
5.3	Low temperature expansion .....	75
5.3.1	Alternate high temperature expansion .....	78
5.3.2	Discussion.....	79
5.4	Example application: magnetic catalysis .....	80
6	ELECTRIC FIELDS AT FINITE TEMPERATURE.....	84
6.1	The worldline formalism at finite temperature.....	86
6.1.1	Fluctuation prefactors.....	89
6.2	Discussion .....	93
6.2.1	Morse-theoretic analysis .....	95
6.2.2	Higher-order effects.....	97
6.3	Conclusions .....	99
6.4	Appendix: zero-temperature fluctuation prefactor .....	100
6.5	Appendix: equivalence with proper-time formalism .....	103
7	ELECTRIC FIELDS AT FINITE TEMPERATURE II .....	104
7.1	Proper-time formula.....	104
7.2	Chemical potential and nonabelian effects.....	109
7.3	Uniform asymptotics.....	111
7.4	Virial representation.....	114
7.5	The thermal Schwinger process in spinor QED .....	117

7.6	Disagreements on thermal Schwinger effects .....	120
8	THE SIGN PROBLEM .....	123
8.1	Computational complexity of Monte Carlo .....	124
8.2	Duality transformation .....	130
8.3	Application to coupled models .....	134
8.3.1	ICQ model .....	136
8.3.2	ICY model.....	137
8.3.3	ICDW model and spatially modulated phases .....	137
8.3.4	The $i\phi^3$ theory .....	142
8.4	The Bose gas at finite density.....	142
8.5	Conclusions .....	144
	REFERENCES .....	145
A	APPENDIX.....	158
A.1	Representations of the Hurwitz zeta function .....	158
A.2	Proof of Mehler's formula.....	159

## LIST OF FIGURES

Figure 1.1:	Chromoelectric flux tube. ....	3
Figure 2.1:	Semiclassical tunneling in the Dirac sea. ....	15
Figure 2.2:	Integration contour for the Euler–Heisenberg Lagrangian with an electric field. ....	25
Figure 3.1:	Worldline instanton in an electric field. ....	41
Figure 3.2:	Spectrum of small fluctuations about worldline instantons. ....	43
Figure 3.3:	Action for a circular trajectory as a function of the radius. ....	47
Figure 3.4:	Functional integration contour for unstable fluctuations about the worldline instanton. ....	47
Figure 5.1:	Constituent mass as a function of temperature, for various magnetic field intensities. ....	81
Figure 5.2:	Polyakov loop as a function of temperature, for various magnetic field intensities. ....	82
Figure 6.1:	Four possible types of finite-temperature worldline instantons. ....	88
Figure 6.2:	Free energy from worldline instantons. ....	93
Figure 6.3:	One-loop thermal correction to the vacuum decay rate for scalars in an electric field. ....	94
Figure 6.4:	Action of an arbitrary finite-temperature arc trajectory as a function of the angle. ....	96
Figure 6.5:	Set of trajectories formed by varying $\dot{x}(0)$ . The envelope of such trajectories is the caustic. ....	98
Figure 6.6:	One-loop thermal correction to the vacuum decay rate for scalars in an electric field, including HTL effects. ....	99

Figure 7.1:	Uniform approximation of one-loop thermal correction to the vacuum decay rate for scalars in an electric field.....	114
Figure 7.2:	Decay rate obtained from integrating over transverse momenta. ....	115
Figure 7.3:	One-loop thermal correction to the vacuum decay rate for spinors in an electric field.....	119
Figure 8.1:	Propagator in the ICQ model.....	135
Figure 8.2:	Propagator in the ICY model. ....	138
Figure 8.3:	Field configurations in the ICDW model. ....	139
Figure 8.4:	Field configurations in the ICDW model in three dimensions. ....	140
Figure 8.5:	Spectral histogram in the ICDW model.....	141

## ACKNOWLEDGEMENTS

I am indebted to my mentor and friend Michael Ogilvie for all the time and dedication over these years. His breadth and depth of knowledge are rivaled only by his patience. I also extend thanks to the members of my mentoring committee. I learned much from Mark Alford and Willem Dickhoff, and their doors were open when I needed them. I appreciate the time and availability of Bhupal Dev and Renato Feres.

I thank the Physics Department staff for all their hard work keeping the ship afloat. Financial support from the McDonnell International Scholars Academy is gratefully acknowledged.

Lastly, I am grateful to my family for all the support and encouragement. My parents provided me with everything I could hope for, and always kept a warm home where I could escape the turmoil of real life. My wonderful better half Joy cannot be thanked enough for her patience and unconditional love.

Leandro Medina de Oliveira

*Washington University in Saint Louis*

*May 2018*

To my family.

# ABSTRACT OF THE DISSERTATION

Quantum Fields in Extreme Backgrounds

by

Leandro Medina de Oliveira

Doctor of Philosophy in Physics

Washington University in St. Louis, 2018

Professor Michael C. Ogilvie, Chair

Quantum field theories behave in interesting and nontrivial ways in the presence of intense electric and/or magnetic fields. Describing such behavior correctly, particularly at finite (nonzero) temperature and density, is of importance for particle physics, nuclear physics, astrophysics, condensed matter physics, and cosmology. Incorporating these conditions as external parameters also provides useful probes into the nonperturbative structure of gauge theories.

In this work, formalism for describing matter in a variety of extreme conditions is developed and implemented. We develop several expansions of one-loop finite temperature effects for spinor particles in the presence of magnetic fields, including the effects of confinement, encoded in a nontrivial Polyakov loop. The worldline instanton formalism is extended to the case of finite temperature, which yields a long-sought thermal extension to the celebrated formula of Schwinger for pair production in a constant electric field. The technique is further extended to include the effects of finite density and confinement, as well as some restricted classes of nonabelian electric fields.

A persistent source of difficulty in the study of gauge theories at finite density, and/or in the presence of external electric fields, is the so-called sign problem. We advance a novel duality-based approach for lattice simulation of scalar field theories with complex actions, which yields new insights on the old problem of spatial modulations arising in systems with competing interactions. The approach shows promise for simulating scalar theories at finite density and in the presence of external electric fields, and is capable of handling systems in the universality class of the  $i\phi^3$  theory, which determines the critical indices of the Lee-Yang edge transition.



# CHAPTER 1

## INTRODUCTION

The standard model of particle physics depicts fundamental interactions in terms of *gauge theories*, which incorporate local symmetries as a preeminent part of the description of charges and forces. However, gauge theories can be very difficult to study, partly because, once distilled to their simplest realization, they contain no adjustable parameters, and standard perturbative techniques that rely on the smallness of a coupling constant are of limited utility. Naively, it does not appear possible to improve understanding by studying these theories in regimes where they simplify, and then restore the complexity gradually. They seem, in a sense, irreducibly complex.

Fortunately, the naive picture is not correct. There are useful probes into the structure of gauge theories which also correspond to quantities of phenomenological interest. Such probes include, for example, finite (nonzero) temperature and density, as well as external fields. At high temperatures, because of asymptotic freedom, the coupling constant is expected to be small, and it is possible to contrast perturbative and semiclassical techniques with fully non-perturbative lattice gauge theory calculations. At high temperatures, field theories reduce in dimensionality by 1, which potentially enables interesting relationships between models that can greatly aid understanding. At finite density, the situation is complicated by the so-called *sign problem*—the Euclidean path integral is represented as a sum over complex weights, which

makes lattice simulations considerably more difficult. Therefore, our understanding relies mostly on other tools, which include, for example, effective models and strong coupling expansions. Interestingly, in the presence of external fields, we have examples of both situations: as a consequence of Landau quantization [1], systems subjected to strong *magnetic* fields have their dimensionality reduced by 2 (rather than by 1 as the case of high temperature), and *electric* fields are associated with complex weights. External fields therefore provide a useful environment in which to test the limits of our calculational tools, which, if validated, may be usefully applied to regimes not accessible to lattice simulations.

Recently there has been considerable progress in understanding the most striking features of QCD with analytical tools. Perturbatively, the expression for the free energy of an  $SU(N)$  gauge theory at finite temperature naturally favors the deconfined phase. The development of various gauge theory models that are confining when the radius of a compact direction is small, and small coupling expansions are expected to be reliable, has enabled study of confinement within perturbation theory. The most developed case is that of  $R^3 \times S^1$ , familiar from the study of field theories at finite temperature, where the length  $L$  of  $S^1$  can be usefully identified with the inverse temperature  $\beta = 1/T$ . In these models, the length of the compact direction can be tuned to interpolate between the high temperature regime, where small-coupling expansions are reliable, and a confined phase at low temperature. It is possible to do so in such a way that there is no discontinuity or phase transition in between, and so insights gained where theoretical tools are known to work may be applied to regimes where study is much more challenging [2].

Electric fields are of special interest. The vacuum is unstable in the presence of an electric field, and decays by producing pairs of particles. Many distinct perspectives equivalently describe this wholly nonperturbative phenomenon. It may be viewed as a tunneling process [3], a loss of

unitarity due to a modification of the propagator in the presence of the electric field [4], or a geometrical effect analogous to Hawking radiation, with a Bogoliubov transformation connecting the number operators in the asymptotic past and future [5]. Many different techniques have been developed within each broad theme. Since it is a nonperturbative effect, it is exponentially suppressed with a factor of  $e^{-m_e^2/eE}$ . The exponent is of order unity only for fields exceeding  $E_c = m^2/e \approx 10^{18}$  V/m. For this reason, the effect has never been experimentally observed. The development of novel calculational approaches that make it possible to compute the decay rate for fields with realistic inhomogeneities has revealed that certain configurations permit a significant enhancement of the particle production rate, making the effect potentially within the observational capability of near-future intense light facilities [5]. Interestingly, some of these approaches have yielded a result that interpolates between the nonperturbative static field particle production process described here, and a perturbative many-photon process [6].

The nonperturbative aspect of pair production is of interest for models of parton fragmentation due to its suspected connection to hadronization and string breaking. Heuristically speaking, as a bound quark and antiquark pair separates, the chromoelectric field lines between them gather in a narrow tube-shaped region, giving rise to a linear potential. For sufficiently large separations, the energy stored in the field exceeds twice the quark mass, pair production becomes energetically possible and the string breaks [7–9]. In (noncentral) heavy-ion collisions there are

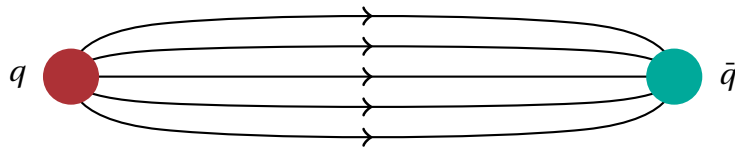


Figure 1.1: Chromoelectric flux tube between a  $q\bar{q}$  pair.

also significant magnetic interactions between the two nuclei that must be considered in the

description of the quark-gluon plasma. Large electric and magnetic fields are experimentally accessible to heavy-ion collider experiments such as ALICE or the RHIC [10].

In condensed matter physics, the discovery of the quantum Hall effect in 1975 has enabled a fruitful investigation of a variety of phenomena in two-dimensional systems, from topological insulators to particles with fractional statistics [11]. Some of these systems, due to their rich topological structure, are potential laboratories for experimental investigation of exotic field theories.

In cosmology and astrophysics there is consistent interest in describing the properties of nuclear matter in the presence of strong external fields. Both electric and magnetic fields were present in the hot environment of the early universe [12, 13]. On the surface of compact stars, magnetic fields can reach energies comparable to the current quark masses. In the core, the fields can reach energies comparable to the pion mass, well into the QCD scale. There, effects due to the magnetic field are certainly expected to be important [14]. In fact, one of the most intriguing predictions of the theory of quantum fields in a magnetic background has been recently confirmed by observational evidence from a neutron star [15]. A large degree of polarization, expected only if the quantum electrodynamics prediction of *birefringence of the magnetized vacuum* is realized in nature, was found in radiation from source RX J1856.5–3754.

The study of gauge theories in the presence of external fields lies at the intersection between particle physics, condensed matter physics, astrophysics, and cosmology. Understanding a number of physical systems requires a solid appreciation of how quantum fields behave when a background field is imposed. For systems that are hot and/or dense, it is additionally necessary to understand how the effects of temperature and density operate when external fields are also present. Where applicable, the striking features of QCD, such as confinement and chiral symmetry breaking, may also play a role, and, in turn, be affected by the background.

The subject has a long and venerable history, which in fact predates quantum field theory itself. An important early development was the effective Lagrangian of Heisenberg and Euler [16]. Even though the authors were not aware of the many subtle conceptual issues underlying quantum field theory more generally, such as the correct treatment of infinities, they were able to write down an expression which encodes essentially all lowest-order quantum effects due to constant (or slowly varying) external fields, in what later would become known as quantum electrodynamics. Their results are central to this subject and will be approached many times, in many different ways, throughout this text.

The numerous experimental applications of gauge theories in external fields, particularly at finite temperature and density, together with ample theoretical motivation, make this study both relevant and timely.

This dissertation is structured as follows. In chapter 2, the fundamentals of quantum mechanics in the presence of background fields are reviewed, with special attention to the effective Lagrangian of Heisenberg and Euler, as well as the nonperturbative *Schwinger process* of pair production in a constant electric field. Chapter 3 introduces the powerful and elegant worldline formalism, which is used to rederive Schwinger's pair production formula. The method is then extended to allow calculation of the transverse momentum distribution of created particles.

Chapter 4 is an introduction to finite temperature field theory. In chapter 5 I present a treatment of thermal magnetic effects, with intended application to the quark-gluon plasma. New expressions that smoothly connect the weak and strong field regimes are derived. In chapter 6, Schwinger's pair production result is generalized to scalar QED at finite temperature using the worldline instanton formalism; various further generalizations are presented in chapter 7. I give the finite-temperature version of the transverse momentum distribution formula. A derivation of the finite temperature decay rate in a uniform WKB framework is also provided.

Chapter 8 concerns the so-called *sign problem* and its relevance to lattice simulations of systems in extreme backgrounds. I present a counter-argument to the well-known **NP**-hardness result. A duality-based technique for simulating scalar fields with complex actions is introduced, and simulation results are presented. Lastly, I explain how this technique can be used to simulate a Bose gas at finite density, or a system of charged scalars in an electric field.

Usual particle physics conventions apply: natural units ( $\hbar = c = k_b = \epsilon_0 = \mu_0 = 1$ ) are used throughout, spacetime indices are written as lower-case Greek letters, repeated indices are summed over, etc.

## CHAPTER 2

### QUANTUM THEORY IN EXTERNAL FIELDS

In classical mechanics, the interactions of particles with electric and magnetic fields are governed by the Lorentz force law

$$\mathbf{F} = q(\mathbf{E} + \mathbf{v} \times \mathbf{B}). \quad (2.1)$$

It results that trajectories in a constant magnetic field are circles, where the angular rotation frequency is given by the usual cyclotron frequency  $\omega = qB/m$ , and radius  $R = p/qB$ , with  $p$  the particle's linear momentum. Using De Broglie's relation  $p = h/\lambda$ , and demanding that the wave be single-valued over the circle, we conclude that the wavelength  $\lambda$  and momentum  $p$  can attain only discrete values

$$\lambda = \sqrt{\frac{2\pi\hbar}{nqB}}, \quad p = \sqrt{\hbar nqB}, \quad n = 1, 2, 3, \dots \quad (2.2)$$

Therefore, the kinetic energy of this particle is also restricted to discrete values  $T_n$ ,

$$T_n = \hbar \frac{qB}{2m} n. \quad n = 1, 2, 3, \dots \quad (2.3)$$

This is *almost* right—in fact, the correct energies, which we will derive in detail in section 2.1, are the so-called *Landau levels*, given by [1]

$$E_n = \hbar \frac{qB}{m} \left( n + \frac{1}{2} \right), \quad n = 1, 2, 3, \dots \quad (2.4)$$

which differs from the above by a factor of 2 and a zero-point energy contribution. Nevertheless, this simple heuristic derivation illustrates one of the interesting features of quantum particles in a magnetic field. The energy levels are quantized, as they are for a particle in a confining potential, even though the magnetic portion of the Lorentz force (2.1) is nonconservative and cannot be written as the gradient of a potential, of any type. *Unlike* a particle in a confining potential, the energy of a classical particle in a magnetic field is the same irrespective of where the orbit is centered, which suggests that the quantum mechanical energy levels are highly degenerate. This is indeed the case, and this fact carries profound consequences. Examples include the *quantum Hall effect* [11], which is the observation of quantized conductivities in cold two-dimensional electron systems when a strong magnetic field is applied, and the *magnetic catalysis* of the chiral condensate [17], which I discuss in detail in chapter 5.

Electric fields present their own subtle issues. Maxwell's equations absent sources

$$\nabla \cdot \mathbf{E} = 0 \qquad \qquad \qquad \nabla \cdot \mathbf{B} = 0 \qquad \qquad (2.5)$$

$$\nabla \times \mathbf{E} = -\frac{\partial \mathbf{B}}{\partial t} \qquad \qquad \qquad \nabla \times \mathbf{B} = \frac{\partial \mathbf{E}}{\partial t} \qquad \qquad (2.6)$$

are completely symmetric with respect to an exchange between electric and magnetic fields  $\mathbf{B} \Leftrightarrow \mathbf{E}$  together with the time reversal  $t \rightarrow -t$ , so, even though the Lorentz force law (2.1) treats electric and magnetic fields asymmetrically, it might appear reasonable to expect a behavior similar to that described above for magnetic fields. As we will see, this is not the case: while, at least in some examples, much of the mathematical technology used to handle systems with an infinite number of discrete Landau levels does carry over to the case of electric fields, there are also qualitative differences that require some conceptual refinement.



A nonrelativistic particle subject to the action of a homogeneous, uniform electric field pointing in the  $\hat{z}$  direction may be described by the following Hamiltonian:

$$H = \frac{\mathbf{p}^2}{2m} + eEz. \quad (2.7)$$

It is immediately apparent that this Hamiltonian is not bounded from below. This is of course not a fundamental difficulty (though it may be a calculational one, particularly at finite temperature [18]), since any electric or magnetic field corresponding to a real, physical system should have finite extent, but the fact that there is a difficulty at all (which does not seem present for magnetic fields) hints at possible issues concerning the stability of the vacuum. This intuition happens to be correct; sufficiently strong electric fields can induce vacuum decay via production of particle-antiparticle pairs. In honor of Schwinger's calculation of the effective action [4], this has come to be known as the *Schwinger effect*, but the subject has a longer history well worth visiting.

It was found early on that a potential barrier presented paradoxical issues for a relativistic wave theory of electrons. Klein found that an electron incident on an infinitely high, infinitely steep potential wall is, contrary to expectation, always transmitted [19, 20]. Sauter then considered the problem of an electron incident on a potential wall of finite slope, which corresponds to a region with a finite electric field, obtaining similar results [21]. Over time it was realized that the correct theory of relativistic electrons is not a theory of particles, but of fields. These early paradoxical results were hinting at the interesting effect of particle production by a constant electric field.

The work of Heisenberg and Euler was prescient: even without a full understanding of quantum field theory, they were able to write the correct effective Lagrangian incorporating quantum mechanical effects in the description of electromagnetic fields [16]. While a proper understanding of the subtleties underlying these phenomena in quantum field theory would not be available

until Schwinger's important 1951 paper [4], Heisenberg and Euler were able to anticipate many of the physical effects expected to happen when external fields are sufficiently large, such as the production of particles mentioned above, as well as scattering of light by light.

Unfortunately, many of these effects are extraordinarily faint, and have thus far eluded experimental confirmation. The production of particles by intense electric fields has never been observed, though it is hoped that the effect might be accessible to current or near future extreme light facilities such as XFEL or ELI [5]. While such facilities cannot attain the required static field strengths, evidence suggests that skillful shaping of laser pulses may lower the required intensities to an attainable level (see for example [6]). Scattering of light by light has been recently observed in the ATLAS experiment [22], but Heisenberg and Euler's prediction pertains to constant or slowly varying electromagnetic fields, rather than the photon-photon processes that take place in a collider experiment. Thus, while encouraging, the result is not a direct test of Euler and Heisenberg's results in the regimes where these are applicable.

In this chapter I review various important calculations of zero temperature effects in the presence of external fields, with especial attention to the effective Lagrangian of Euler and Heisenberg. These results are both historically important and physically illuminating; the final results will also be referred to constantly in the remainder of this text.

## 2.1 MAGNETIC FIELDS IN QUANTUM MECHANICS

Consider a spinless particle with electric charge  $q$  in a constant, uniform magnetic field of strength  $B$  pointing in the  $\hat{z}$  direction. The Hamiltonian describing the dynamics is

$$\hat{H} = \frac{1}{2m} (\hat{\mathbf{p}} - q\hat{\mathbf{A}})^2. \quad (2.8)$$

In the gauge where  $\hat{\mathbf{A}} = (0, Bx, 0)$ , we have

$$H = \frac{1}{2m} [\hat{p}_x^2 + (\hat{p}_y - qB\hat{x})^2 + \hat{p}_z^2]. \quad (2.9)$$

Clearly,  $\hat{p}_y$  and  $\hat{p}_z$  commute with  $H$ , which can be readily expressed in diagonal form:

$$H = \frac{1}{2m} \left[ \hat{p}_x^2 + (qB)^2 \left( \hat{x} - \frac{p_y}{qB} \right)^2 + p_z^2 \right]. \quad (2.10)$$

For simplicity, in the remainder of this discussion the irrelevant  $z$  direction will be suppressed. Notice that this is the Hamiltonian of a harmonic oscillator in the  $x$  direction, centered at  $p_y/qB$ , with frequency  $\omega = qB/m$ . The wavefunctions in the 12-plane are, therefore, given in terms of Hermite polynomials

$$\psi_n(x) = \frac{1}{\sqrt{2^n n!}} \left( \frac{\omega}{\pi} \right)^{1/4} H_n(\omega^{1/2} x) e^{-\omega x^2/2}. \quad (2.11)$$

with energies

$$E_n = \frac{qB}{m} \left( n + \frac{1}{2} \right). \quad (2.12)$$

The seemingly different treatment of the two spatial directions is merely an artifact of our choice of gauge. Wavefunctions are not directly observable and are thus not required to be gauge invariant. The important point to notice is that the energies  $E_n$  do not depend on the value of  $p_y$ : as suggested by the heuristic derivation, each Landau level is highly degenerate.

To quantify this degeneracy, place the system in a cubic box of side  $L \gg m/(qB)^2$ . There are two constraints on  $p_y$ :

- Periodic boundary conditions require  $p_y = \frac{2\pi n}{L}$ ,  $n \in \mathbb{Z}$ .
- The center of the oscillator must be inside the box, so  $\frac{p_y}{qB} < L$ .

Taken together, these two constraints give

$$n < L^2 \frac{qB}{2\pi} \quad (2.13)$$

for a density of states of  $qB/2\pi$  per unit area.

In symmetric gauge, there is an elegant method for calculating this density of states. The reader interested in this argument, as well as the theory of magnetic fields in condensed matter systems, may refer to David Tong's lecture notes on the quantum Hall effect [23].

## 2.2 THE KLEIN PARADOX

The earliest work suggesting issues of fundamental importance in the quantum mechanical treatment of electric fields was that of Klein [19, 20]. Klein solved the one-dimensional Dirac equation in a step potential of the form

$$V(x) = \begin{cases} 0 & x < 0 \\ V_0 & x \geq 0. \end{cases} \quad (2.14)$$

The reflection and transmission coefficients are given by

$$R_K = \left( \frac{1 - \kappa}{1 + \kappa} \right)^2 \quad T_K = \frac{4\kappa}{(1 + \kappa)^2} \quad (2.15)$$

where

$$\kappa \equiv \sqrt{\frac{(V - E + m)(E + m)}{(V - E - m)(E - m)}}. \quad (2.16)$$

The surprising conclusion, unexplainable in the wave mechanics paradigm of 1929, is that the transmission coefficient is nonvanishing for  $E < V_0$ , and in fact, approaches unity as  $V_0 \rightarrow \infty$  and  $E \gg m$ . This counterintuitive result became known as the ‘‘Klein paradox’’.

Sauter subsequently refined this picture by considering a continuous potential of the form [21]

$$V(x) = \begin{cases} 0 & x < 0 \\ V_0(x/L) & 0 \leq x < L \\ V_0 & x \geq L \end{cases} \quad (2.17)$$

which corresponds to a uniform, homogeneous electric field  $E = -V_0/L$  in the region  $0 \leq x < L$ . For sufficiently narrow barriers ( $L < V_0/m^2$ ) the transmission and reflection coefficients reduce to those of the step function (2.15); but even for shallow barriers the transmission coefficient is nonzero and given by

$$T_S = e^{-\pi m^2/eE}. \quad (2.18)$$

Shortly thereafter Dirac published his famous work on the negative energy solutions of his equation [24], signaling a departure from the wavefunction point of view towards the modern field theoretic perspective. In light of these developments, the correct interpretation of the Klein paradox finally became clear: the solutions of the Dirac equation do not represent particle wavefunctions directly but rather quantized modes; the nonzero transmission coefficient represents a probability of creation of an electron positron pair. The first work to assess the paradox within quantum field theory was due to Hund [25].

### 2.3 WKB CALCULATION

The previous results have been suggestive of a tunneling interpretation for the process of pair production. A WKB type calculation should be able to reveal that more directly. For a review of this calculation, as well as an assortment of various other methods, refer to the article by Holstein [3].

The spectrum of a Klein-Gordon particle of mass  $m$  contains both positive and negative energies, separated by a gap of width  $2m$ . In the presence of a weak electric field, the energy levels become

tilted, as indicated in figure 2.1. If all negative energy levels are filled, as in the Dirac sea picture, a process where a particle tunnels from a level in the negative portion of the spectrum to one in the positive portion, leaving behind a hole, becomes possible. The barrier penetration factor given in the WKB approximation is

$$T_S = \exp \left[ - \int_{z_-}^{z_+} dz k_z(z) \right] \quad (2.19)$$

where  $z_-$  and  $z_+$  are the turning points of the classical motion. For a particle of frequency  $\omega$  the momentum  $k_z$  in the forbidden region is

$$k_z = \sqrt{m^2 + k_{\perp}^2 - (\omega - eEz)^2} \quad (2.20)$$

with turning points

$$z_{\pm} = \pm \frac{1}{eE} \sqrt{m^2 + k_{\perp}^2 - \omega^2}. \quad (2.21)$$

The potential barrier is thus in the shape of a semicircle, and the barrier penetration factor is simply

$$T_S = \exp \left[ -\pi \frac{m^2 + p_{\perp}^2}{eE} \right]. \quad (2.22)$$

This, as we will see in section 2.4.2, leads to the correct pair production probability once integrated over all modes.

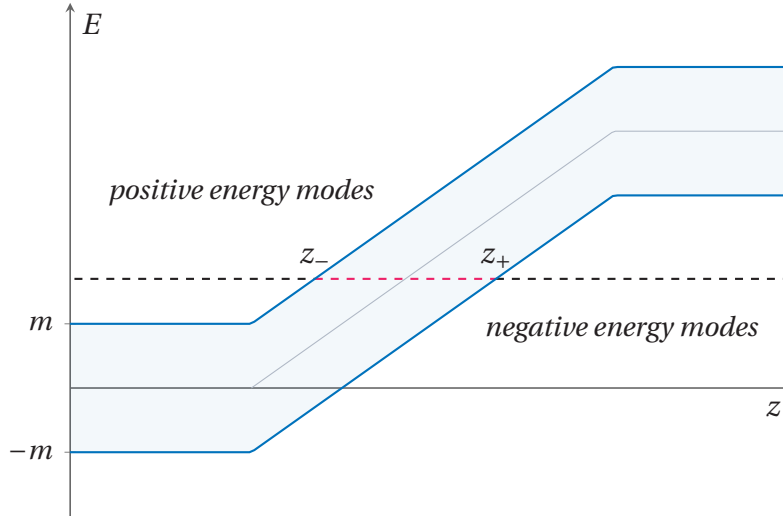


Figure 2.1: Semiclassical picture of tunneling between negative and positive energy modes, for a charged particle in an electric field of finite extent. The shaded region is classically forbidden.

#### 2.4 EULER–HEISENBERG EFFECTIVE LAGRANGIAN

A natural question is whether the interactions between light and matter can manifest as modifications of Maxwell’s equations encoding quantum effects such as the polarization of the vacuum or the possibility of matter creation by intense electric fields. Euler and Heisenberg’s 1935 computation of the effective action demonstrated that they can [16].

Effective actions can be informally described as objects which modify the classical action in order to take into account quantum mechanical effects up to a given order in perturbation theory. When extremized, such modified actions yield a set of classical equations of motion which incorporate some quantum effects. Euler and Heisenberg’s effective action is an object of this type. The modified Maxwell’s equations obtained from it are nonlinear, which is often regarded as a dielectric-like behavior of the vacuum [26], but this is not essential: equally valid is the point of view that quantum mechanics induces interactions between light and light. The Euler–Heisenberg Lagrangian is a function of  $\mathbf{E}$  and  $\mathbf{B}$ , the values of external electric and

magnetic fields, which are taken as constant and uniform. If the fields are inhomogeneous and/or nonconstant, it may still be useful as the leading term in a derivative expansion.

The case of a charged spinless particle, studied first by Weisskopf in 1936 [27], is simplest. Consider a complex scalar in the background of a gauge field, assumed to be classical. The purpose of this assumption is twofold: first, it allows for a semi-phenomenological study of quantum corrections to Maxwell's equations. Second, it provides a useful means with which to nonperturbatively probe the structure of the quantum vacuum [26]. The matter portion of the partition function reads

$$Z[A] = \int [d\phi^*][d\phi] \exp\left\{i \int d^4x [(D_\mu\phi^*)(D_\mu\phi) + m^2\phi^*\phi]\right\}, \quad (2.23)$$

where  $m$  is the scalar's mass,  $D_\mu \equiv \partial_\mu + ieA_\mu$  is the gauge covariant derivative, and  $A_\mu$  a  $U(1)$  gauge field with corresponding field strength tensor  $F_{\mu\nu} = \partial_\mu A_\nu - \partial_\nu A_\mu$ . As written, this functional integral is defined only up to an arbitrary normalization. The appropriate choice of normalization generically depends on the specific problem being considered; for example, if the masses are dynamically generated, it might be desirable to normalize with respect to the massless theory, a situation which will be relevant in section 5.4. Here, I assume that the mass is some fundamental parameter that does not depend on the magnetic field, and normalize with respect to the partition function associated with a scalar of the same mass and vanishing external background. With this choice, the *effective action*  $W^{(1)}[A]$  is given by

$$e^{iW^{(1)}[A]} = \frac{Z[A]}{Z[0]}, \quad (2.24)$$

or equivalently

$$W^{(1)}[A] \equiv -i \log \left\{ \frac{Z[A]}{Z[0]} \right\}. \quad (2.25)$$

The superscript (1) indicates a one-loop result. This definition is natural when studying the properties of quantum fields in the presence of an external background, and appears frequently



in discussions of spontaneous symmetry breaking beyond tree level [28]. An alternate definition of the effective action is often given where it is a functional of classical external *sources*, rather than fields. In that form it can be understood as the generating functional of connected Green's functions; the form given here generates one-particle irreducible Green's functions. Both forms are thus important for perturbation theory, and are related to one another by a Legendre transform. A clear and comprehensive treatment of the various aspects of effective actions can be found in Brown's quantum field theory textbook [29].

It is easier to compute the effective action if the action functional is Wick-rotated to Euclidean space, with the replacement  $t \rightarrow ix_4$ . It is also useful to define the *effective Lagrangian* in the obvious way,

$$W^{(1)}[A] = \int dt d^3x \mathcal{L}_M[A] = i \int d^4x \mathcal{L}_E[A]. \quad (2.26)$$

The subscripts  $M$  and  $E$  stand for *Minkowski* and *Euclidean*, respectively. The Euclidean Lagrangian in particular is also often called the *effective potential*. Following common practice in the literature, all effective Lagrangians in this text are assumed to be defined in Euclidean space, and the subscript  $E$  will be dropped; the term “effective potential” will be regarded as synonymous. An integration by parts places the partition function in the standard Gaussian form

$$Z[A] = \int [d\phi^*][d\phi] \exp\left\{-\int d^4x \phi^* (-D^2 + m^2)\phi\right\}. \quad (2.27)$$

The Lagrangian is quadratic on the scalar fields, so they can be integrated out. In the general case where there are higher-order interactions, a suitable linearization allows this expression to be evaluated perturbatively. With the choice of normalization mentioned above, the effective action is easily written in terms of functional determinants [30]:

$$\frac{Z[A]}{Z[0]} = \frac{\det^{-1}[-D^2 + m^2]}{\det^{-1}[-\partial^2 + m^2]}. \quad (2.28)$$

Using the standard identity  $\log \det = \text{tr} \log$ , we obtain the convenient representation

$$W^{(1)}[A] = i \text{tr} \log \left[ \frac{-D^2 + m^2}{-\partial^2 + m^2} \right] \quad (2.29)$$

where the trace is over spacetime indices. The problem has been reduced to finding the spectrum of the operator  $(-D^2 + m^2)$ , and computing the (suitably regularized) product of eigenvalues.

The physical case of spinor electrodynamics is similar. The theory is defined by the Lagrangian

$$\mathcal{L} = \bar{\psi}(iD - m)\psi - \frac{1}{4}F^{\mu\nu}F_{\mu\nu} \quad (2.30)$$

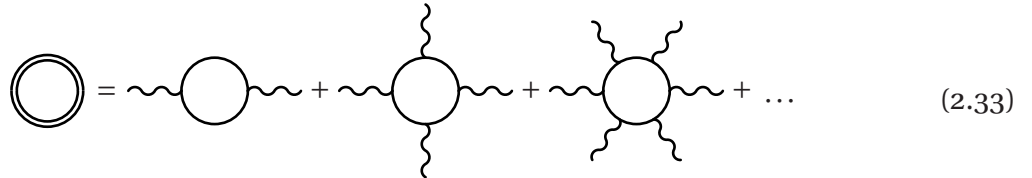
where  $\not{a} \equiv \gamma_\mu a^\mu$ . After integrating out the matter fields, the effective action (normalized with respect to zero field) reads

$$S^{(1)}[A] = -i \log \left[ \frac{\det(iD - m)}{\det(i\partial - m)} \right]. \quad (2.31)$$

Once again using  $\log \det = \text{tr} \log$ , we can write

$$S^{(1)}[A] = -i \text{tr} \log \left( \frac{iD - m}{i\partial - m} \right) = -i \text{tr} \log \left( 1 - \frac{e\not{A}}{i\partial - m} \right) \quad (2.32)$$

where the trace is over both spacetime and spinor indices. Expansion of the logarithm yields a familiar perturbative expansion [31]



$$\text{Diagram} = \text{Diagram}_1 + \text{Diagram}_2 + \text{Diagram}_3 + \dots \quad (2.33)$$

Note that, as a consequence of charge conjugation invariance, diagrams with odd numbers of external photon lines vanish (Furry's theorem [32]).

This perturbative expansion encodes the leading contributions to several important processes, such as vacuum polarization and light by light scattering (see for example the second term in

the right-hand side), and is useful in its own right. However, for us it is chiefly of theoretical interest (see section 2.4.3). We will concentrate instead on an evaluation of the left-hand side in the soluble special case of constant fields.

The cyclic property of the trace, together with  $\gamma_5^2 = 1$ , shows

$$\det(i\mathcal{D} - m) = \det(\gamma_5^2(i\mathcal{D} - m)) = \det(\gamma_5(i\mathcal{D} - m)\gamma_5) = \det(-i\mathcal{D} - m), \quad (2.34)$$

which yields immediately

$$\log \det(i\mathcal{D} - m) = \frac{1}{2} \log \det(\mathcal{D}^2 + m^2). \quad (2.35)$$

The effective action can now be written in terms of a positive-definite operator, in a form similar to the scalar expression (2.29):

$$S^{(1)} = -\frac{i}{2} \log \left[ \frac{\det(\mathcal{D}^2 + m^2)}{\det(\partial^2 + m^2)} \right] = -\frac{i}{2} \text{tr} \log \left[ \frac{\mathcal{D}^2 + m^2}{\partial^2 + m^2} \right] \quad (2.36)$$

$$= -\frac{i}{2} \text{tr} \log \left[ \frac{-\mathcal{D}^2 + m^2}{-\partial^2 + m^2} \right]. \quad (2.37)$$

In the second line, I performed a Wick-rotation to Euclidean space. The squared Dirac operator  $\mathcal{D}^2$  differs from the scalar Klein-Gordon operator by the addition of a spin term,

$$\mathcal{D}^2 = \gamma^\mu \gamma^\nu (\partial_\mu + ieA_\mu)(\partial_\nu + ieA_\nu) \quad (2.38)$$

$$= \gamma^\mu \gamma^\nu (\partial_\mu \partial_\nu + ie(\partial_\mu A_\nu + A_\mu \partial_\nu) - e^2 A_\mu A_\nu) \quad (2.39)$$

$$= \frac{\{\gamma^\mu, \gamma^\nu\}}{2} (\partial_\mu \partial_\nu + ie((\partial_\mu A_\nu) + A_\nu \partial_\mu + A_\mu \partial_\nu) - e^2 A_\mu A_\nu) \quad (2.40)$$

$$+ ie \frac{[\gamma^\mu, \gamma^\nu]}{2} (\partial_\mu A_\nu)$$

$$= (\partial^2 + 2ieA^\mu \partial_\mu - e^2 A^2 + ie(\partial_\mu A^\mu) + \frac{1}{2} e\sigma^{\mu\nu} F_{\mu\nu}) \quad (2.41)$$

$$= D^2 + \frac{1}{2} e\sigma^{\mu\nu} F_{\mu\nu}. \quad (2.42)$$

In the fourth equality, I defined  $\sigma^{\mu\nu} \equiv \frac{i}{2}[\gamma^\mu, \gamma^\nu]$ . In the third, the chain rule was used. The four-divergence term  $ie(\partial_\mu A^\mu)$  is irrelevant provided field configurations fall off sufficiently fast at infinity; it will be omitted from now on. Note that the solutions of the Dirac equation are easily obtained from the solutions of the “squared” Dirac equation by the following observation [33]:

$$(\mathcal{D}^2 + m^2)\Psi = (i\mathcal{D} - m)[(-i\mathcal{D} - m)\Psi] = 0. \quad (2.43)$$

In other words, if  $\Psi$  is a solution of the squared Dirac equation, the spinor  $\psi = (-i\mathcal{D} - m)\Psi$  is a solution of the usual Dirac equation.

We are now in position to evaluate the determinant directly in the case of constant fields. The eigenvalues of the (Euclidean) squared Dirac operator are given by

$$(-\partial^2 - 2ieA^\mu\partial_\mu + e^2A^2 - \frac{1}{2}e\sigma^{\mu\nu}F_{\mu\nu} + m^2)\Psi = E\Psi. \quad (2.44)$$

For a constant magnetic field pointing in the  $\hat{\mathbf{z}}$  direction, the eigenvalues have contributions from free particle degrees of freedom in the 3d-plane, plus the usual Landau levels

$$E = 2eB(n + \frac{1}{2} \pm \frac{1}{2}) + p_3^2 + p_4^2 + m^2. \quad (2.45)$$

The same considerations for density of states shown in section 2.1 apply here—the Landau levels are highly degenerate, with a density of states factor of  $eB/2\pi$  per unit area. The one-loop contribution to the effective action then reads,

$$\mathcal{L}^{(1)}[B] = - \sum_{n,\pm} \frac{eB}{2\pi} \int \frac{d^2p_\perp}{(2\pi)^2} \log[2eB(n + \frac{1}{2} \pm \frac{1}{2}) + p_\perp^2 + m^2] \quad (2.46)$$

where the normalization factor has been temporarily suppressed. The logarithm is represented as a Schwinger proper-time integral,

$$\mathcal{L}^{(1)}[B] = \sum_{n,\pm} \frac{eB}{2\pi} \int \frac{d^2p_\perp}{(2\pi)^2} \int_0^\infty \frac{ds}{s} e^{-s[2eB(n + \frac{1}{2} \pm \frac{1}{2}) + p_\perp^2 + m^2]}. \quad (2.47)$$

The integral over  $p_\perp$  is a Gaussian and can be done immediately. Notice that, for dimensional consistency, the proper time parameter  $s$  must have dimensions of inverse energy squared. It will be convenient in what follows to define it as dimensionless, so I make the substitution  $s \rightarrow s/eB$ . Then effecting the sum over polarizations we have

$$\mathcal{L}^{(1)}[B] = \sum_n \frac{(eB)^2}{8\pi^2} \int_0^\infty \frac{ds}{s^2} e^{-s(m^2/eB)} e^{-2sn} [1 + e^{-2s}]. \quad (2.48)$$

The sum over Landau levels is a geometric series,

$$\sum_{n=0}^\infty e^{2sn} = \frac{1}{1 - e^{2s}}, \quad (2.49)$$

so we may write

$$\mathcal{L}^{(1)}[B] = \frac{(eB)^2}{8\pi^2} \int_0^\infty \frac{ds}{s^2} e^{-s(m^2/eB)} \coth(s). \quad (2.50)$$

This integral is divergent at small  $s$ , which corresponds to the usual ultraviolet divergences of quantum field theory. Let us split the finite and infinite parts:

$$\begin{aligned} \mathcal{L}^{(1)}[B] &= \frac{(eB)^2}{8\pi^2} \int_0^\infty \frac{ds}{s^2} e^{-s(m^2/eB)} \left( \coth(s) - \frac{1}{s} - \frac{s}{3} \right) \\ &\quad + \frac{(eB)^2}{8\pi^2} \int_0^\infty \frac{ds}{s^2} e^{-s(m^2/eB)} \left( \frac{1}{s} + \frac{s}{3} \right). \end{aligned} \quad (2.51)$$

The most severe divergence is quadratic and appears in the first term in the second line. This divergence is cured by restoring the normalization factor neglected in equation (2.46), which is written in terms of the functional determinant at zero field. After performing a Wick rotation  $\partial^2 \rightarrow -\partial^2$ , and with the aid of a proper time representation for the logarithm, as in equation (2.47), we may write

$$\text{tr log}[-\partial^2 + m^2] = 2 \int \frac{d^4k}{(2\pi)^4} \int_0^\infty \frac{ds}{s} e^{-s(k^2+m^2)} \quad (2.52)$$

$$= \frac{1}{8\pi^2} \int_0^\infty \frac{ds}{s^3} e^{-sm^2} \quad (2.53)$$

$$= \frac{(eB)^2}{8\pi^2} \int_0^\infty \frac{ds}{s^3} e^{-s(m^2/eB)}. \quad (2.54)$$

Agreeably, this is identical to the offending term, so the quadratic divergence cancels. Only the second divergent term in equation (2.51) is left.

$$\frac{(eB)^2}{24\pi^2} \int_0^\infty \frac{ds}{s} e^{-s(m^2/eB)} = \frac{(eB)^2}{24\pi^2} \log\left(\frac{eB}{m^2}\right). \quad (2.55)$$

This term is physical: it represents the renormalization of electric charge. Its significance was not fully realized until the later work of Schwinger [4], which I describe in section 2.5.

We are now free to focus on the finite part of the effective Lagrangian. It reads

$$\mathcal{L}^{(1)}[B] = \frac{(eB)^2}{8\pi^2} \int_0^\infty \frac{ds}{s^2} e^{-s(m^2/eB)} \left( \coth(s) - \frac{1}{s} - \frac{s}{3} \right). \quad (2.56)$$

This is the famous *Euler–Heisenberg effective Lagrangian* for the case of a constant magnetic field. For more details on what follows, refer to the review by Dunne [26].

This expression can be related to a representation of the Hurwitz zeta function,

$$\zeta_{\text{H}}(s; z) \equiv \sum_{n=0}^{\infty} \frac{1}{(n+z)^s}, \quad (2.57)$$

or rather, its derivative with respect to the first argument, which appears naturally in the context of zeta-function regularization of functional determinants:

$$\zeta'_{\text{H}}(-1; z) = \frac{1}{12} - \frac{z^2}{4} - \zeta_{\text{H}}(-1, z) \log z - \frac{1}{4} \int_0^\infty \frac{dt}{t^2} e^{-2zt} \left( \coth(t) - \frac{1}{t} - \frac{t}{3} \right). \quad (2.58)$$

This identity will be derived in detail in Appendix A.1.

The case of a constant *electric* field can be obtained via the analytic continuation  $B \rightarrow iE$ ,  $s \rightarrow is$ . This formal substitution is motivated by the fact that, if only one of  $\mathbf{E}$  or  $\mathbf{B}$  is nonzero, the unique Lorentz invariant is  $B^2 - E^2$ , thus the change  $B^2 \rightarrow -E^2$  should leave the physics unchanged [26]. However, the argument fails if rotational invariance in Euclidean space is lost

(as in, for example, the case of finite temperature, c.f. chapter 6). The result is

$$\mathcal{L}^{(1)}[E] = \frac{(eE)^2}{8\pi^2} \int_0^\infty \frac{ds}{s^2} e^{-s(m^2/eE)} \left( \cot(s) - \frac{1}{s} + \frac{s}{3} \right). \quad (2.59)$$

The complete expression for a general constant background field is given by

$$\mathcal{L}^{(1)}[A] = \frac{1}{8\pi^2} \int_0^\infty \frac{ds}{s^2} e^{-sm^2} \left( \frac{e^2 bas}{\tanh(ebs) \tan(eas)} - \frac{1}{s} - \frac{s}{3} (b^2 - a^2) \right) \quad (2.60)$$

where  $a$  and  $b$  are defined in terms of the Lorentz invariants as<sup>1</sup>

$$a^2 - b^2 = \mathbf{E}^2 - \mathbf{B}^2 = -\frac{1}{2} F_{\mu\nu} F^{\mu\nu} \quad (2.61)$$

$$ab = \mathbf{E} \cdot \mathbf{B} = -\frac{1}{4} F_{\mu\nu} \tilde{F}^{\mu\nu}. \quad (2.62)$$

Expanding this expression to lowest nonlinear order we obtain

$$\mathcal{L}^{(1)}[A] = \frac{e^2}{360\pi^2 m^4} [(\mathbf{E}^2 - \mathbf{B}^2)^2 + 7(\mathbf{E} \cdot \mathbf{B})^2] + \dots \quad (2.63)$$

which encodes the low-energy limit of the amplitude for scattering of light by light (see the second term on the RHS of equation (2.33)), and is the leading quantum mechanical correction to Maxwell's equations.

The corresponding expression for spinless particles was obtained by Weisskopf [27]. It reads

$$\mathcal{L}_{scalar}^{(1)}[A] = -\frac{1}{16\pi^2} \int_0^\infty \frac{ds}{s^2} e^{-sm^2} \left( \frac{e^2 bas}{\sinh(ebs) \sin(eas)} - \frac{1}{s} + \frac{s}{6} (b^2 - a^2) \right). \quad (2.64)$$

#### 2.4.1 Vacuum decay

The Euler–Heisenberg effective Lagrangian (2.60) encodes all of the physics of constant fields accessible at one-loop. It may be expected that the particle-antiparticle production process

---

<sup>1</sup>An alternate convention where  $a$  and  $b$  are swapped can be encountered in the literature [34–36]. The conventions presented here are those of reference [26].

suggested in the work of Klein and Sauter [19, 21] is manifested in some form. As determined by Schwinger, this is indeed the case [4]. In Minkowski space, the state vector overlap between the vacuum state in the asymptotic past and in the asymptotic future can be computed immediately in the functional integral formalism

$$\langle 0_{\text{out}} | 0_{\text{in}} \rangle = \frac{Z[A]}{Z[0]} = e^{iW[A]}, \quad (2.65)$$

which coincides with the defining expression for the effective action. This quantity is sometimes called the *vacuum persistence amplitude*. If the effective action is purely real, the vacuum persistence amplitude is a pure phase—a system initially in the vacuum state will remain there. On the other hand, if the effective action is complex, the amplitude of the vacuum state will, depending on the choice of boundary conditions, grow or decay over time, and particle-antiparticle pairs will be produced (or destroyed). The probability of detecting the system in its vacuum state in the asymptotic far future is given by

$$|\langle 0_{\text{out}} | 0_{\text{in}} \rangle|^2 = e^{-2\text{Im}\{W^{(1)}[A]\}} \approx 1 - 2VT \text{Im}\{\mathcal{L}^{(1)}[A]\}. \quad (2.66)$$

An important difference between the cases of electric and magnetic backgrounds is that, in the case of electric fields, because of the cotangent in equation (2.59), the integrand has poles on the real axis. The expression thus requires disambiguation. The correct sense in which to avoid the poles is given by the usual convergence prescription for Minkowski space functional integrals,  $m^2 \rightarrow m^2 - i\epsilon$ . This is equivalent to avoiding each pole by a semicircular path in the upper half-plane. The effective Lagrangian will thus acquire an imaginary contribution from the residues at each pole.



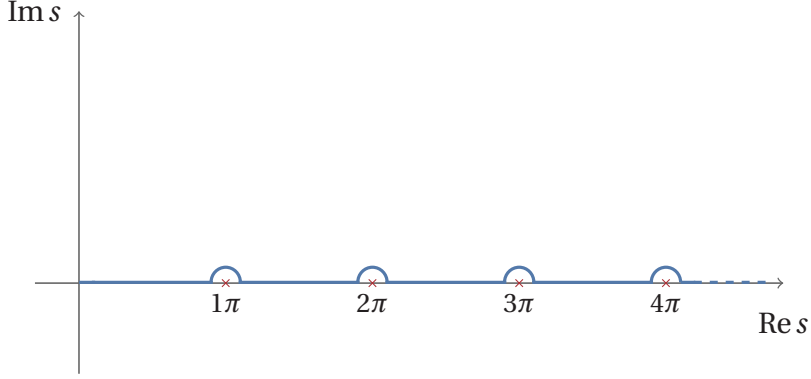


Figure 2.2: Proper-time integration contour in the Euler–Heisenberg effective Lagrangian for a constant electric field, equation (2.59). Note that there is no pole at the origin—ultraviolet divergences have been subtracted off.

Thus the *vacuum decay rate per unit volume* may be computed from the Euler–Heisenberg Lagrangian with the aid of the residue theorem:

$$\Gamma = 2 \operatorname{Im}\{\mathcal{L}^{(1)}[E]\} = \frac{(eE)^2}{4\pi^3} \sum_{n=1}^{\infty} \frac{1}{n^2} e^{-\frac{m^2}{eE}\pi n}. \quad (2.67)$$

This is known as *Schwinger’s formula*. Notice that the expression is *non-perturbative* in the coupling constant  $e$ , which is typical of tunneling processes. We will recast it in the familiar form of an instanton calculation in section 3.2.

#### 2.4.2 Nikishov’s virial representation

For physical applications it may be necessary to know not only the mean rate of vacuum decay, but also the momentum distribution of created pairs. This information is obscured in equation (2.67). To address this difficulty we may return to equation (2.47) and proceed while leaving the  $p_{\perp}$  integration undone. The counterpart of equation (2.67) then reads

$$\Gamma = 2 \operatorname{Im}\{\mathcal{L}^{(1)}[E]\} = \frac{eE}{\pi} \int \frac{d^2 p_{\perp}}{(2\pi)^2} \sum_{n=1}^{\infty} \frac{1}{n} e^{-\frac{m^2 + p_{\perp}^2}{eE}\pi n}. \quad (2.68)$$

The series is recognized as a Taylor expansion of the logarithm,

$$\Gamma = 2 \operatorname{Im}\{\mathcal{L}^{(1)}[E]\} = -\frac{eE}{\pi} \int \frac{d^2 p_{\perp}}{(2\pi)^2} \log\left(1 - e^{-\frac{m^2 + p_{\perp}^2}{eE} \pi}\right). \quad (2.69)$$

This formula is closely related to the virial representation of Nikishov [37, 38],

$$2VT \operatorname{Im}\{\mathcal{L}^{(1)}[E]\} = \pm V \sum_r \int \frac{d^3 p}{(2\pi)^3} \log(1 \pm \bar{n}_{p,r}), \quad (2.70)$$

$$\bar{n}_{p,r} = \exp\left(-\frac{m^2 + p_{\perp}^2}{eE} \pi\right)$$

where  $\bar{n}_{p,r}$  is the mean number of particles produced with momentum  $p$  and spin projection  $r$ , and the upper (lower) signs refer to the production of charged scalars (spinors). Notice that, even though this expression seems reminiscent of a one-loop thermal effective action, the sign is opposite to what would be expected for a particle's statistics. The distribution is degenerate with respect to both  $r$  and  $p_3$ , the component of momentum along the direction parallel to the electric field.

The appearance of  $p_3$  in this formula might be surprising. To understand it, note that the quantity  $p_3/eE$  is analogous to the center of the oscillator coordinate in the case of a constant magnetic field (see section 2.1). For an electric field, the oscillator is inverted; the motion in the field in the classical limit approaches a hyperbolic trajectory rather than a circular one. The coordinate  $p_3/eE$  then represents the time at the center of the hyperbola: the particle decelerates for  $t < p_3/eE$  and accelerates for  $t > p_3/eE$ . In other words, the integration over  $p_3$  in equation (2.70) is tantamount to an integration over particle production time [37].

### 2.4.3 Borel summability

The decay rate of the vacuum in the presence of a constant electric field is a non-perturbative expression, that is, the process appears in no finite order in perturbation theory. It is reasonable to ask, however, whether it is possible to extract this nonperturbative result from an appropriate

resummation of the perturbative series. Indeed it is [39, 26]. I outline Dunne's argument below. For more details on Borel summation, refer to the book on divergent series by Hardy [40].

A useful tool for the analysis of divergent series is Borel summation. As an example, consider an alternating, divergent series

$$f(g) = \sum_{n=0}^{\infty} (-1)^n n! g^n. \quad (2.71)$$

A new function  $\tilde{f}(g)$  can be formally defined by inserting the definition of the Gamma function  $n! = \int_0^{\infty} dt t^n e^{-t}$ , and swapping integration and summation:

$$\tilde{f}(g) = \int_0^{\infty} dt e^{-t} \sum_{n=0}^{\infty} (-1)^n (tg)^n = \frac{1}{g} \int_0^{\infty} dt \frac{e^{-t/g}}{1+t}. \quad (2.72)$$

This expression, called the *Borel sum* of  $f$ , is well-defined and convergent for all  $g > 0$ . The original, divergent series is then best understood as an asymptotic expansion for this finite function of  $g$ .

For a more general power series  $A(z)$

$$A(z) = \sum_{n=0}^{\infty} a_n z^n \quad (2.73)$$

we define the *Borel transform*  $\mathcal{B}A(t)$

$$\mathcal{B}A(t) = \sum_{n=0}^{\infty} \frac{a_n}{n!} t^n. \quad (2.74)$$

The *Borel sum*  $\tilde{A}(z)$  is

$$\tilde{A}(z) = \int_0^{\infty} dt e^{-t} \mathcal{B}A(tz). \quad (2.75)$$

The Borel transform  $\mathcal{B}A(t)$  need not converge for all  $t$  in order for the method to be useful. If  $\mathcal{B}A(t)$  converges to an analytic function in a finite region containing  $t = 0$ , it is natural to use its analytic continuation to define the Borel sum, provided the resulting integral exists.

One class of series that are particularly useful in physics is given by [41]

$$f(g) \sim \sum_{n=0}^{\infty} (-1)^n \alpha^n \Gamma(\beta n + \gamma) g^n \quad (2.76)$$

$$\tilde{f}(g) = \frac{1}{\beta} \int_0^{\infty} \frac{dt}{t} \left( \frac{1}{1+t} \right) \left( \frac{t}{\alpha g} \right)^{\gamma/\beta} \exp \left[ - \left( \frac{t}{\alpha g} \right)^{1/\beta} \right]. \quad (2.77)$$

Such series arise naturally in the context of perturbation expansions with a small coupling  $g$ .

#### 2.4.4 Constant magnetic field

We will make use of the previous result for studying the Euler–Heisenberg Lagrangian. We start by inserting the expansion [42]

$$z \coth z = \sum_{n=0}^{\infty} \frac{2^{2k} B_{2n}}{(2n)!} z^{2n}, \quad (2.78)$$

where  $B_{2n}$  are the Bernoulli numbers, into equation (2.56), which yields

$$\mathcal{L}^{(1)}[B] = \frac{m^4}{8\pi^2} \sum_{n=0}^{\infty} \frac{B_{2n+4}}{(2n+4)(2n+3)(2n+2)} \left( \frac{2eB}{m^2} \right)^{2n+4}. \quad (2.79)$$

As anticipated in equation (2.33), only even powers of  $e$  appear. The series is of the form  $\sum a_n g^n$ , where  $g = (2eB/m^2)^2$  and

$$a_n = \frac{B_{2n+4}}{(2n+4)(2n+3)(2n+2)} \quad (2.80)$$

$$= (-1)^{n+1} \frac{2}{(2\pi)^{2n+4}} \Gamma(2n+2) \zeta(2n+4) \quad (2.81)$$

$$\sim (-1)^{n+1} \frac{2}{(2\pi)^{2n+4}} \Gamma(2n+2) \left[ 1 + \frac{1}{2^{2n+4}} + \dots \right] \quad (2.82)$$

where in the last step the Riemann zeta function

$$\zeta(s) \equiv \sum_{n=1}^{\infty} \frac{1}{n^s} \quad (2.83)$$

was expanded about large argument. The leading-order term now has the form of equation (2.76), and thus

$$\tilde{\mathcal{L}}^{(1)}[B] \sim \frac{(eB)^2}{8\pi^4} \int_0^\infty \frac{dt}{1+t} \exp\left(-\frac{m^2}{eB} \pi \sqrt{t}\right) \quad (2.84)$$

$$\sim \left(\frac{eB}{2\pi^2}\right)^2 \int_0^\infty ds \frac{s}{\pi^2 + s^2} e^{-s(m^2/eB)}. \quad (2.85)$$

Just as in the example series (equation (2.71)), this is a well-defined, unambiguous result. It represents the leading term in the Borel sum of  $\mathcal{L}^{(1)}[B]$ . In fact, the full Borel sum recovers the original expression (2.56) for the Euler–Heisenberg Lagrangian [26].

#### 2.4.5 Constant electric field

The power series expansion of the Euler–Heisenberg Lagrangian for the case of a constant electric field (2.59) reads

$$\mathcal{L}^{(1)}[E] = \frac{m^4}{8\pi^2} \sum_{n=0}^{\infty} \frac{(-1)^n B_{2n+4}}{(2n+4)(2n+3)(2n+2)} \left(\frac{2eE}{m^2}\right)^{2n+4}. \quad (2.86)$$

This series is non-alternating, so it can be expected that Borel summation will fail. Given the leading term,

$$\mathcal{L}^{(1)}[E] \sim \frac{m^4}{8\pi^2} \sum_{n=0}^{\infty} \frac{2}{(2\pi)^{2n+4}} \Gamma(2n+2) \left(\frac{2eE}{m^2}\right)^{2n+4}, \quad (2.87)$$

we may write formally

$$\tilde{\mathcal{L}}^{(1)}[E] \sim \frac{(eE)^2}{8\pi^4} \int_0^\infty \frac{dt}{1-t} \exp\left(-\frac{m^2}{eE} \pi \sqrt{t}\right) \quad (2.88)$$

$$\sim \left(\frac{eE}{2\pi^2}\right)^2 \int_0^\infty ds \frac{s}{\pi^2 - s^2} e^{-s(m^2/eE)}. \quad (2.89)$$

Notice that this expression can also be obtained from the Borel sum for a constant magnetic background (2.85) by the formal substitution  $B \rightarrow iE$  and contour rotation  $s \rightarrow is$ , as in the full Euler–Heisenberg Lagrangian.

Once more, our formal substitutions have resulted in an expression that is ill-defined due to a pole in the integrand—Borel summation has indeed failed. However, here too the ambiguity can be lifted by taking into account the correct causal boundary conditions codified in the  $i\epsilon$  prescription [43]. Once this is done, an imaginary part can be obtained which coincides with the leading term in equation (2.67). Remarkably, we were able to obtain nonperturbative information solely by analyzing the large order behavior of perturbation theory. By taking into account further terms in the asymptotic expansion (2.87), it is possible to reconstitute the full Schwinger formula (2.67).

## 2.5 SCHWINGER'S PROPER TIME METHOD

Heisenberg and Euler were able to derive an impressive array of effects in quantum electrodynamics in the presence of external fields, but at the time their derivations could be considered somewhat heuristic due to the lack of a firm field theoretic understanding of key concepts such as renormalization and gauge invariance. This was rectified by Schwinger, who placed several of the results of previous sections on a firmer field theoretic foundation [4, 44]. Several things are worth noting about this derivation. First, gauge invariance is manifest in every step of the calculation. Second, unlike in the previous calculation of Euler and Heisenberg, the role of logarithmic divergences and charge renormalization was properly understood. Third, Schwinger was able to reduce the computation of correlation functions in a quantum field theory to the conceptually simpler task of solving a nonrelativistic Schrödinger equation. It is this latter property that will be of most use for our purposes.

Schwinger's key insight comes from the following observation: in Minkowski space, the Green's function for QED satisfies the equation

$$(i\mathcal{D} - m)G(x, x') = \delta^4(x - x'). \quad (2.90)$$

Spinor indices are suppressed. Note that this is an operator equation, as  $A_\mu$  is not at this point a classical vector field, but rather an operator valued distribution. If we write  $G(x, x')$  as a matrix element of an operator  $G$ , that is,  $G(x, x') \equiv \langle x' | G | x \rangle$ , we can rewrite the above as

$$(\mathcal{P} - m)G = \mathbb{1} \quad (2.91)$$

where  $P^\mu = iD^\mu$ . Hereafter I write  $\mathbb{1}$  simply as 1. Now recall the observation in equation (2.43).

We may represent the Green's function as

$$G = -(\mathcal{P} + m) \frac{1}{-\mathcal{P}^2 + m^2} \quad (2.92)$$

$$= -(\mathcal{P} + m) i \int_0^\infty ds \exp[-i(-\mathcal{P}^2 + m^2)s]. \quad (2.93)$$

If we now write  $H \equiv -\mathcal{P}^2$  and restore the spacetime dependence,

$$G(x, x') = -i(i\mathcal{D} + m) \int_0^\infty ds e^{-im^2s} \langle x' | e^{-iHs} | x \rangle, \quad (2.94)$$

we notice something remarkable. The factor  $\langle x' | e^{-iHs} | x \rangle$  has the exact form of a matrix element of the time-evolution operator in nonrelativistic quantum mechanics, with the “proper time”  $s$  taking on the role of the time variable

$$U(x, x'; s) \equiv \langle x' | e^{-iHs} | x \rangle. \quad (2.95)$$

The time-evolution matrix element  $U(x, x'; s)$  contains essentially all of the physics. We can say loosely that this theory of quantum fields in  $d$  spacetime dimensions is equivalent to the quantum mechanics of nonrelativistic particles in  $d$  “spatial” dimensions and one proper time dimension.

There is now a clear objective. The differential equation satisfied by the time-evolution operator is

$$i\partial_s U(x, x'; s) = H U(x, x'; s), \quad (2.96)$$

where

$$H = -\mathbf{P}^2 = D^2 - \frac{1}{2}e\sigma^{\mu\nu}F_{\mu\nu}, \quad (2.97)$$

subject to the boundary conditions

$$U(x, x'; 0) = \delta^4(x - x') \quad (2.98)$$

$$\lim_{s \rightarrow -\infty} U(x, x'; s) = 0. \quad (2.99)$$

We seek the matrix elements of  $H$  in the appropriate basis so that the equations above are easy to solve. To proceed we need the commutation relations

$$[x^\mu, p^\nu] = -ig^{\mu\nu}, \quad [P^\mu, P^\nu] = -ieF^{\mu\nu}. \quad (2.100)$$

In the cases of interest to us, it will be convenient to employ the Heisenberg picture. The time-dependent operators  $x^\mu(s)$  and  $P^\mu(s)$  satisfy the equations of motion

$$\frac{dx^\mu}{ds} = i[H, x^\mu] = -2P^\mu \quad (2.101)$$

$$\frac{dP^\mu}{ds} = i[H, P^\mu] = -2eF_{\mu\rho}P^\rho - ie\partial^\rho F_{\mu\rho} - \frac{1}{2}e\partial_\mu\sigma^{\mu\nu}F_{\rho\nu}. \quad (2.102)$$

In the second equation above, all terms but the first vanish for the case of a constant field, and thus the system may be readily integrated. Using a matrix notation for compactness, we write

$$P(s) = e^{-2eFs} P(0) \quad (2.103)$$

$$x(s) - x(0) = \left( \frac{e^{-2eFs} - 1}{eF} \right) P(0). \quad (2.104)$$

These two expressions can be combined to write  $P(s)$  as a function of  $x(s)$  and  $x(0)$ .

$$P(s) = -\frac{eFe^{-eFs}}{2\sinh(eFs)} [x(s) - x(0)] \quad (2.105)$$



and then, using the antisymmetry of  $F$ , we establish

$$P^2(s) = [x(s) - x(0)]^\top K [x(s) - x(0)], \quad (2.106)$$

$$K \equiv \frac{e^2 F^2}{4 \sinh^2(eFs)}. \quad (2.107)$$

We wish to order the operators so that all the  $x(s)$  is to the left of the  $x(0)$ . By making use of the commutator

$$[x_\mu(s), x_\nu(0)] = i \left( \frac{e^{-2eFs} - 1}{eF} \right)_{\mu\nu}, \quad (2.108)$$

the Hamiltonian may be written as

$$H = -x(s)^\top K x(s) + 2x(s)^\top K x(0) - x(0)^\top K x(0) + \frac{i}{2} \text{tr}[eF \coth(eFs)] - \frac{1}{2} e\sigma F. \quad (2.109)$$

The differential equation satisfied by the time-evolution operator matrix element is

$$i\partial_s U(x, x'; s) = \left\{ -(x - x')^\top K (x - x') + \frac{i}{2} \text{tr}[eF \coth(eFs)] - \frac{1}{2} e\sigma F \right\} U(x, x'; s). \quad (2.110)$$

This may be integrated immediately, which yields

$$U(x, x'; s) = C(x, x') s^{-2} \exp \left\{ -\frac{i}{4} (x - x')^\top eF \coth(eFs) (x - x') - \frac{1}{2} \text{tr} \log \left[ \frac{\sinh(eFs)}{eFs} \right] + \frac{i}{2} e\sigma Fs \right\}. \quad (2.111)$$

The factor  $C(x, x')$  can be found by solving the equations

$$\langle x' | e^{-iHs} P_\mu(s) | x \rangle = \left[ i\partial_\mu^x - eA_\mu(x) \right] \langle x' | e^{-iHs} | x \rangle \quad (2.112)$$

$$\langle x' | e^{-iHs} P_\mu(0) | x \rangle = \left[ -i\partial_\mu^{x'} - eA_\mu(x') \right] \langle x' | e^{-iHs} | x \rangle \quad (2.113)$$

which lead to

$$\left[ i\partial_\mu^x - eA_\mu(x) - \frac{1}{2} eF(x - x') \right] C(x, x') = 0 \quad (2.114)$$

$$\left[ -i\partial_\mu^{x'} - eA_\mu(x') - \frac{1}{2} eF(x - x') \right] C(x, x') = 0. \quad (2.115)$$

The solution is just an Aharanov-Bohm phase factor:

$$C(x, x') = \frac{-i}{(4\pi)^2} \exp \left[ -ie \int_{x'}^x dy \cdot A(y) \right], \quad (2.116)$$

whose presence we might expect on physical grounds. The normalization is fixed by the boundary condition (2.98). Finally we obtain

$$U(x, x'; s) = \frac{-i}{(4\pi s)^2} \exp \left\{ -\frac{i}{4}(x-x')^\top eF \coth(eFs)(x-x') \right. \\ \left. - \frac{1}{2} \text{tr} \log \left[ \frac{\sinh(eFs)}{eFs} \right] - ie \int_{x'}^x dy \cdot A(y) + \frac{i}{2} e\sigma F s \right\}. \quad (2.117)$$

This expression can be combined with equation (2.94) to give the full, *nonperturbative* expression for the fermion propagator in the presence of a constant external field. This can then be used to compute directly a number of quantum electrodynamics effects in nontrivial backgrounds, such as the birefringence of the vacuum, photon splitting, or external-field-enhanced variants of scattering of light by light, such as Delbrück scattering [45, 46, 33].

I will use equation (2.117) to compute the effective action in the presence of a constant external field. In the proper time language we may express the one-loop effective Lagrangian as

$$\mathcal{L}^{(1)} = \frac{i}{2} \int_0^\infty \frac{ds}{s} e^{-is(m^2 - ie)} \text{tr} U(x, x; s), \quad (2.118)$$

c.f. equation (2.33). For brevity, I will omit the  $-ie$  term in the following expressions, but keep in mind that it is always there. Equation (2.117) simplifies somewhat in the coincident limit that appears in this expression. Deforming the contour by making the substitution  $s \rightarrow -is$ ,

$$\mathcal{L}^{(1)} = -\frac{1}{32\pi^2} \int_0^\infty \frac{ds}{s^3} e^{-sm^2} \exp \left( -\frac{1}{2} \text{tr} \log \left[ \frac{\sin(eFs)}{eFs} \right] \right) \text{tr} e^{\frac{1}{2} e\sigma F s}. \quad (2.119)$$

To illustrate the use of the formula we specialize to the case of a constant electric field pointing in the  $\hat{\mathbf{z}}$ -direction:

$$\mathcal{L}^{(1)} = -\frac{1}{32\pi^2} \int_0^\infty \frac{ds}{s^3} e^{-sm^2} \frac{eEs}{\sin(eEs)} \cdot 4 \cos(eEs) \quad (2.120)$$

$$= -\frac{1}{8\pi^2} \int_0^\infty \frac{ds}{s^3} e^{-sm^2} \frac{eEs}{\tan(eEs)}. \quad (2.121)$$

As in equation (2.50), this expression is divergent as  $s \rightarrow 0$ , so the divergences must be subtracted off. The finite part is, after making the substitution  $s \rightarrow s/eE$  and Wick-rotating to Euclidean space,

$$\mathcal{L}^{(1)} = \frac{(eE)^2}{8\pi^2} \int_0^\infty \frac{ds}{s^2} e^{-sm^2} \left( \cot(s) - \frac{1}{s} - \frac{s}{3} \right) \quad (2.122)$$

where, as before, the first subtraction is chosen to make the effective action vanish at zero external field, and the second is a charge renormalization. Analogously, for a constant magnetic field,

$$\mathcal{L}^{(1)} = \frac{(eB)^2}{8\pi^2} \int_0^\infty \frac{ds}{s^2} e^{-sm^2} \left( \coth(s) - \frac{1}{s} - \frac{s}{3} \right). \quad (2.123)$$

We have been able to rederive the exact form of the Euler–Heisenberg Lagrangian in the proper-time method (compare equations (2.56) and (2.59)). However, this was done without a need for the formal substitution  $B \rightarrow iE$ . Expression (2.119) allows for any choice of constant, homogeneous background field. By diagonalizing the  $F$  and  $\sigma F$  matrices it is possible to evaluate the Dirac traces exactly, which recovers equation (2.60) for the effective action, in terms of the Lorentz invariants defined in equations (2.61) and (2.62). It is worth emphasizing that at no point a gauge was chosen; the expression was explicitly gauge invariant at every step of the calculation.

## CHAPTER 3

### THE WORLDLINE FORMALISM

Schwinger's method is powerful and elegant, and was historically important both for clarifying the role of renormalization that was unknown to Heisenberg and Euler, as well as a clear demonstration that it is possible to maintain manifest gauge invariance at every step of the calculation in QED. However, it obscures the simple tunneling interpretation suggested by the calculation of Sauter (sections 2.2 and 2.3). In field theories, tunneling processes are typically realized by incorporating the effect of saddle point approximations to the path integral. The field configurations at the saddle point are known as *instantons*. It is worthwhile to ask whether the process of pair production in an electric field can be understood in terms of instanton-type contributions.

This interpretation was obtained by Affleck et al. [47], who, building on the earlier work of Feynman [48, 49], sought a semiclassical expansion of Schwinger's expression for the electron propagator (2.117). Consider the representation given in equation (2.95), which is just the observation that the kernel  $U(x, x'; s)$  can be seen as a time-evolution matrix element in a (5-dimensional) nonrelativistic quantum theory. Schwinger's approach was to compute this matrix element directly via the Heisenberg equations of motion. An equivalent choice is to express the nonrelativistic quantum mechanics problem using the path integral formalism, which, as we will see, suggests a powerful approximation scheme.

There is also a suggestive derivation of this formalism from string theory [50–52], where the proper-time parameter is identified with one of the coordinates describing the worldsheet. From such a point of view, the gauge theory diagrams have the same form as perturbative contributions in a string theory in the limit of infinite string tension. This point of view has been immensely useful in the computation of amplitudes in nonabelian gauge theory [53]. However, this rich subject falls outside the scope of this dissertation.

### 3.1 PRELIMINARIES

In the calculations of section 2.5 I followed some of the conventions set by Schwinger; namely, the proper-time was defined such that the formal analogy between the Green’s function and a nonrelativistic quantum mechanics time evolution operator is clearest. In what follows I use different conventions, which agree with those of Dunne and Schubert [54]. For clarity, the initial presentation is restricted to the case of a charged scalar, with Euclidean Lagrangian density

$$\mathcal{L} = (D_\mu \phi^*)(D_\mu \phi) + m^2 \phi^* \phi. \quad (3.1)$$

We write the Green’s function

$$G = \frac{1}{P^2 + m^2} = \int_0^\infty ds \exp[-s(P^2 + m^2)] \quad (3.2)$$

(c.f. equation (2.93)), which implicitly defines a *Euclidean* proper time  $s$ . The spacetime matrix elements of the Green’s function are then

$$G(x, x') = \int_0^\infty ds e^{-sm^2} \langle x' | e^{-sP^2} | x \rangle \quad (3.3)$$

with the corresponding Euclidean proper-time evolution operator

$$U(x, x'; s) \equiv \langle x' | e^{-sP^2} | x \rangle. \quad (3.4)$$

Though the role of proper-time is slightly obscured in this formulation, standard functional integration methods are still applicable [52, 55]. As usual, one subdivides the proper-time interval  $(0, s)$  into sufficiently small segments so that the noncommutativity of the operators in the exponential can be ignored. For the  $n$ -th interval  $(s_n, s_n + \delta s)$ , we may write

$$\langle x_{n+1} | e^{-p^2 \delta s} | x_n \rangle = \int \frac{dp}{2\pi} e^{-\delta s p^2} \langle x_{n+1} | p \rangle \langle p | x_n \rangle \quad (3.5)$$

$$= \int \frac{dp}{2\pi} e^{-\delta s (p^\mu + e A^\mu)^2 - i p (x_{n+1} - x_n)} \quad (3.6)$$

$$= \mathcal{N}_n e^{-\delta s (\frac{1}{4} \dot{x}_n^2 - i e A \cdot \dot{x}_n)} \quad (3.7)$$

where  $\dot{x} \equiv (x_{n+1} - x_n)/\delta s$  and  $\mathcal{N}_n$  is a normalization factor to be absorbed in the functional integral measure. We can now write the path integral corresponding to the kernel (3.4),

$$U(x, x'; s) = \int_x^{x'} [dx] \exp \left[ - \int_0^s d\tau \left( \frac{1}{4} \dot{x}^2 + i e A \cdot \dot{x} \right) \right]. \quad (3.8)$$

### 3.2 ZERO-TEMPERATURE EFFECTIVE ACTION

One of the conceptual advantages of Feynman's path integral is the clarity of the semiclassical limit, which is used to great effect in the instanton method. That is the role of expression (3.8): it provides a means for finding semiclassical expressions for propagators and quantities that can be written directly in terms of propagators, such as the effective action. This insight was first applied to the problem of pair production in an external electric field by Affleck et al. [47], but, due in part to our choice of conventions, the exposition below parallels that of Dunne and Schubert [54]. Recalling expression (2.118), we write

$$S_{eff}^{(1)} = \int_0^\infty \frac{ds}{s} e^{-sm^2} \oint [dx] \exp \left[ - \int_0^s d\tau \left( \frac{1}{4} \dot{x}^2 + i e A \cdot \dot{x} \right) \right], \quad (3.9)$$

where the circle in the integral symbol indicates the functional integral is over all closed paths, that is, those satisfying  $x^\mu(s) = x^\mu(0)$ . This condition requires comment. In reference [54], the

authors state the integral is to be taken over *periodic* paths, not merely closed ones. This is based on the beautiful work of Gutzwiller [56] and Littlejohn [57], who established that, in trace formulas (which have a very similar structure to equation (3.9)), only periodic orbits contribute. If the spacetime manifold is topologically trivial, this implies the condition of periodicity of the paths themselves. However, nontrivial manifolds will eventually appear in the study of vacuum decay at finite temperature; the periodicity of the orbits does not necessarily imply the periodicity of the paths, and the weaker condition of merely closed paths is more appropriate. See chapter 6 for details.

The above expression can be simplified further. If we effect the rescaling  $\tau = su, s \rightarrow s/m^2$ , we can write

$$S_{eff}^{(1)} = \int_0^\infty \frac{ds}{s} e^{-s} \oint [dx] \exp \left[ - \int_0^1 du \left( \frac{m^2}{4s} \dot{x}^2 + ieA \cdot \dot{x} \right) \right]. \quad (3.10)$$

It is now possible to perform the proper time integral explicitly, which yields

$$S_{eff}^{(1)} = 2 \oint [dx] K_0 \left( m \sqrt{\int_0^1 du \dot{x}^2} \right) \exp \left[ -ie \int_0^1 du A \cdot \dot{x} \right]. \quad (3.11)$$

Using the large argument formula [58]

$$K_0(z) \sim \left( \frac{\pi}{2z} \right)^{1/2} e^{-z}, \quad (3.12)$$

it is then possible to write

$$S_{eff}^{(1)} \sim \sqrt{\frac{2\pi}{m}} \oint [dx] \left( \int_0^1 du \dot{x}^2 \right)^{-1/4} \exp \left[ - \left( m \sqrt{\int_0^1 du \dot{x}^2} + ie \int_0^1 du A \cdot \dot{x} \right) \right]. \quad (3.13)$$

This expression could also have been obtained from equation (3.10) directly via Laplace's method, as was done in the work of Affleck et al. [47]. The critical point is

$$s_0 = \frac{m}{2} \sqrt{\int_0^1 du \dot{x}^2}. \quad (3.14)$$

Physically, the large-argument condition for the reliability of this approximation corresponds to a weak field limit, such as  $eE \ll m^2$ , as we will see when we specialize to an electric background [54].

### 3.2.1 Worldline instantons

We are now in position to derive a semiclassical approximation for equation (3.13). The problem reduces to finding instanton solutions for the associated worldline action

$$\bar{S} = m\sqrt{\int_0^1 du \dot{x}^2} + ie \int_0^1 du A \cdot \dot{x}. \quad (3.15)$$

This entails solving the following equations of motion:

$$\frac{1}{\sqrt{\int_0^1 du \dot{x}^2}} m \dot{x}_\mu = ie F_{\mu\nu} \dot{x}_\nu. \quad (3.16)$$

Notice that  $\sqrt{\int_0^1 du \dot{x}^2}$  is a constant of the motion, as can be verified by contracting the above with  $\dot{x}_\mu$ .

We impose a constant and uniform (Minkowski-space) electric field in the  $\hat{z}$ -direction by taking  $A_3 = -iEx_4$ , with the other three components either zero or constant. Then the only non-zero components of  $F$  are  $F_{34} = -F_{43} = +iE$ . The general solution of the equations of motion (3.16) for  $x_\mu(\tau)$  is a circular orbit of radius  $R = m/eE$  centered about  $(\bar{x}_3, \bar{x}_4)$

$$x_3 = \frac{m}{eE} \cos\left(\frac{a}{R}u + \varphi\right) + \bar{x}_3 \quad (3.17)$$

$$x_4 = \frac{m}{eE} \sin\left(\frac{a}{R}u + \varphi\right) + \bar{x}_4 \quad (3.18)$$

where the parameter  $a = \sqrt{\int_0^1 du \dot{x}^2}$  is determined from the condition that the paths be closed, as required by the path integral (3.9), and the phase  $\varphi$  is an arbitrary (modulus) parameter. In the case of constant field,  $a$  equals the arc length, so clearly we must have  $a = 2\pi pR$ , with  $p$  a



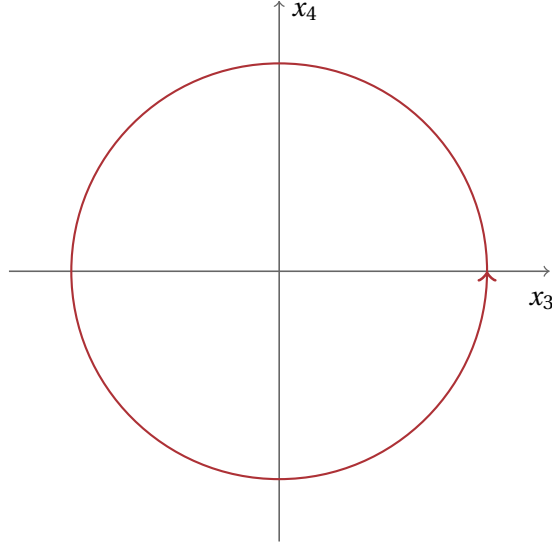


Figure 3.1: A worldline instanton for the case of a constant electric field with  $p = 1$ . The trajectory is a circle of radius  $r = m/eE$ . The arrow indicates the direction of increasing proper-time  $u$ .

positive integer. The solution is then

$$x_3^p = \frac{m}{eE} \cos(2\pi p u + \varphi) + \bar{x}_3 \quad (3.19)$$

$$x_4^p = \frac{m}{eE} \sin(2\pi p u + \varphi) + \bar{x}_4. \quad (3.20)$$

Such paths are known as *worldline instantons*. The value of the action for a worldline instanton of winding  $p$  is

$$\bar{S}_{0p} = \frac{m^2}{eE} \pi p. \quad (3.21)$$

The 0 in the subscript stands for 0 winding and indicates that this is a zero-temperature result. This notation will be introduced properly in Chapter 6, but is retained here for consistency. The values of  $\bar{S}_{0p}$  coincide with the exponents in Schwinger's formula, equation (2.67), as they must if this formalism is to reproduce the known results in Chapter 2.

### 3.2.2 Fluctuation prefactors

Calculating the pre-exponential factor in the semiclassical evaluation of the effective action (3.13) requires characterizing small oscillations about the classical solution. The case of circle instantons with winding  $p = 1$  was treated by Affleck et al. [47]. I generalize their derivation to the case  $p > 1$  below [59]. Expanding the effective action about its functional extremum we obtain

$$S_{eff}^{(1)} \sim \sum_{p=1}^{\infty} \sqrt{\frac{2\pi eE}{m^2 \vartheta_{0p}}} \mathcal{N} \det^{-\frac{1}{2}}(M_{p,\mu\nu}) e^{-\bar{S}_{0p}}, \quad (3.22)$$

$$M_{p,\mu\nu} \equiv \left. \frac{\delta^2 \bar{S}}{\delta x_\mu \delta x_\nu} \right|_{x^p}.$$

In this formula,  $\mathcal{N}$  is a normalization factor to be fixed shortly, and  $\vartheta_{0p} = 2\pi p$  is the total angle swept by a wordline instanton which winds around its center  $p$  times (with  $a_{0p}$  defined analogously as the arc length parameter of such a solution). These definitions are special to the case of a constant electric field. If the field has spatial or temporal inhomogeneities, the instanton is no longer circular [54];  $a_{0p}$  and  $\vartheta_{0p}$  can no longer be identified as arc lengths or angles and must be defined directly in terms of  $s_{0p} = \frac{m}{2} (\int_0^1 du \dot{x}^2)^{1/2}$ , equation (3.14).

The determinant factor is often the most difficult to determine. However, in the case of a constant electric field, it is possible to compute explicitly the full spectrum of small fluctuations about the wordline instanton. The second variation operator is

$$M_{p,\mu\nu} = eE \left[ \left( -\frac{\delta_{\mu\nu}}{\vartheta_{0p}} \frac{\partial^2}{\partial u^2} + ieF_{\mu\nu} \frac{\partial}{\partial u} \right) \delta(u-u') - \frac{\vartheta_{0p}}{R^2} x_\mu^p(u) x_\nu^p(u') \right]. \quad (3.23)$$

The determinant of this operator is defined as the product of all eigenvalues (subject to periodic boundary conditions), together with some suitable regularization prescription, which we handle simultaneously with the normalization factor  $\mathcal{N}$ . The last term is problematic in general, as it is nonlocal in the proper-time  $u$ ; solving the fluctuation problem for spacetime dependent electric fields would typically require solving an integro-differential eigenvalue

<i>eigenvalue</i>	<i>eigenvector(s)</i>
$2\pi eE \frac{q^2}{p}$	$(\cos(2\pi qu), 0, 0, 0),$ $(\sin(2\pi qu), 0, 0, 0)$
$2\pi eE \left( \frac{q^2}{p} - q \right)$	$(0, 0, \cos(2\pi qu), \sin(2\pi qu)),$ $q \neq p$ $(0, 0, \sin(2\pi qu), -\cos(2\pi qu))$
$-2\pi p eE$	$(0, 0, \cos(2\pi pu), \sin(2\pi pu))$

Figure 3.2: Eigenvalues and eigenvectors of the second variation operator about circle worldline instanton solutions for a constant electric field, with winding  $p$ . The parameter  $q$  takes values over all nonzero integers unless otherwise stated. Translational zero modes are not listed.

problem. However, for the specific case of circle instantons, all eigenfunctions may be found by inspection.

The oscillations in the 1 and 2 directions are trivially sines and cosines, as there is no electric field and the second term inside the parentheses vanishes. In the 3 and 4 directions, because  $F_{34}$  is nonzero, oscillations in both directions are coupled together. There are also five zero modes: four corresponding to the usual spacetime translations of the instanton, and one corresponding to translations of the starting point of the solution, that is, translations of the modulus parameter  $\varphi$  in equations (3.19) and (3.20). Because of the orthogonality of trigonometric functions, the nonlocal term from the functional Hessian (3.23) vanishes for all modes except the one associated with expansions and contractions of the circle solution, and the corresponding eigenvalue is negative as a result. There are also  $p - 1$  pairs of unstable modes associated with fluctuations in the 34 plane with frequency  $q < p$ . The full set of eigenvalues and eigenvectors of the functional Hessian can be found in Table 3.2.

The presence of negative eigenvalues indicates that this trajectory is a saddle (rather than a maximum or a minimum) in functional space. If there is an odd number of negative eigenvalues, the determinant is overall negative and the square root in equation (3.22) yields an overall purely imaginary prefactor. Thus, one expects such worldline instantons represent contributions to

the vacuum decay rate. However, if there is more than one negative eigenvalue, as in the case of worldline instantons with  $p > 1$ , there are subtle interpretational issues [60–62]. Here we have guidance from the treatment of Schwinger [4] and the various derivations in Chapter 2, which establishes that the naive prescription is correct and all eigenvalues are included; the pairs of minus signs cancel as expected.

The zero mode associated with translations of the proper-time variable  $x^\mu(u) \rightarrow x^\mu(u + \varphi/2\pi p)$  is handled as follows. One considers an infinitesimal translation

$$x^\mu(u + \varphi/2\pi p) \approx x^\mu(u) + \varphi \left. \frac{d}{d\varphi} x^\mu(u + \varphi/2\pi p) \right|_{\varphi=0} \quad (3.24)$$

and writes the second term in terms of normalized eigenfunctions. Per this standard argument [63], a factor of

$$R \int_0^{2\pi} \frac{d\varphi}{\sqrt{2\pi}} = \sqrt{2\pi} \frac{m}{eE} \quad (3.25)$$

must be included in the functional integral.

The product of eigenvalues in Table 3.2 is clearly divergent. This divergence associated with the normalization of the functional integral. We fix this normalization by evaluating the following exactly solvable path integral

$$\oint [dx] \exp \left[ -\frac{m^2}{4s_0 p} \int_0^1 du \dot{x}^2 \right] = \int d^4x \langle x | e^{-s_0 p (p/m)^2} | x \rangle \quad (3.26)$$

in two different ways. Inserting a complete set of states in the integrand on the right we obtain

$$\langle x | e^{-s_0 p (p/m)^2} | x \rangle = \int \frac{d^4p}{(2\pi)^4} e^{-s_0 p (p/m)^2} = \frac{m^4}{(4\pi s_0 p)^2}. \quad (3.27)$$

One may also evaluate the left-hand side as a functional Gaussian, which gives

$$\begin{aligned} \oint [dx] \exp \left[ -\frac{m^2}{4s_0 p} \int_0^1 du \dot{x}^2 \right] &= (\int d^4x) \mathcal{N} \left[ \det'(M_{p,\mu\nu}^{free}) \right]^{-1/2}, \\ M_{p,\mu\nu}^{free} &\equiv -\frac{m^2}{4s_0 p} \frac{d^2}{du^2} \end{aligned} \quad (3.28)$$

where the prime indicates that the determinant is computed with the zero modes removed. I define the “free” second variation operator as the operator obtained from  $M_{p,\mu\nu}$  by removing terms corresponding to the effect of the external field. Comparing with equation (3.22), we can write

$$\mathcal{L}^{(1)} \sim \frac{(eE)^2}{16\pi^4} \sum_{p=1}^{\infty} \frac{1}{p^2} \sqrt{\frac{2\pi}{peE}} \left[ \frac{\det'(M_{p,\mu\nu})}{\det'(M_{p,\mu\nu}^{free})} \right]^{-1/2} e^{-\tilde{S}_{0p}}. \quad (3.29)$$

The eigenvalues problem for  $M_{p,\mu\nu}^{free}$  is trivial for all four directions, that is, its eigenvalues are the same as those given in the first row of Table 3.2. Thus we may write

$$\frac{\det'(M_{p,\mu\nu})}{\det'(M_{p,\mu\nu}^{free})} = \frac{(-2\pi peE)}{(2\pi peE)^2} \prod_{\substack{q \neq 0 \\ q \neq p}} \frac{\left(\frac{q^2}{p} - q\right)^2}{\left(\frac{q^2}{p}\right)^2} \quad (3.30)$$

$$= -\frac{1}{2\pi peE} \left[ \lim_{z \rightarrow 1} \frac{\sin(\pi pz)}{\pi pz(1-z)} \right]^2 \quad (3.31)$$

$$= -\frac{1}{2\pi peE} [(-1)^{p+1}]^2. \quad (3.32)$$

The second line comes from a standard identity [42],

$$\frac{\sin(x)}{x} = \prod_{n=1}^{\infty} \left(1 - \frac{x^2}{n^2\pi^2}\right) = \prod_{n \neq 0} \left(1 - \frac{x}{n\pi}\right). \quad (3.33)$$

As mentioned previously, the determinant is negative. The factor in brackets is positive or negative depending on whether there is an even or odd number of *pairs* of negative eigenvalues from the second line in Table 3.2. Finally we can assemble the final expression

$$\mathcal{L}^{(1)} \sim \frac{i}{2} \frac{(eE)^2}{(2\pi)^3} \sum_{p=1}^{\infty} \frac{(-1)^{p+1}}{p^2} e^{-\frac{m^2}{eE}\pi p}, \quad (3.34)$$

in agreement with the results of Weisskopf for the vacuum decay rate in scalar electrodynamics [27]. An additional factor of 1/2 was included in accordance with a standard argument [63]. A functional integral can formally be decomposed by expressing the integrand in an orthonormal basis and integrating over the coefficient. An appropriate basis for the integration over fluctuations about the worldline instanton is the one given in Table 3.2. However, since there

are negative eigenvalues, the individual integrals over each direction in functional space do not converge. Considering specifically the lone negative eigenvalue corresponding to expansions and contractions of the circle, one may write the action as a function of the radius  $\rho$  for a circular trajectory (which satisfies the equations of motion (3.16) only when  $\rho = R = m/eE$ ),

$$S(\rho) = \frac{m}{eE} 2\pi \left( \rho - \frac{\rho^2}{2R} \right). \quad (3.35)$$

This action is plotted in Figure 3.3. It approaches negative infinity for large  $\rho$ , which means the integration over  $\rho$  diverges exponentially<sup>2</sup>. Thus, the functional integral (3.13) must be defined together with a prescription for analytic continuation, which is in turn determined by the causal boundary conditions. This is in correspondence with the  $i\epsilon$  prescription used in the various derivations in Chapter 2. The appropriate steepest descent contour is composed of two straight lines: one from the origin  $(0, 0)$  to the saddle point at  $(R, 0)$ , and one from the saddle point to  $(R, +i\infty)$ . The integration in the imaginary direction is done over only one half of the Gaussian peak, which explains the factor of 1/2 that was included in equation (3.34).

---

<sup>2</sup>Note that, in the formulation I employed, in which the integral over proper-time was done before the functional integral (see the steps between equation (3.10) and (3.13)),  $\rho$  is by definition a non-negative number.

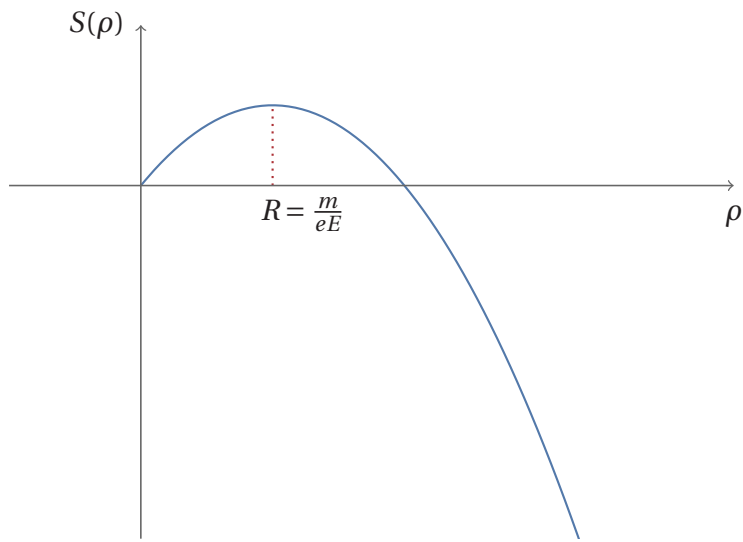


Figure 3.3: Action for a circular trajectory of arbitrary radius  $\rho$ . Only when  $\rho = R = m/eE$  this solution satisfies the equations of motion (3.16).

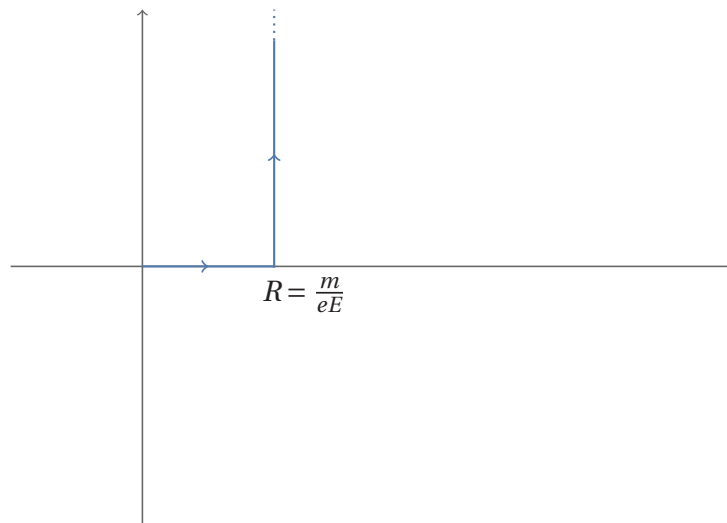


Figure 3.4: Integration contour for the direction in functional space corresponding to the negative eigenvalue in the spectrum of small fluctuations about the circle worldline instanton solution.

### 3.3 SPINORS

The various expressions for one-loop effective actions in the presence of external fields developed in Chapter 2 give great insight into the structure of such formulas. This understanding allows for a straightforward generalization of the results of the preceding sections to the physically relevant case of spinor electrodynamics. Inspecting equations (2.36) and (2.97), it is possible to deduce that the path integral representation for the effective action in the case of a charged fermion differs from the corresponding charged scalar expression by a global factor  $-1/2$  as well as the last term in equation (2.97), which represents the coupling of spin to the external electromagnetic field. As explained in the article of Dunne and Schubert [54], this term can be accounted for by including a 'spin factor'

$$Sp[x, A] = \text{Tr} \mathcal{P} \exp \left[ \frac{i}{2} \sigma_{\mu\nu} \int_0^\tau ds F_{\mu\nu}(x(\tau)) \right] \quad (3.36)$$

under the path integral [54]. The trace is over Dirac indices and the symbol  $\mathcal{P}$  denotes path-ordering, which is irrelevant for the case of constant fields as all  $F_{\mu\nu}$  commute. For an external Euclidean electric field, the exponent in equation (3.36) is purely imaginary. It does not, therefore, affect the location of the saddle point in the integral over proper-time  $s$ , nor the functional saddle point identified by the equations of motion (3.16). Most of the analysis performed in the previous sections is therefore still applicable. The spin factor is simply carried along the worldline instanton. For the case of a constant electric field, it reduces to

$$Sp[x, A] = 4 \cos(eEs) = 4 \cos(\pi p) = 4(-1)^p \quad (3.37)$$

(c.f. equation (2.120)). Therefore, the vacuum decay rate due to the applied electric field reduces to

$$\text{Im} \mathcal{L}^{(1)} \sim \frac{(eE)^2}{(2\pi)^3} \sum_{p=1}^{\infty} \frac{1}{p^2} e^{-\frac{m^2}{eE} \pi p}, \quad (3.38)$$



which is Schwinger’s formula (2.67). Remarkably, even though this result is a saddle-point approximation, it coincides with the exact result.

Another (perhaps more sophisticated) way of handling spinors in the worldline formalism is to write the spin factor as an integral over Grassmann variables [52]. The one-loop effective action in the presence of a gauge field is

$$\begin{aligned} \mathcal{L}[A] = & -\frac{1}{2} \int_0^\infty \frac{ds}{s} e^{-sm^2} \oint [dx] \int_A [d\psi] \\ & \times \exp \left[ - \int_0^s ds \left( \frac{1}{4} \dot{x}^2 + \frac{1}{2} \psi \cdot \dot{\psi} + ie A_\mu \dot{x}^\mu - ie \psi^\mu F_{\mu\nu} \psi^\nu \right) \right] \end{aligned} \quad (3.39)$$

where the subscript  $A$  on the Grassmann integral indicates anti-periodic boundary conditions. Thus, the path integral is split into a bosonic “orbital” part and a fermionic “spin” part. This form is particularly useful for amplitude computations and other applications of the worldline formalism, as the worldline action, thought of as a one-dimensional field theory, has a supersymmetry. In fact, the worldline path integral describing a Dirac particle is  $\mathcal{N} = 1$  supergravity. However, the form (3.36) is more appropriate for the purpose of obtaining saddle-point approximations.

### 3.4 VIRIAL REPRESENTATION

Nikishov’s virial representation was derived in Chapter 2 in order to determine the momentum distribution of created pairs. It would be useful to be able to obtain the same results from the worldline formalism, which permits the evaluation of the effective action in various inhomogeneous field configurations [64].

I give this generalization here. The Green’s function (3.2)

$$G = \int_0^\infty ds \exp[-s(P^2 + m^2)] \quad (3.40)$$

can be written in the position basis in the “parallel” 3,4 directions, and in the momentum basis in the “perpendicular” 1,2 directions,

$$G(x_{\parallel}, x'_{\parallel}, p_{\perp}, p'_{\perp}) = \int_0^{\infty} ds e^{-sm^2} \langle x'_{\parallel}, p'_{\perp} | e^{-sD^2} | x_{\parallel}, p_{\perp} \rangle. \quad (3.41)$$

The remaining transformations that were used to obtain the worldline representation can proceed only along the 3,4 directions and leave the 1,2 directions untouched. The one-loop effective action for a scalar in “partial” worldline form is

$$S_{eff}^{(1)} = \int \frac{d^2 p_{\perp}}{(2\pi)^2} \int_0^{\infty} \frac{ds}{s} e^{-s(m^2 + p_{\perp}^2)} \oint [dx] \exp \left[ - \int_0^s d\tau \left( \frac{1}{4} \dot{x}^2 + ieA \cdot \dot{x} \right) \right]. \quad (3.42)$$

This form suggests defining the quantity

$$m_{\perp}^2 \equiv m^2 + p_{\perp}^2 \quad (3.43)$$

which has a physical interpretation as the relativistic mass squared of the created particles.

With the replacement  $m \rightarrow m_{\perp}$ , all manipulations proceed as before, with only minor modifications. In particular, the target space for the path integral in (3.42) is two-dimensional, so the relevant normalization is

$$\oint [dx] \exp \left[ - \frac{m_{\perp}^2}{4s_0 p} \int_0^1 du \dot{x}^2 \right] = \frac{m_{\perp}^2}{4\pi s_0 p} \quad (3.44)$$

(c.f. equations (3.26) and (3.27)). The remainder of the calculation is the same regardless of dimensionality. The instanton radius  $R_{\perp} = m_{\perp}/eE$  is larger than  $m/eE$ , reflecting the fact that the production of particles with larger transverse momentum is more strongly suppressed. The one-loop effective action results

$$\mathcal{L}^{(1)} \sim i \frac{eE}{2\pi} \int \frac{d^2 p_{\perp}}{(2\pi)^2} \sum_{p=1}^{\infty} \frac{(-1)^{p+1}}{p} e^{-\frac{m_{\perp}^2}{eE} \pi p}. \quad (3.45)$$

Doing the  $p_{\perp}$  integral recovers equation (3.34). Doing the sum over  $p$  gives

$$\mathcal{L}^{(1)} \sim i \frac{eE}{2\pi} \int \frac{d^2 p_{\perp}}{(2\pi)^2} \log\left(1 + e^{-\frac{m^2 + p_{\perp}^2}{eE} \pi}\right), \quad (3.46)$$

in agreement with equations (2.69) and (2.70). Of course, the same derivation is valid for spinor particles as well; the end result differs only by an overall sum over polarizations and the sign in the logarithm. Once again it bears emphasizing that the sign is opposite what should be expected from spin-statistics: the virial expression for fermions contains a minus sign, while the one for bosons contains a plus sign.

This construction provides an interesting means of investigating pair production of massless particles, which may be relevant, for example, in QCD. The parameter  $m_{\perp}$  is generically nonzero even if  $m = 0$ , and the above argument applies. The total decay rate is given by

$$2\mathcal{L}_{bosons}^{(1)} = \sum \frac{(eE)^2}{48\pi}, \quad 2\mathcal{L}_{fermions}^{(1)} = \sum \frac{(eE)^2}{24\pi}, \quad (3.47)$$

where the sum is over polarization states.

## CHAPTER 4

### FINITE TEMPERATURE FIELD THEORY

In this chapter I briefly review various concepts, definitions and conventions useful for discussing the thermodynamics of quantum fields. The subject, of course, is vast, and only a small portion of it will be reproduced here. The interested reader may refer to the book of Kapusta and Gale [65] for details.

The fundamental object in the description of quantum mechanical systems when full knowledge of the quantum state is unavailable is the density matrix

$$\hat{\rho} = \exp\left\{-\beta(\hat{H} - \sum_i \mu_i \hat{N}_i)\right\} \quad (4.1)$$

where  $\beta = 1/T$  is the inverse temperature,  $H$  the Hamiltonian, and the  $\mu_i$  are chemical potentials corresponding to conserved charges  $\hat{N}_i$ . The ensemble average of any observable  $\hat{A}$  can be computed with the prescription

$$\langle \hat{A} \rangle = \frac{\text{Tr } \hat{A} \hat{\rho}}{\text{Tr } \hat{\rho}} \quad (4.2)$$

The quantity in the denominator

$$Z = \text{Tr } \hat{\rho} \quad (4.3)$$

is called the *grand canonical partition function*. We define the free energy  $F$  by

$$Z = \exp(-\beta VF), \quad (4.4)$$

which should be reminiscent of the definition of the quantum mechanical free energy encountered earlier in the context of zero temperature effective actions (2.25). This analogy may be taken further for computing of the partition function for field theories at finite temperature. For example, for a scalar field  $\phi$  in four dimensions, we can write the partition function

$$Z = \int [d\phi] \exp\left(-\int_0^\beta dx_4 \int d^3x \mathcal{L}_E(\phi, \partial_\mu\phi)\right), \quad (4.5)$$

where the fields are assumed to satisfy periodic boundary conditions on the Euclidean time direction

$$\phi(\mathbf{x}, x_4) = \phi(\mathbf{x}, x_4 + \beta). \quad (4.6)$$

An analogous expression holds for the thermal partition function describing a fermionic particle, with the fields  $\psi$  satisfying anti-periodic boundary conditions

$$\psi(\mathbf{x}, x_4) = -\psi(\mathbf{x}, x_4 + \beta). \quad (4.7)$$

The spectrum of oscillations in the Euclidean time direction is discrete. The angular frequencies associated with such oscillations are

$$\omega_n = \begin{cases} (2n)\pi T & \text{bosons} \\ (2n+1)\pi T & \text{fermions,} \end{cases} \quad (4.8)$$

known as *Matsubara frequencies*. The discreteness of the spectrum has marked consequences for the effective action defined in (2.25). For example, to one loop, the zero-temperature effective potential for a real scalar field  $\phi$  in the presence of suitable sources that set  $\langle\phi\rangle = \phi_c$  is given by

$$V_{eff}^{(T=0)} = V(\phi_c) + \frac{1}{2} \int \frac{d^4k}{(2\pi)^4} \log(k^2 + V''(\phi_c)) \quad (4.9)$$

At finite temperature, the integral over momentum modes is replaced by a sum, so

$$V_{eff} = V(\phi_c) + \frac{1}{2\beta} \sum_n \int \frac{d^3k}{(2\pi)^3} \log\left[\left(\frac{2\pi n}{\beta}\right)^2 + \mathbf{k}^2 + V''(\phi_c)\right]. \quad (4.10)$$

The sum over Matsubara modes can be brought into the logarithm as a product. With the notation  $\omega_{\mathbf{k}}^2 \equiv \mathbf{k} + V''(\phi_c)$  we can write

$$V_{eff} = V(\phi_c) + \frac{1}{2\beta} \int \frac{d^3k}{(2\pi)^3} \log \left[ \prod_n (\omega_n^2 + \omega_{\mathbf{k}}^2) \right]. \quad (4.11)$$

A factor of  $\prod_n \omega_n^2$  can be removed from the product, as it represents only an infinite, temperature dependent constant contribution to the normalization of the functional integral [66]. Thus

$$V_{eff} = V(\phi_c) + \frac{1}{\beta} \int \frac{d^3k}{(2\pi)^3} \log \left[ \beta \omega_{\mathbf{k}} \prod_{n=1}^{\infty} \left( 1 + \frac{\omega_{\mathbf{k}}^2}{\omega_n^2} \right) \right] \quad (4.12)$$

$$= V(\phi_c) + \frac{1}{\beta} \int \frac{d^3k}{(2\pi)^3} \log \left[ \beta \omega_{\mathbf{k}} \prod_{n=1}^{\infty} \left( 1 + \frac{\beta^2 \omega_{\mathbf{k}}^2}{4\pi^2 n^2} \right) \right]. \quad (4.13)$$

The argument of the logarithm is recognized as a representation of the hyperbolic sine [42]

$$\sinh(z) = z \prod_{k=1}^{\infty} \left( 1 + \frac{z^2}{\pi^2 k^2} \right), \quad (4.14)$$

therefore

$$V_{eff} = V(\phi_c) + \frac{1}{\beta} \int \frac{d^3k}{(2\pi)^3} \log [2 \sinh(\beta \omega_{\mathbf{k}})] \quad (4.15)$$

$$= V(\phi_c) + \int \frac{d^3k}{(2\pi)^3} \left\{ \omega_{\mathbf{k}} + \frac{1}{\beta} \log(1 - e^{-\beta \omega_{\mathbf{k}}}) \right\}. \quad (4.16)$$

The first term in braces is recognized as a vacuum energy contribution, while the second is  $-p$ , where  $p$  is the pressure of a relativistic Bose gas with mass  $m = \sqrt{V''(\phi_c)}$ . This justifies the interpretation of the one-loop effective potential as the free energy of the system, when this expression is evaluated on a global minimum.

#### 4.1 GAUGE THEORIES AT FINITE TEMPERATURE

The study of phase transitions and critical phenomena, particularly the Landau-Ginsburg theory and related developments [67], has generated fruitful results for many areas of physics.

There, the free energy is taken to be a functional a set of *order parameters* whose abrupt changes across phase transitions typically (but not always) represent the breaking of various symmetries. More details on the Landau-Ginsburg picture in the context of gauge theories may be found in Ogilvie [2]. The prototypical example of a phase transition is that of a ferromagnetic spin system, where the order parameter is the net magnetization, and the corresponding symmetry is rotational invariance.

There is a natural analogue of magnetization which can be defined for a nonabelian gauge theory and acts as the order parameter for the deconfinement transition. The *Polyakov loop* operator for a gauge field  $A_\mu$ , abelian or nonabelian, is defined as the path-ordered exponential

$$P(x) \equiv \mathcal{T} \exp \left[ i g \int_0^\beta dy_4 A_4(\mathbf{x}, y_4) \right] \quad (4.17)$$

where where the symbol  $\mathcal{T}$  stands for ordering in the Euclidean time direction<sup>3</sup>, and the timelike path begins and ends at  $(\mathbf{x}, x_4)$ . The operator  $P$  takes on values in the gauge group and transforms according to its adjoint representation:  $P(x) \rightarrow g(x)P(x)g^\dagger(x)$  so that the trace of powers of  $P$ ,  $\text{Tr} P^n$ , is gauge-invariant. The usefulness of this quantity stems from the fact that it can be related to the free energy of a static isolated quark in the representation  $R$  of the gauge group:

$$e^{-\beta F_R} = \langle \text{Tr}_R P(x) \rangle, \quad (4.18)$$

as the Polyakov loop factor can be understood as a nonabelian Aharanov-Bohm-like geometric phase accumulated by a heavy particle in the representation  $R$  which winds around once in the Euclidean time direction. Clearly, if  $\langle \text{Tr}_R P(x) \rangle$  vanishes, the free energy  $F_R = \infty$ , which indicates that static isolated particles in the representation  $R$  are confined.

---

<sup>3</sup>For all cases considered in this dissertation this is of no consequence: external fields are taken to be constant, or gauge-transformable to constant, and thus all the  $A_4$  commute.

The symmetry associated with the confinement transition is the center symmetry of the global symmetry implied by the gauge symmetry of the theory. The center of a group is the set of elements which commute with every other element. For  $SU(N)$ , this is  $Z(N)$ . Under a rotation by an element  $z \in Z(N)$ , the Polyakov loop transforms as

$$\mathrm{Tr}_R P(x) \rightarrow z^{k_R} \mathrm{Tr}_R P(x) \quad (4.19)$$

where  $k_R$  is an integer known as the  $N$ -ality of the representation  $R$ . If  $k_R$  is nonzero, unbroken center symmetry implies the vanishing of the Polyakov loop expectation value

$$\langle \mathrm{Tr}_R P(x) \rangle = 0 \quad (4.20)$$

and therefore confinement of particles in representation  $R$ . The trace of  $P$  is an order parameter for the deconfinement phase transition in pure gauge theories, which is associated with loss of center symmetry above a critical temperature  $T_d$ . When quark effects are included,  $\langle \mathrm{Tr} P \rangle$  may or may not indicate a phase transition. However,  $\langle \mathrm{Tr} P \rangle$  is quite generally small at low temperatures and densities, indicating a large free energy cost for the presence of a single added static quark, and tends towards larger values at temperatures and/or densities are increased. In the absence of a real phase transition, in the case where quark effects prevent exact unbroken center symmetry from being realized, there is still a crossover between confined and deconfined regimes.

For sufficiently high temperatures, the dimensionality of the system is reduced and the dynamics are effectively those of a  $Z(N)$  spin system. Note that the situation in gauge theory is opposite the most common case in condensed matter systems, in which a symmetry which is broken at low temperatures is restored at high temperatures for entropic reasons.

In particular we may be interested in the groups  $SU(2)$  and  $SU(3)$ . For  $SU(2)$  it will be useful to employ the parameterization



$$P = \begin{pmatrix} e^{i\theta} & 0 \\ 0 & e^{-i\theta} \end{pmatrix} \quad (4.21)$$

and for  $SU(3)$

$$P = \begin{pmatrix} e^{i(\theta+\psi)} & 0 & 0 \\ 0 & e^{-i(\theta+\psi)} & 0 \\ 0 & 0 & e^{-2i\psi} \end{pmatrix}. \quad (4.22)$$

In both cases, it was assumed that the gauge field can be made diagonal by an appropriate transformation. Generically for  $SU(N)$ , the Polyakov loop may be written as  $\text{diag}(e^{i\theta_1}, \dots, e^{i\theta_{n-1}})$ , where the  $\theta_j$ , are commonly, if inaccurately, referred to as *Polyakov loop eigenvalues*.

#### 4.2 EFFECTIVE ACTION IN THE PRESENCE OF A POLYAKOV LOOP

In this section, low and high temperature expansions of the effective action in the presence of a Polyakov loop background are derived. These results are useful for applications, and in particular they elucidate how the center symmetry becomes broken at high temperatures. These derivations will also be the template for some further extensions, particularly in Chapter 5, and some of the results obtained here will be useful as a benchmark for checking the correctness of results obtained by other methods. The development presented here is that of Meisinger and Ogilvie [68].

The steps leading to equation (4.16) may be retraced in the presence of a nontrivial Polyakov loop. This is accomplished by replacing the Matsubara frequency contribution to the spectrum in each of the copies of (4.10) as

$$\omega_n^2 \rightarrow (\omega_n + \varphi)^2 \quad (4.23)$$

where  $\varphi \equiv \theta_j$  is one of the Polyakov loop eigenvalues defined above. In  $d + 1$  dimensions, the finite temperature contribution to the effective potential will be a sum of terms of the form

$$\frac{1}{\beta} \int \frac{d^d k}{(2\pi)^d} \log(1 \pm e^{-\beta\omega_{\mathbf{k}} + i\varphi}) + \frac{1}{\beta} \int \frac{d^d k}{(2\pi)^d} \log(1 \pm e^{-\beta\omega_{\mathbf{k}} - i\varphi}) \quad (4.24)$$

where the minus (plus) sign is taken for bosonic (fermionic) contributions. The first term corresponds to the sum over positive Matsubara frequencies and can thus be identified with particle contributions, and the second, respectively, with antiparticle contributions. In what follows I will specialize to the case of a single bosonic particle moving in a Polyakov loop background, with the understanding that the corresponding fermionic expression may be obtained with the replacement [68]

$$V_F(\varphi) = -V_B(\pi + \varphi). \quad (4.25)$$

Note that these expressions are valid for a single bosonic (resp. fermionic) degree of freedom: degeneracies associated with e.g. spin degrees of freedom or the dimensionality of the group representation are not included. The effective potential for a boson of spin  $s$  in the fundamental representation of  $SU(N)$  is thus

$$f_B = s \sum_j V_B(\theta_j) \quad (4.26)$$

where  $s$  is a spin degeneracy factor, which is 2 if the particle is massless and  $2s + 1$  otherwise [69].

For a gauge boson, which is in the adjoint representation, we may write

$$f_{gauge} = \frac{s}{2} \sum_{j,k=1}^N \left(1 - \frac{1}{N} \delta_{jk}\right) V_B(\theta_j - \theta_k) \quad (4.27)$$

where the factor of  $1/2$  corrects for overcounting the particle and antiparticle contributions present in  $V_B$ , and the  $\delta_{jk}$  removes a singlet contribution.

#### 4.2.1 Low temperature expansions

At low temperatures, the Boltzmann factor  $e^{-\beta\omega_{\mathbf{k}}}$  is likely small, so a Taylor expansion of the logarithm is reliable. Additionally performing the angular integrations we obtain

$$V_B = \sum_{\pm} \frac{1}{\beta} \int \frac{d^d \mathbf{k}}{(2\pi)^d} \log(1 - e^{-\beta\omega_{\mathbf{k}} + i\varphi}) \quad (4.28)$$

$$= -\frac{4\pi^{d/2}}{\Gamma(d/2)(2\pi)^d \beta} \int dk k^{d-1} \sum_{n=1}^{\infty} \frac{1}{n} e^{-n\beta\omega_{\mathbf{k}}} \cos(n\varphi). \quad (4.29)$$

With the substitution  $k = m \sinh t$  this becomes

$$V_B = -\frac{4\pi^{d/2}}{\Gamma(d/2)(2\pi)^d} \sum_{n=1}^{\infty} \frac{\cos(n\varphi)}{n\beta} m^d \int_0^{\infty} dt \cosh t (\sinh t)^{d-1} e^{-n\beta m \cosh t} \quad (4.30)$$

$$= \frac{4\pi^{d/2}}{\Gamma(d/2)(2\pi)^d} \sum_{n=1}^{\infty} \frac{\cos(n\varphi)}{n^2 \beta^2} m^d \frac{d}{dm} \int_0^{\infty} dt (\sinh t)^{d-1} e^{-n\beta m \cosh t} \quad (4.31)$$

$$= \frac{4\pi^{d/2}}{\Gamma(d/2)(2\pi)^d} \sum_{n=1}^{\infty} \frac{\cos(n\varphi)}{n^2 \beta^2} m^d \frac{d}{dm} \left[ \frac{\Gamma(d/2)}{\sqrt{\pi}} \left( \frac{2}{n\beta m} \right)^{(d-1)/2} K_{(d-1)/2}(n\beta m) \right]. \quad (4.32)$$

The derivative can be computed with use of recursion relations for modified Bessel functions:

$$K'_\nu(z) = -K_{\nu+1}(z) + \frac{\nu}{z} K_\nu(z) \quad (4.33)$$

which imply

$$\frac{d}{dz} \left[ \left( \frac{2}{z} \right)^\nu K_\nu(z) \right] = \left( \frac{2}{z} \right)^\nu \left( K'_\nu(z) - \frac{\nu}{z} K_\nu(z) \right) = -\left( \frac{2}{z} \right)^\nu K_{\nu+1}(z). \quad (4.34)$$

Therefore

$$V_B = \frac{4\pi^{(d-1)/2}}{(2\pi)^d} m^d \sum_{n=1}^{\infty} \frac{\cos(n\varphi)}{n\beta} \frac{d}{dz} \left[ \left( \frac{2}{z} \right)^{\nu} K_{\nu}(z) \right]_{\substack{z=n\beta m, \\ \nu=(d-1)/2}} \quad (4.35)$$

$$= \frac{4\pi^{(d-1)/2}}{(2\pi)^d} m^d \sum_{n=1}^{\infty} \frac{\cos(n\varphi)}{n\beta} \left[ - \left( \frac{2}{z} \right)^{\nu} K_{\nu+1}(z) \right]_{\substack{z=n\beta m, \\ \nu=(d-1)/2}} \quad (4.36)$$

$$= - \frac{4\pi^{(d-1)/2}}{(2\pi)^d} m^d \sum_{n=1}^{\infty} \frac{\cos(n\varphi)}{n\beta} \left( \frac{2}{n\beta m} \right)^{\frac{d-1}{2}} K_{(d+1)/2}(n\beta m) \quad (4.37)$$

$$= - \frac{4m^{d+1}}{(2\pi)^{(d+1)/2}} \sum_{n=1}^{\infty} \frac{\cos(n\varphi)}{(n\beta m)^{(d+1)/2}} K_{(d+1)/2}(n\beta m). \quad (4.38)$$

The corresponding expression for fermions is

$$V_F = \frac{4m^{d+1}}{(2\pi)^{(d+1)/2}} \sum_{n=1}^{\infty} (-1)^n \frac{\cos(n\varphi)}{(n\beta m)^{(d+1)/2}} K_{(d+1)/2}(n\beta m) \quad (4.39)$$

where the powers  $(-1)^n$  correspond to antiperiodic boundary conditions on the path integral.

#### 4.2.2 High temperature expansions

If the number of spatial dimensions  $d$  is odd, it is possible to resum expressions (4.38) and (4.39) to obtain asymptotic expressions valid at high temperature. The starting point is the identity [42]

$$\sum_{p=1}^{\infty} K_0(pz) \cos(p\varphi) = \frac{1}{2} \left[ \gamma + \log\left(\frac{z}{4\pi}\right) \right] + \frac{\pi}{2} \sum'_{\ell} \left[ \frac{1}{\sqrt{z^2 + (\varphi - 2\pi\ell)^2}} - \frac{1}{2\pi|\ell|} \right] \quad (4.40)$$

where the notation  $\sum'_{\ell}$  indicates that the singular term  $1/2\pi|\ell|$  is omitted when  $\ell = 0$ . With repeated application of recurrence relation (4.33) it is possible to derive similar expressions for

$$\sum_{\nu=1}^{\infty} \frac{1}{p^{\nu}} K_{\nu}(pr) \cos(p\varphi) \quad (4.41)$$

which is the main result needed for the desired expansions. The details may be found in reference [68]; I quote only the final results relevant for  $d = 1$  and  $d = 3$ :

$$\sum_{p=1}^{\infty} \frac{1}{p} K_1(pz) \cos(p\varphi) = -\frac{1}{4} \left[ \log\left(\frac{z}{4\pi}\right) + \gamma - \frac{1}{2} \right] + \frac{1}{z} \left[ \frac{1}{4} \varphi^2 - \frac{\pi}{2} \varphi + \frac{\pi^2}{6} \right] - \frac{\pi}{2z} \sum_{\ell}' \left[ \sqrt{z^2 + (\varphi - 2\pi\ell)^2} - |\varphi - 2\pi\ell| - \frac{z^2}{4\pi|\ell|} \right] \quad (4.42)$$

$$\begin{aligned} \sum_{p=1}^{\infty} \frac{1}{p^2} K_2(pz) \cos(p\varphi) &= \frac{1}{16} z^2 \left[ \log\left(\frac{z}{4\pi}\right) + \gamma - \frac{3}{4} \right] \\ &\quad - \frac{1}{2} \left[ \frac{1}{4} \varphi^2 - \frac{\pi}{2} \varphi + \frac{\pi^2}{6} \right] + \frac{2}{z^2} \left[ -\frac{1}{48} \varphi^4 + \frac{\pi}{12} \varphi^3 - \frac{\pi^2}{12} \varphi^2 + \frac{\pi^4}{90} \right] \\ &\quad - \frac{\pi}{2z^2} \sum_{\ell}' \left\{ \frac{1}{3} [z^2 + (\varphi - 2\pi\ell)^2]^{3/2} - \frac{1}{3} |\varphi - 2\pi\ell|^3 \right. \\ &\quad \left. - \frac{1}{2} |\varphi - 2\pi\ell| z^2 - \frac{z^4}{16\pi|\ell|} \right\}. \end{aligned} \quad (4.43)$$

In both formulas,  $\varphi$  is assumed to lie in the range  $(0, 2\pi)$ . With this, we have the complete expression for the high temperature expansion of  $V_B$  in three spatial dimensions:

$$\begin{aligned} V_B(\varphi) &= -\frac{m^2}{\pi^2 \beta^2} \sum_{n=1}^{\infty} \frac{1}{n^2} K_2(n\beta m) \cos(n\varphi) \\ &= -\frac{2}{\pi^2 \beta^4} \left[ \frac{\pi^4}{90} - \frac{\pi^2}{12} \varphi^2 + \frac{\pi}{12} \varphi^3 - \frac{1}{48} \varphi^4 \right] \\ &\quad + \frac{m^2}{2\pi^2 \beta^2} \left[ \frac{1}{4} \varphi^2 - \frac{\pi}{2} \varphi + \frac{\pi^2}{6} \right] - \frac{m^4}{16\pi^2} \left[ \log\left(\frac{\beta m}{4\pi}\right) + \gamma - \frac{3}{4} \right] \\ &\quad - \frac{1}{2\pi \beta^4} \sum_{\ell}' \left\{ \frac{1}{3} [(\beta m)^2 + (\varphi - 2\pi\ell)^2]^{3/2} - \frac{1}{3} |\varphi - 2\pi\ell|^3 \right. \\ &\quad \left. - \frac{1}{2} |\varphi - 2\pi\ell| \beta^2 m^2 - \frac{(\beta m)^4}{16\pi|\ell|} \right\}. \end{aligned} \quad (4.45)$$

The first term in the first line of (4.45) is the black body free energy for two degrees of freedom. This leading term is minimized when  $\varphi = 0$ , which, as we will see, means that the deconfined phase is favored at high temperatures. The second term is the one commonly associated with symmetry restoration at finite temperature, as the  $m^2 T^2/12$  term contributes a positive mass of order  $T$ —notice that  $m$  is not a bare mass and may depend on the expectation values of

fields. The logarithm in the third term often combines with similar contributions from zero-temperature effective actions in such a way that the temperature sets the scale for running coupling constants. The last term is associated with the loss of analyticity in finite temperature perturbation theory [68].

### 4.3 RECOVERING CONFINEMENT

The high-temperature expansion of the one-loop effective potential for a boson moving in a Polyakov loop background, equation (4.45), together with equation (4.27), can be used to build the high temperature expansion of the one-loop effective potential for the gauge bosons, which shows that the free energy is minimized when all the Polyakov loop eigenvalues are equal (and zero, as demanded by the fact that elements of  $SU(N)$  have unit determinant). At high temperatures, the Polyakov loop approaches the identity matrix, which is not invariant under the center group  $Z(N)$ , signaling deconfinement.

It is worth asking whether it is possible to recover a confined regime at sufficiently high temperatures, where, as a consequence of asymptotic freedom, the one-loop result is reliable. One clear possibility is to consider theories with fermions in the adjoint representation, satisfying periodic boundary conditions on the Euclidean time direction [70, 71]. This type of model maintains center symmetry at arbitrarily small values of  $\beta$ , which permits confinement to be studied analytically. However, since our main goal in this section is to obtain a deconfinement transition in rough agreement with lattice data [2], I will introduce the two models given in [72], which for our purposes may be regarded as phenomenological. Both models have a physical inspiration, but of two very different types; it is hoped that the differences might give insight into what features are universal. Phenomenological studies of QCD at finite density have indeed revealed regimes in which the two models differ [73].

### 4.3.1 Model A

For bosons in the adjoint representation, the second term in (4.27) is minimized when  $\varphi = \theta_j - \theta_k = \pi$ , which means that the model favors phases  $e^{i\theta_j}$  as far apart as possible on the unit circle. This is known as *eigenvalue repulsion* and it is precisely the sort of behavior that is required in order to favor unbroken center symmetry. However, such a term does not appear in the pure gauge theory since it represents a mass contribution.

In *model A*, I ignore this difficulty and simply add to the free energy, by hand, the second term in (4.27), and adjust the parameter  $m$  so that the confinement-deconfinement transition occurs at the correct temperature  $T_d = 270$  MeV for the pure gauge theory. The phase transition then occurs as a result of the competition between the perturbative free energy, which dominates at high temperatures, and the deformation, which dominates for temperatures  $T < T_d$ . An equivalent way to write the deforming term is

$$V_d^A = \frac{M^2 T^2}{2\pi^2} \sum_{n=1}^{\infty} \frac{1}{n^2} \text{Tr}_{Adj} P^n. \quad (4.46)$$

For  $SU(2)$ , we have  $T_d = (3/2)^{1/2} M/\pi$  so the mass parameter must be set to  $m = 693$  MeV. This parameter should not be thought of as a mass for the gauge bosons: it is purely phenomenological.

### 4.3.2 Model B

*Model B* begins from the assumption that color confinement operates on a specific length scale  $R$ . Net color charges are allowed only in volumes smaller than  $R^3$ , with color neutrality enforced on larger scales. Space is then divided into cells of volume  $R^3$ , each with partition

function given by

$$Z_{cell} = \exp[-\beta R^3 f_{cell}] = \int (d\theta) \exp[-\beta R^3 f_{gauge}(\theta)] \quad (4.47)$$

with  $f_{gauge}(\theta)$  given by equation (4.27), and  $(d\theta)$  the  $SU(N)$  Haar measure. I then make the further assumption that the eigenvalues  $\theta$  are the same in every cell, so that a true phase transition is possible in the infinite volume limit. The deformation term for model B is then,

$$V_d^B(\theta) = -\frac{1}{\beta R^3} \log[J(\theta)] \quad (4.48)$$

where  $J(\theta)$  is the Jacobian

$$J(\theta) = A \prod_{j < k} \sin^2\left(\frac{\theta_j - \theta_k}{2}\right), \quad (4.49)$$

with  $A$  a normalization constant to be determined from the requirement  $\int (d\theta) = 1$ . This measure is maximized when the angles  $\theta_j$  are spread out over the unit circle as far from one another as possible, a clear manifestation of eigenvalue repulsion. At temperatures much higher than the inverse of the scale set by  $R$ , the center-breaking perturbative one-loop free energy dominates. For  $SU(2)$ , the correct deconfinement temperature  $T_d = 270$  MeV is obtained by setting the distance  $R = 1.315$  fm.

An alternate, equivalent form of the deforming potential is

$$V_d^B = \frac{T}{R^3} \sum_{n=1}^{\infty} \frac{1}{n} \text{Tr}_{Adj} P^n. \quad (4.50)$$

Comparing this expression with the corresponding one from model A, equation (4.46), shows that even though both models were obtained by very different methods, starting from very different assumptions, the final expressions are closely related.



## CHAPTER 5

### MAGNETIC FIELDS AT FINITE TEMPERATURE

As outlined in the introduction, a number of physical systems are characterized by strong external fields as well as high temperatures and/or densities. If such systems are gauge theories, it may also be necessary to contend with confinement and chiral symmetry breaking. Therefore, an understanding of the interplay between these different conditions, as well as mathematical technology for calculating their effects accurately, are of great importance. Examples of hot and/or dense systems where external magnetic fields are significant include the early universe, where the energy scale of magnetic fields  $\sqrt{eB}$  is of the order of  $\approx 2$  GeV, heavy ion collisions such as at the ALICE or RHIC experiments, where  $\sqrt{eB} \approx 0.1\dots 0.5$  GeV, and compact stars, where  $\sqrt{eB} \approx 1$  MeV [33, 74].

As we have seen in chapter 2, a perturbative understanding of systems with intense magnetic fields is centered on the concept of *Landau levels*, which are the discrete energy eigenvalues found in a magnetic system. At finite temperature, Landau levels naturally play a pronounced role, as more levels become accessible with increasing temperature. With strong magnetic fields, the lowest Landau level is particularly important. The density of states enhancement that accompanies the squeezing of a continuous energy spectrum into a discrete one also has profound physical consequences. The low-lying eigenvalues are of special importance to

the formation of the chiral condensate [75], and to the restoration of chiral symmetry at high temperatures.

The goal in this chapter is to develop expansions that may be used for computing thermal magnetic effects in nonabelian gauge theories. Our focus is on the physical case of charged spinors in a  $U(1)$  magnetic field, but the techniques presented here may be easily generalized to treat charged scalars or vector particles, and abelian chromomagnetic backgrounds, if desired.

## 5.1 EFFECTIVE ACTION FOR SPINORS IN A MAGNETIC FIELD

First I develop techniques for computing the fermion determinant in the presence of an abelian magnetic field as well as a nonabelian gauge field background which is meant to represent a nontrivial Polyakov loop. I take the fermion field to be in the fundamental representation of the gauge group and to satisfy anti-periodic boundary conditions, but the method can be generalized to periodic and/or adjoint fermions without difficulty. The procedure presented here is adapted from the work of Meisinger and Ogilvie [76], which concerns the case of an  $SU(2)$  gauge boson moving in an abelian chromomagnetic background.

In previous chapters the letter  $A$  was used to denote an external gauge field, assumed to be in  $U(1)$ . In this chapter we have both  $U(1)$  fields, which I continue to denote as  $A$ , as well as  $SU(2)$  fields, which are denoted  $G$ . The electric charge will be denoted  $q$ , while  $SU(2)$  charges are absorbed within the field  $G$ .

The background fields are taken to be

$$A_2 = Bx_1 \quad G_4 = \frac{\theta}{\beta} \tau_3 \quad (5.1)$$

where  $\beta$  is the inverse temperature  $1/T$  and  $\tau_3$  is the third Pauli matrix  $\text{diag}(1, -1)$ . This corresponds to a magnetic field in the  $\hat{z}$ -direction and an abelian Polyakov loop parameterized by

the angle  $\theta$  in the 3-direction of the gauge group. The corresponding covariant derivative is given by

$$\gamma \cdot D = \gamma \cdot \partial - i\gamma^4 G_4 - iq\gamma^2 A_2 \quad (5.2)$$

I follow a similar procedure as the one used in section 2.4 to evaluate the effective Lagrangian of Euler and Heisenberg, where the functional determinant was computed directly from the spectrum. The energy of a fermionic mode in the given background (5.1) is

$$E_{mode}^2 = \left(\omega_n \pm \frac{\theta}{\beta}\right)^2 + \omega_{\pm}^2(r, p_3) \quad (5.3)$$

where  $\omega_n = (2n + 1)\pi T$  are the Matsubara frequencies and

$$\omega_{\pm}^2(r, p_3) = 2qB\left(r + \frac{1}{2} \pm \frac{1}{2}\right) + p_3^2 + m^2. \quad (5.4)$$

Notice that the energy of the lowest Landau level  $r = 0$  has no magnetic contribution, which is understood as a consequence of the Atiyah–Singer index theorem [77–79]. Then the effective potential

$$V = - \sum_{r=0}^{\infty} \sum_{n,\pm,\pm} \frac{qB}{2\pi\beta} \int \frac{dp_3}{2\pi} \log \left[ \left(\omega_n \pm \frac{\theta}{\beta}\right)^2 + \omega_{\pm}^2(r, p_3) \right]. \quad (5.5)$$

By using a standard identity (see equation (4.16) and its derivation) this can be split into a finite temperature contribution

$$V_T = - \sum_{r=0}^{\infty} \sum_{\pm,\pm} \frac{qB}{2\pi} \int \frac{dp_3}{2\pi} \left[ \frac{1}{\beta} \log \left( 1 + e^{-\beta\omega_{\pm}(r, p_3) \pm i\theta} \right) \right] \quad (5.6)$$

and a sum over zero-point energies, written in unregularized form,

$$V_{(T=0)} = -2 \sum_r \sum_{\pm} \frac{qB}{2\pi} \int \frac{dp_3}{2\pi} \omega_{\pm}(r, p_3). \quad (5.7)$$

In fact, this is just the Euler–Heisenberg Lagrangian (2.56) for two spinors moving in a magnetic field, with one important difference. In section 2.4, I regarded the fermion mass as a parameter; here, for typical applications we may be interested in how this mass is dynamically generated,

so there is no corresponding term in the normalization of the path integral to subtract the  $1/s^3$  divergence. I compute both divergent terms using a Lorentz-invariant proper-time cutoff,

$$\frac{(qB)^2}{6\pi} \int_{1/\Lambda^2}^{\infty} \frac{ds}{s} e^{-m^2 s} = \frac{(qB)^2}{12\pi^2} \Gamma\left(0, \frac{m^2}{\Lambda^2}\right) \quad (5.8)$$

$$\frac{1}{2\pi} \int_{1/\Lambda^2}^{\infty} \frac{ds}{s^3} e^{-m^2 s} = \frac{1}{8\pi^2} \left[ e^{-\frac{m^2}{\Lambda^2}} \Lambda^2 (\Lambda^2 - m^2) - m^4 \text{Ei}\left(-\frac{m^2}{\Lambda^2}\right) \right], \quad (5.9)$$

where  $\Gamma(s, x)$  is the upper incomplete Gamma function, and  $\text{Ei}(x)$  is the exponential integral. Note that the proper-time variable is dimensionful in these expressions; the shift  $s \rightarrow s/qB$  done in equation (2.48) has been left undone. Otherwise, the physical cutoff value would depend on the applied magnetic field, which is undesirable.

We may use expression (2.58), derived in Appendix A.1, to write the finite part in terms of the Hurwitz zeta function,

$$\int_0^{\infty} \frac{dt}{t^2} e^{-2zt} \left( \coth t - \frac{1}{t} - \frac{t}{3} \right) = \frac{1}{3} - z^2 - \zeta'(-1, z) - 4 \left( z - 2z^2 - \frac{1}{3} \right) \log z, \quad (5.10)$$

where the prime denotes differentiation with respect to the first argument. Thus the finite portion can be written

$$\begin{aligned} V_{(T=0)}^{finite} = & -\frac{(qB)^2}{12\pi^2} \left( \log\left(\frac{2qB}{m^2}\right) - 1 \right) - \frac{m^4}{8\pi^2} \left( \log\left(\frac{2qB}{m^2}\right) + \frac{1}{2} \right) \\ & - \frac{(qB)m^2}{4\pi^2} \log\left(\frac{m^2}{2qB}\right) - \frac{(qB)^2}{\pi^2} \zeta'_H\left(-1, \frac{m^2}{2qB}\right). \end{aligned} \quad (5.11)$$

The final expression for the zero-temperature contribution to the effective potential is obtained by adding to this expression the divergent terms calculated in (5.8) and (5.9).

I now proceed to develop various asymptotic expansions of the one-loop finite-temperature effective action which are more convenient for applications than the integral representation (5.6).

### 5.1.1 Strong field expansion

Expanding the logarithm in equation (5.6) we obtain

$$V_T = - \sum_{r=0}^{\infty} \sum_{\pm} \frac{qB}{2\pi} \int \frac{dp_3}{2\pi} \left[ \frac{2}{\beta} \sum_{n=1}^{\infty} (-1)^{n+1} \frac{\cos(n\theta)}{n} e^{-n\beta\omega_{\pm}(r,p_3)} \right]. \quad (5.12)$$

The contribution of each Landau level  $r$  has the form

$$u(\pm, r) = - \frac{2}{\beta} \frac{qB}{2\pi} \sum_{n=1}^{\infty} (-1)^{n+1} \frac{\cos(n\theta)}{n} \times \int \frac{dp_3}{2\pi} \exp \left[ -n\beta \sqrt{2qB(r + \frac{1}{2} \pm \frac{1}{2}) + p_3^2 + m^2} \right] \quad (5.13)$$

which is rewritten using the representation [42]

$$K_1(n\beta\alpha) = \frac{1}{2\alpha} \int_{-\infty}^{\infty} dk e^{-n\beta\sqrt{k^2+\alpha^2}} \quad (5.14)$$

yielding

$$u(\pm, r) = - \frac{qB}{\pi^2\beta} \sqrt{2qB(r + \frac{1}{2} \pm \frac{1}{2}) + m^2} \times \sum_{n=1}^{\infty} (-1)^{n+1} \frac{\cos(n\theta)}{n} K_1 \left[ n\beta \sqrt{2qB(r + \frac{1}{2} \pm \frac{1}{2}) + m^2} \right]. \quad (5.15)$$

Note that  $u(+, r) = u(-, r + 1)$ , and the lowest Landau level contribution  $u(-, 0)$  stands alone.

Adding all of them we obtain the final strong field expansion

$$V_T = - \frac{qB}{\pi^2\beta} \sum_{n=1}^{\infty} (-1)^{n+1} \frac{\cos(n\theta)}{n} \left[ mK_1(n\beta m) + 2 \sum_{r=0}^{\infty} \sqrt{qB(2r+1) + m^2} K_1 \left( n\beta \sqrt{qB(2r+1) + m^2} \right) \right]. \quad (5.16)$$

The density of states factor  $qB/2\pi$  justifies regarding this expression as a strong field expansion: clearly, a number  $O(qB/mT)$  of terms must be taken for this series to approach the correct expression for zero field (4.39).

## 5.2 HIGH TEMPERATURE EXPANSION

Expanding the logarithm in (5.6) as a proper-time integral, the effective potential may be written

$$V = \sum_{r=0}^{\infty} \sum_{n,\pm} \frac{qB}{2\pi\beta} \int \frac{dp_3}{2\pi} \int_0^{\infty} \frac{ds}{s} e^{-s[(\omega_n \pm \frac{\theta}{\beta})^2 + 2qB(r + \frac{1}{2} \pm \frac{1}{2}) + p_3^2 + m^2]}. \quad (5.17)$$

Notice that  $(\omega_n + \frac{\theta}{\beta})^2 = (\omega_{-(n+1)} - \frac{\theta}{\beta})^2$ , and the sum over Matsubara frequencies runs over all  $n$ , so we can without prejudice choose either the plus or minus sign in the corresponding term and include an overall factor of 2, the dimension of the fundamental representation of the gauge group. The integral over 3-momentum may be done exactly,

$$V = \sum_{r=0}^{\infty} \sum_{n,\pm} \frac{qB\sqrt{\pi}}{2\pi^2\beta} \int_0^{\infty} \frac{ds}{s^{3/2}} e^{-s[(\omega_n - \frac{\theta}{\beta})^2 + 2qB(r + \frac{1}{2} \pm \frac{1}{2}) + m^2]}, \quad (5.18)$$

and, as was done in the steps between equations (2.47) and (2.51), we can effect the sum over Landau levels and polarization states,

$$\begin{aligned} \sum_{r=0}^{\infty} \sum_{\pm} e^{-s2qB(r + \frac{1}{2} \pm \frac{1}{2})} &= (1 + e^{-s2qB}) \sum_{r=0}^{\infty} e^{-r(s2qB)} \\ &= \frac{1 + e^{-s2qB}}{1 - e^{-s2qB}} = \coth(qBs), \end{aligned} \quad (5.19)$$

so

$$V = \sum_n \frac{qB\sqrt{\pi}}{2\pi^2\beta} \int_0^{\infty} \frac{ds}{s^{3/2}} \coth(qBs) e^{-s[(\omega_n - \frac{\theta}{\beta})^2 + m^2]}. \quad (5.20)$$

To extract the high temperature asymptotic behavior we employ a  $\vartheta_4$  resummation identity:

$$\sum_n \exp\left[-\frac{s}{\beta^2}((\theta - \pi) - 2\pi n)^2\right] = \frac{\beta}{\sqrt{4\pi s}} \sum_p \exp\left[-\frac{\beta^2 p^2}{4s} + ip(\theta - \pi)\right]. \quad (5.21)$$

Because  $e^{i\pi} = e^{-i\pi} = -1$ ,

$$V = \sum_p \frac{qB}{4\pi^2} \int_0^{\infty} \frac{ds}{s^2} \coth(qBs) e^{-sm^2 - \frac{\beta^2 p^2}{4s} + ip(\theta + \pi)} \quad (5.22)$$

The term with  $p = 0$  does not depend on temperature, so I will discard it for now; it will be treated shortly. The remaining sum is symmetric under  $p \leftrightarrow -p$ , so we can collect like terms and write

$$V_T = \frac{qB}{2\pi^2} \int_0^\infty \frac{ds}{s^2} e^{-sm^2} \coth(qBs) \sum_{p=1}^\infty e^{-\frac{\beta^2 p^2}{4s}} \cos(p(\theta + \pi)). \quad (5.23)$$

I now shift  $s \rightarrow s/qB$  in order to remove any dimensionful factors from the hyperbolic cotangent

$$V_T = \frac{(qB)^2}{2\pi^2} \int_0^\infty \frac{ds}{s^2} e^{-sm^2/qB} \coth(s) \sum_{p=1}^\infty e^{-\frac{\beta^2 p^2}{4s}} qB \cos(p(\theta + \pi)), \quad (5.24)$$

as the first two terms in the series expansion

$$\coth(s) = \sum_{k=0}^\infty \frac{2^{2k} B_{2k}}{(2k)!} s^{2k-1} = \frac{1}{s} + \frac{s}{3} + \sum_{k=2}^\infty \frac{2^{2k} B_{2k}}{(2k)!} s^{2k-1} \quad (5.25)$$

are especially important for determining the high temperature behavior. We define

$$f_0 = \frac{(qB)^2}{2\pi^2} \int_0^\infty \frac{ds}{s^2} e^{-sm^2/qB} \left[ \frac{1}{s} \right] \sum_{p=1}^\infty e^{-\frac{\beta^2 p^2}{4s}} qB \cos(p(\theta + \pi)) \quad (5.26)$$

$$f_1 = \frac{(qB)^2}{2\pi^2} \int_0^\infty \frac{ds}{s^2} e^{-sm^2/qB} \left[ \frac{s}{3} \right] \sum_{p=1}^\infty e^{-\frac{\beta^2 p^2}{4s}} qB \cos(p(\theta + \pi)) \quad (5.27)$$

$$f_{k \geq 2} = \frac{(qB)^2}{2\pi^2} \int_0^\infty \frac{ds}{s^2} e^{-sm^2/qB} \left[ \sum_{k=2}^\infty \frac{2^{2k} B_{2k}}{(2k)!} s^{2k-1} \right] \times \sum_{p=1}^\infty e^{-\frac{\beta^2 p^2}{4s}} qB \cos(p(\theta + \pi)) \quad (5.28)$$

So that

$$V_T = f_0 + f_1 + f_{k \geq 2}. \quad (5.29)$$

Now we use integral representations of the modified Bessel functions of the second kind [42]

$$K_\nu(z) = \frac{1}{2} \left( \frac{z}{2} \right)^\nu \int_0^\infty \frac{ds}{s^{\nu+1}} \exp \left[ -s - \frac{z^2}{4s} \right] \quad (5.30)$$

to rewrite

$$f_0 = \frac{4m^2}{\pi^2 \beta^2} \sum_{p=1}^{\infty} \frac{\cos(p(\theta + \pi))}{p^2} K_2(p\beta m) \quad (5.31)$$

$$f_1 = \frac{(qB)^2}{3\pi^2} \sum_{p=1}^{\infty} \cos(p(\theta + \pi)) K_0(p\beta m). \quad (5.32)$$

To do these sums we use the known identities (equation 8.526 in reference [42]):

$$\sum_{p=1}^{\infty} (-1)^p K_0(pz) \cos(p\theta) = \frac{1}{2} \left[ \log\left(\frac{z}{4\pi}\right) + \gamma \right] + \frac{\pi}{2} \sum_{\ell}' \left[ \frac{1}{\sqrt{z^2 + (\theta - (2\ell - 1)\pi)^2}} - \frac{1}{2\pi|\ell|} \right] \quad (5.33)$$

$$\begin{aligned} \sum_{p=1}^{\infty} \frac{(-1)^p}{p} K_1(pz) \cos(p\theta) &= -\frac{1}{4} z \left[ \log\left(\frac{z}{4\pi}\right) + \gamma - \frac{1}{2} \right] + \frac{1}{z} \left[ \frac{\theta^2}{4} - \frac{\pi^2}{12} \right] \\ &\quad - \frac{\pi}{2z} \sum_{\ell}' \left[ \sqrt{z^2 + (\theta - (2\ell - 1)\pi)^2} - |\theta - (2\ell - 1)\pi| - \frac{z^2}{4\pi|\ell|} \right] \end{aligned} \quad (5.34)$$

$$\begin{aligned} \sum_{p=1}^{\infty} \frac{(-1)^p}{p^2} K_2(pz) \cos(p\theta) &= -\frac{2}{z^2} \left[ \frac{7\pi^4}{720} - \frac{\pi^2 \theta^2}{24} + \frac{\theta^4}{48} \right] - \frac{1}{2} \left[ \frac{\theta^2}{4} - \frac{\pi^2}{12} \right] \\ &\quad + \frac{1}{16} z^2 \left[ \log\left(\frac{z}{4\pi}\right) + \gamma - \frac{3}{4} \right] \\ &\quad + \frac{\pi}{2z^2} \sum_{\ell}' \left\{ \frac{1}{3} [z^2 + (\theta - (2\ell - 1)\pi)^2]^{3/2} - \frac{1}{3} |\theta - (2\ell - 1)\pi|^3 \right. \\ &\quad \left. - \frac{1}{2} |\theta - (2\ell - 1)\pi| z^2 - \frac{z^4}{16\pi|\ell|} \right\} \end{aligned} \quad (5.35)$$

where  $\gamma$  is the Euler-Mascheroni constant. Here the notation  $\sum_{\ell}'$  indicates that the singular term  $1/|\ell|$  is omitted when  $\ell = 0$ . Then

$$\begin{aligned} f_0 &= -\frac{8}{\pi^2 \beta^4} \left[ \frac{7\pi^4}{720} - \frac{\pi^2 \theta^2}{24} + \frac{\theta^4}{48} \right] - \frac{2m^2}{\pi^2 \beta^2} \left[ \frac{\theta^2}{4} - \frac{\pi^2}{12} \right] \\ &\quad + \frac{m^4}{4\pi^2} \left[ \log\left(\frac{\beta m}{4\pi}\right) + \gamma - \frac{3}{4} \right] \\ &\quad + \frac{2}{\pi \beta^4} \sum_{\ell}' \left\{ \frac{1}{3} [\beta^2 m^2 + (\theta - (2\ell - 1)\pi)^2]^{3/2} - \frac{1}{3} |\theta - (2\ell - 1)\pi|^3 \right. \\ &\quad \left. - \frac{1}{2} |\theta - (2\ell - 1)\pi| \beta^2 m^2 - \frac{\beta^4 m^4}{16\pi|\ell|} \right\}, \end{aligned} \quad (5.36)$$

$$f_1 = \frac{(qB)^2}{3\pi^2} \left\{ \frac{1}{2} \left[ \log\left(\frac{\beta m}{4\pi}\right) + \gamma \right] + \frac{\pi}{2} \sum_{\ell}' \left[ \frac{1}{\sqrt{\beta^2 m^2 + (\theta - (2\ell - 1)\pi)^2}} - \frac{1}{2\pi|\ell|} \right] \right\}. \quad (5.37)$$



Now we turn to  $f_{k \geq 2}$ ,

$$f_{k \geq 2} = \frac{(qB)^2}{4\pi^2} \int_0^\infty \frac{ds}{s^2} e^{-sm^2/qB} \left[ \sum_{k=2}^\infty \frac{2^{2k} B_{2k}}{(2k)!} t^{2k-1} \right] \sum_{p \neq 0} \exp \left[ -\frac{p^2}{4s} \beta^2 qB + ip(\theta + \pi) \right], \quad (5.38)$$

where we undo the  $\vartheta_4$  transformation:

$$f_{k \geq 2} = -\frac{(qB)^{3/2}}{2\pi^{3/2}\beta} \sum_{k=2}^\infty \frac{2^{2k} B_{2k}}{(2k)!} \int_0^\infty ds s^{2k-5/2} e^{-sm^2/qB} \times \left\{ \frac{\beta\sqrt{qB}}{\sqrt{4\pi s}} - \sum_{\ell} \exp \left[ -s \frac{1}{\beta^2 qB} (\theta - (2\ell - 1)\pi)^2 \right] \right\}. \quad (5.39)$$

To evaluate the sum over Bernoulli numbers we use the generating function

$$\frac{s}{e^s - 1} = \sum_{k=0}^\infty \frac{1}{k!} B_k s^k = 1 - \frac{s}{2} + \frac{s^2}{12} + \sum_{k=2}^\infty \frac{B_{2k}}{(2k)!} s^{2k}. \quad (5.40)$$

With the above, the first term in  $f_{k \geq 2}$  gives a zero temperature contribution

$$\begin{aligned} f_{k \geq 2, (T=0)} &= -\frac{(qB)^2}{4\pi^2} \sum_{k=2}^\infty \frac{2^{2k} B_{2k}}{(2k)!} \int_0^\infty ds s^{2k-3} e^{-sm^2/qB} \\ &= -\frac{(qB)^2}{4\pi^2} \int_0^\infty \frac{ds}{s^3} e^{-sm^2/qB} \sum_{k=2}^\infty \frac{2^{2k} B_{2k}}{(2k)!} s^{2k} \\ &= -\frac{(qB)^2}{4\pi^2} \int_0^\infty \frac{ds}{s^3} e^{-sm^2/qB} \left[ \frac{2s}{e^{2s} - 1} - 1 + s - \frac{s^2}{3} \right] \\ &= -\frac{(qB)^2}{4\pi^2} \int_0^\infty \frac{ds}{s^2} e^{-sm^2/qB} \left[ \coth(s) - \frac{1}{s} - \frac{s}{3} \right] \end{aligned} \quad (5.41)$$

which of course can be recognized as the negative of the expression of Heisenberg and Euler (2.56) for two charged fermion fields in a magnetic field. Recall the  $p = 0$  contribution from equation (5.22)

$$V_{(T=0)} = \frac{(qB)^2}{4\pi^2} \int_0^\infty \frac{ds}{s^2} e^{-sm^2/qB} \coth(s), \quad (5.42)$$

which is now canceled exactly by the first term in the last line of equation (5.41). We are left with the second and third terms, which we have already computed,

$$\begin{aligned} V_{(T=0)} &= \frac{(qB)^2}{4\pi^2} \int_{1/\Lambda^2}^{\infty} \frac{ds}{s^3} e^{-sm^2/qB} \left[ 1 + \frac{s^2}{3} \right] \\ &= \frac{(qB)^2}{12\pi^2} \Gamma\left(0, \frac{m^2}{\Lambda^2}\right) + \frac{1}{8\pi^2} \left[ e^{-\frac{m^2}{\Lambda^2}} \Lambda^2 (\Lambda^2 - m^2) - m^4 \text{Ei}\left(-\frac{m^2}{\Lambda^2}\right) \right], \end{aligned} \quad (5.43)$$

where  $\Lambda$  is an energy scale determining the proper time cutoff. As before, the second term on the last line represents charge renormalization [4]. However, note that, unlike the case discussed in section 2.4, here we may be interested on the question of dynamically generated masses, and so the divergence associated with the  $1/s^3$  subtraction does not cancel out a corresponding term in the normalization of the path integral.

The remaining finite temperature part of  $f_{k \geq 2}$  reads

$$f_{k \geq 2} = \frac{(qB)^{3/2}}{2\pi^{3/2}\beta} \sum_{k=2}^{\infty} \frac{2^{2k} B_{2k}}{(2k)!} \int_0^{\infty} ds s^{2k-5/2} \sum_{\ell} \left[ -s \left( \frac{m^2}{qB} + \frac{(\theta - (2\ell - 1)\pi)^2}{\beta^2 qB} \right) \right] \quad (5.44)$$

$$= \frac{(qB)^{3/2}}{2\pi^{3/2}\beta} \sum_{k=2}^{\infty} \frac{2^{2k} B_{2k}}{(2k)!} \Gamma\left(2k - \frac{3}{2}\right) \sum_{\ell} \left( \frac{qB\beta^2}{m^2\beta^2 + (\theta - (2\ell - 1)\pi)^2} \right)^{2k-3/2}. \quad (5.45)$$

With all the necessary pieces computed, we can finally write the full expression for the high temperature expansion of the effective potential as

$$\begin{aligned}
V = & \frac{(qB)^2}{12\pi^2} \Gamma\left(0, \frac{m^2}{\Lambda^2}\right) + \frac{1}{8\pi^2} \left[ e^{-\frac{m^2}{\Lambda^2}} \Lambda^2 (\Lambda^2 - m^2) - m^4 \text{Ei}\left(-\frac{m^2}{\Lambda^2}\right) \right] \\
& - \frac{8}{\pi^2 \beta^4} \left[ \frac{7\pi^4}{720} - \frac{\pi^2 \theta^2}{24} + \frac{\theta^4}{48} \right] - \frac{2m^2}{\pi^2 \beta^2} \left[ \frac{\theta^2}{4} - \frac{\pi^2}{12} \right] \\
& + \frac{m^4}{4\pi^2} \left[ \log\left(\frac{\beta m}{4\pi}\right) + \gamma - \frac{3}{4} \right] + \frac{(qB)^2}{6\pi^2} \left[ \log\left(\frac{\beta m}{4\pi}\right) + \gamma \right] \\
& + \frac{(qB)^2}{6\pi} \sum_{\ell}' \left[ \frac{1}{\sqrt{\beta^2 m^2 + (\theta - (2\ell - 1)\pi)^2}} - \frac{1}{2\pi|\ell|} \right] \\
& + \frac{2}{\pi \beta^4} \sum_{\ell}' \left\{ \frac{1}{3} [\beta^2 m^2 + (\theta - (2\ell - 1)\pi)^2]^{3/2} - \frac{1}{3} |\theta - (2\ell - 1)\pi|^3 \right. \\
& \quad \left. - \frac{1}{2} |\theta - (2\ell - 1)\pi| \beta^2 m^2 - \frac{\beta^4 m^4}{16\pi|\ell|} \right\} \\
& + \frac{(qB)^{3/2}}{2\pi^{3/2} \beta} \sum_{k=2}^{\infty} \frac{2^{2k} B_{2k}}{(2k)!} \Gamma\left(2k - \frac{3}{2}\right) \sum_{\ell} \left( \frac{qB \beta^2}{m^2 \beta^2 + (\theta - (2\ell - 1)\pi)^2} \right)^{2k-3/2}.
\end{aligned} \tag{5.46}$$

### 5.3 LOW TEMPERATURE EXPANSION

One of the weaknesses of the high temperature expansion derived above is that it is based on a Taylor series expansion of the hyperbolic cotangent, which has a finite radius of convergence. For modestly strong magnetic fields ( $qB > \pi m^2$ ), a substantial portion of the integration volume lies outside the region of convergence and the expansion is likely to be unreliable. The final expression still exhibits the correct asymptotic behavior, even though it is divergent, but utilizing it properly in a real application requires great care. It is worth asking whether an expansion with better convergence properties can be obtained.

Our procedure is to rewrite the hyperbolic cotangent as

$$\coth s = e^{-2s} (\coth s + 1) + 1, \tag{5.47}$$

and expand the inner cotangent in a Taylor series,

$$\coth s = e^{-2s} \left( \frac{1}{s} + \frac{s}{3} + 1 + \dots \right) + 1. \quad (5.48)$$

This expansion still has a finite radius of convergence, but unlike the simple Taylor expansion (5.25), it has the correct leading order asymptotic behavior as  $s \rightarrow \infty$  built in. When truncated after just the first two terms, the relative error of the approximation is less than 0.3%. This approximation can be further improved by iterating,

$$\coth s = e^{-4s} (\coth s + 1) + 2e^{-2s} + 1, \quad (5.49)$$

or more generally

$$\coth s = 1 + \sum_{n=1}^N 2e^{-2ns} + e^{-2(N+1)s} (\coth s + 1). \quad (5.50)$$

If the iteration is carried out infinitely many times, this becomes a well-known asymptotic expansion of the hyperbolic cotangent.

I now use this expansion to develop an approximate expression for the thermal one-loop effective action in a magnetic field. The calculation is carried out in the simplest case  $N = 0$ ; the generalization for larger  $N$ , should one be desired, is entirely straightforward. The starting point is equation (5.23), which after a shift  $s \rightarrow s/qB$  becomes

$$V_T = \frac{(qB)^2}{2\pi^2} \int_0^\infty \frac{ds}{s^2} e^{-sm^2/qB} \coth s \sum_{p=1}^\infty e^{-\frac{\beta^2 p^2}{4s} qB} (-1)^p \cos(p\theta). \quad (5.51)$$

We replace the hyperbolic cotangent by our approximation, obtaining

$$V_T = \frac{(qB)^2}{2\pi^2} \int_0^\infty \frac{ds}{s^2} e^{-sm^2/qB} \left[ e^{-2s} \left( \frac{1}{s} + \frac{s}{3} + 1 \right) + 1 \right] \sum_{p=1}^\infty e^{-\frac{\beta^2 p^2}{4s} qB} (-1)^p \cos(p\theta). \quad (5.52)$$

There are now four integrals, which can be written after appropriate substitutions as

$$\begin{aligned}
V_T = & \frac{(m^2 + 2qB)^2}{2\pi^2} \sum_{p=1}^{\infty} (-1)^p \int_0^{\infty} \frac{ds}{s^3} e^{-s - \frac{\beta^2 p^2}{4s}(m^2 + 2qB)} \cos(p\theta) \\
& + \frac{qB(m^2 + 2qB)}{2\pi^2} \sum_{p=1}^{\infty} (-1)^p \int_0^{\infty} \frac{ds}{s^2} e^{-s - \frac{\beta^2 p^2}{4s}(m^2 + 2qB)} \cos(p\theta) \\
& + \frac{qBm^2}{2\pi^2} \sum_{p=1}^{\infty} (-1)^p \int_0^{\infty} \frac{ds}{s^2} e^{-s - \frac{\beta^2 p^2}{4s}m^2} \cos(p\theta) \\
& + \frac{(qB)^2}{6\pi^2} \sum_{p=1}^{\infty} (-1)^p \int_0^{\infty} \frac{ds}{s} e^{-s - \frac{\beta^2 p^2}{4s}(m^2 + 2qB)} \cos(p\theta).
\end{aligned} \tag{5.53}$$

Each of these is easily done with the integral representations of modified Bessel functions, (5.30).

$$\begin{aligned}
V_T = & \frac{4(m^2 + 2qB)}{\pi^2 \beta^2} \sum_{p=1}^{\infty} \frac{(-1)^p}{p^2} K_2(p\beta\sqrt{m^2 + 2qB}) \cos(p\theta) \\
& + \frac{2qB\sqrt{m^2 + 2qB}}{\pi^2 \beta} \sum_{p=1}^{\infty} \frac{(-1)^p}{p} K_1(p\beta\sqrt{m^2 + 2qB}) \cos(p\theta) \\
& + \frac{2qBm}{\pi^2 \beta} \sum_{p=1}^{\infty} \frac{(-1)^p}{p} K_1(p\beta m) \cos(p\theta) \\
& + \frac{(qB)^2}{3\pi^2} \sum_{p=1}^{\infty} (-1)^p K_0(p\beta\sqrt{m^2 + 2qB}) \cos(p\theta).
\end{aligned} \tag{5.54}$$

This expression has one clear advantage: the first line, in the limit when  $qB \rightarrow 0$ , reduces to the correct low temperature expansion of the free energy of a three-dimensional gas of relativistic fermions, equation (4.39). The third line, for  $qB \gg \beta m$ , reduces to the free energy of a Fermi gas in one spatial dimension. It is much more difficult to obtain both limits simultaneously in either of the previous expansions.

### 5.3.1 Alternate high temperature expansion

Using the same identities (5.33), (5.34), and (5.35), these sums can be performed. We define

$$g_2 = \frac{4(m^2 + 2qB)}{\pi^2 \beta^2} \sum_{p=1}^{\infty} \frac{(-1)^p}{p^2} K_2(p\beta\sqrt{m^2 + 2qB}) \cos(p\theta), \quad (5.55)$$

$$g_{1a} = \frac{2qBm}{\pi^2 \beta} \sum_{p=1}^{\infty} \frac{(-1)^p}{p} K_1(p\beta m) \cos(p\theta), \quad (5.56)$$

$$g_{1b} = \frac{2qB\sqrt{m^2 + 2qB}}{\pi^2 \beta} \sum_{p=1}^{\infty} \frac{(-1)^p}{p} K_1(p\beta\sqrt{m^2 + 2qB}) \cos(p\theta), \quad (5.57)$$

$$g_0 = \frac{(qB)^2}{3\pi^2} \sum_{p=1}^{\infty} (-1)^p K_0(p\beta\sqrt{m^2 + 2qB}) \cos(p\theta), \quad (5.58)$$

such that

$$V_T = g_0 + g_{1a} + g_{1b} + g_2. \quad (5.59)$$

In what follows I shorten  $m_B \equiv \sqrt{m^2 + 2qB}$ . We obtain immediately

$$g_0 = \frac{(qB)^2}{6\pi^2} \left[ \log\left(\frac{\beta m_B}{4\pi}\right) + \gamma \right] + \frac{(qB)^2}{6\pi} \sum_{\ell}' \left[ \frac{1}{\sqrt{\beta^2 m_B^2 + (\theta - (2\ell - 1)\pi)^2}} - \frac{1}{2\pi|\ell|} \right]. \quad (5.60)$$

The terms  $g_{1a}$  and  $g_{1b}$  have the exact same functional dependence on the “mass” parameter, but  $g_{1a}$  is slightly simpler:

$$g_{1a} = -\frac{qBm^2}{2\pi^2} \left[ \log\left(\frac{\beta m}{4\pi}\right) + \gamma - \frac{1}{2} \right] + \frac{2qB}{\pi^2 \beta^2} \left[ \frac{\theta^2}{4} - \frac{\pi^2}{12} \right] - \frac{qB}{\pi \beta^2} \sum_{\ell}' \left[ \sqrt{(\beta m)^2 + (\theta - (2\ell - 1)\pi)^2} - |\theta - (2\ell - 1)\pi| - \frac{\beta^2 m^2}{4\pi|\ell|} \right], \quad (5.61)$$

and  $g_{1b}$  can be obtained with the replacement  $m \rightarrow m_B$ . The remaining term dominates the high-temperature behavior,

$$\begin{aligned}
g_2 = & -\frac{8}{\pi^2 \beta^4} \left[ \frac{7\pi^4}{720} - \frac{\pi^2 \theta^2}{24} + \frac{\theta^4}{48} \right] - \frac{2m_B^2}{\pi^2 \beta^2} \left[ \frac{\theta^2}{4} - \frac{\pi^2}{12} \right] \\
& + \frac{m_B^4}{4\pi^2} \left[ \log\left(\frac{\beta m_B}{4\pi}\right) + \gamma - \frac{3}{4} \right] \\
& + \frac{2}{\pi \beta^4} \sum_{\ell}' \left\{ \frac{1}{3} [\beta^2 m_B^2 + (\theta - (2\ell - 1)\pi)^2]^{3/2} - \frac{1}{3} |\theta - (2\ell - 1)\pi|^3 \right. \\
& \quad \left. - \frac{1}{2} |\theta - (2\ell - 1)\pi| \beta^2 m_B^2 - \frac{\beta^4 m_B^4}{16\pi |\ell|} \right\}.
\end{aligned} \tag{5.62}$$

### 5.3.2 Discussion

It is instructive to compare these expressions with the previous high temperature expansion, equations (5.36) and (5.37). Clearly,  $g_2$  is just  $f_0^4$  with the replacement  $m \rightarrow m_B$ , and the two expressions obviously agree as  $qB \rightarrow 0$ . This indicates that the leading thermal effect due to an intense magnetic field is to suppress the dynamics of the particle. This makes good physical sense: as the magnetic field is increased, a larger portion of the spectral weight is concentrated in the lowest Landau levels, and the system becomes effectively 1+1-dimensional. This high-temperature expansion implements this effective loss of degrees of freedom by increasing the effective particle mass. Similar remarks apply to  $g_0$ , which corresponds to  $f_1$ .

The  $g_1$  terms seem reminiscent of the strong field expansion derived in section 5.1.1, equation (5.16). In particular,  $g_{1a}$  is recognized as the contribution from the lowest Landau level, and in this expansion it is the only one that does not become suppressed with increasing magnetic field. This term has the exact form of the one-loop effective potential for a spinor particle moving in 1+1 dimensions [68].

---

<sup>4</sup>Note that the magnetic field does not appear anywhere in  $f_0$ : it is, in fact, the one-loop effective potential of a Fermi gas at high temperature, in the background of a nontrivial Polyakov loop [68].

It is remarkable that this representation of the effective action encodes both weak and strong field effects in a natural way. It smoothly interpolates between a strong field regime, in which the dynamics are dimensionally reduced, dominated by the lowest Landau level, and a weak field, high-temperature regime, in which the magnetic field is a small correction to a free, 3+1-dimensional gas.

#### 5.4 EXAMPLE APPLICATION: MAGNETIC CATALYSIS

It is interesting to consider how the presence of an external field may affect deconfinement and the breaking of chiral symmetry, which could be said to be the two most striking features of QCD [2]. The Banks-Casher relation [75]

$$\int d^4x \langle \bar{\psi}\psi \rangle = \lim_{m \rightarrow 0} \left\langle \int d\mu \rho(\mu) \frac{m}{\mu^2 + m^2} \right\rangle, \quad (5.63)$$

where  $\rho(\mu)$  is the fermionic spectral density function, implies that the value of the chiral condensate  $\langle \bar{\psi}\psi \rangle$  is chiefly controlled by the spectral density at small energies. As seen in chapter 1, the presence of a magnetic field results in a discrete spectrum of highly degenerate Landau levels. The lowest-lying Landau level for massless fermions has zero energy (see equation (2.46)), so it can be expected that a magnetic field has the effect of enhancing the chiral condensate, a phenomenon known as *magnetic catalysis*. This is indeed observed in lattice simulations at zero temperature. However, the situation at finite temperature is substantially less clear, and lattice evidence points to the opposite effect: for a range of temperatures, the value of the chiral condensate *decreases* as the applied magnetic field is increased, which has been termed *inverse magnetic catalysis*. The causes and detailed workings of this phenomenon are at present poorly understood, though various possible explanations have been advanced in the literature [80–84]. The reader interested in magnetic catalysis may consult Shovkovy’s review [17].



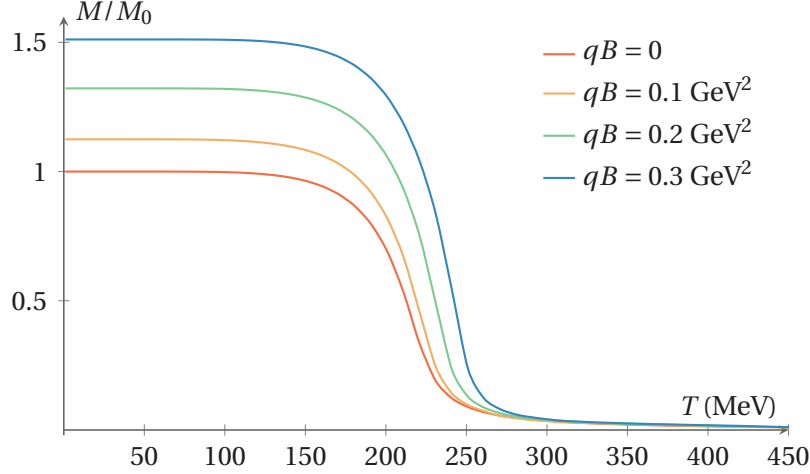


Figure 5.1: Constituent quark mass  $M$  for the PNJL model, as a function of temperature, for several values of the magnetic field  $B$ .

An explanation of inverse magnetic catalysis is beyond the scope of this work. I will show instead an example of how the expansions derived above can be used in a typical physical application. One common approach for investigating the deconfinement transition and the breaking of chiral symmetry at finite temperatures and densities is the so-called *Polyakov–Nambu–Jona-Lasinio model*. In such models, one constructs an effective potential for the Polyakov loop  $P$  as well as the chiral condensate  $\langle \bar{\psi}\psi \rangle$ . This is accomplished by adding to the perturbative expression for the free energy a nonrenormalizable interaction potential of the type

$$V_F = \frac{g_S}{2} [(\bar{\psi}\lambda^a\psi)^2 + (\bar{\psi}i\gamma_5\lambda^a\psi)^2] + g_D [\det \bar{\psi}(1 - \gamma_5)\psi + h.c.]. \quad (5.64)$$

Here  $\lambda^a$  are the generators of the flavor symmetry group,  $g_S$  is the four-fermion coupling constant, and  $g_D$  encodes the strength of an anomaly-induced term. It is possible to show that this interaction can be written in the form [85–88]

$$V_F = \sum_j g_S \sigma_j^2 + 2g_D(N_f - 1) \prod_j \sigma_j \quad (5.65)$$

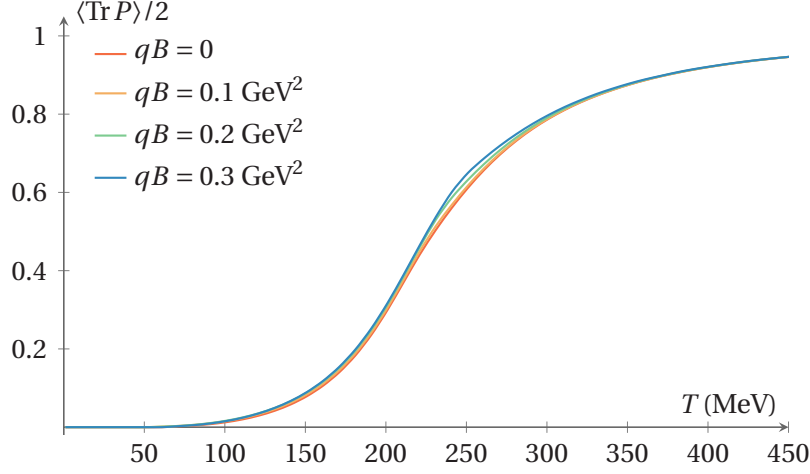


Figure 5.2: The expectation value of the trace of the Polyakov loop  $\text{Tr} P$  in the fundamental representation, as a function of temperature, for several values of the magnetic field  $B$ .

where  $\sigma_j = \langle \bar{\psi}_j \psi_j \rangle$  is the chiral condensate corresponding to the  $j$ -th fermion flavor, whose mass is given by

$$M_j = m_{0j} - 2g_S \sigma_j - 2g_D \prod_{k \neq j} \sigma_k. \quad (5.66)$$

It is convenient to take  $g_D = 0$ , and to take the masses  $m_{0j}$  to be equal to a common mass  $m_0$ .

Thus the common constituent mass is written  $M = m_0 - 2g_S \sigma$ , and the potential term is

$$V_F = \frac{N_f}{4g_S} (M - m_0)^2. \quad (5.67)$$

The model also requires an effective potential for the Polyakov loop. I will use model B of reference [72], introduced here in section 4.3. I take the concrete form

$$V_g = -\frac{\pi^2}{15\beta^4} + \frac{4}{3\pi^2\beta^4} \theta^2 (\theta - \pi)^2 - \frac{1}{(4R)^3 \beta} \log\left(\frac{2}{\pi} \sin^2 \theta\right), \quad (5.68)$$

where the parameter  $R = 1.315$  fm is chosen to fix the correct deconfinement temperature  $T_d = 270$  MeV in the pure gauge theory. The proper-time cutoff scale  $\Lambda$  and the coupling  $g_S$  are free parameters of the model. Since the model is not renormalizable, the physics will depend sensitively on  $\Lambda$ . These parameters are typically fixed, at zero magnetic field, by demanding that the model give correct values for the chiral condensate as well as the pion decay constant  $f_\pi$ . I

do not perform a realistic fit of this simple  $SU(2)$  model, but merely choose parameters which lead to plausible behavior. Setting  $\Lambda = 880$  MeV and  $g_S = 16.48$  GeV<sup>2</sup>, with a current quark mass  $m_0 = 5$  MeV, the zero-temperature constituent mass  $M_0 = 250$  MeV. With massless quarks, the same parameters lead to the restoration of chiral symmetry at a temperature  $T = 200$  MeV. Results from the model are given in figures 5.1 and 5.2.

The constituent masses generated in this model are in broad agreement with similar NJL-type studies [89–91]. The Polyakov loop, however, behaves differently: in these previous studies, the temperature of the deconfinement transition is found to increase in response to the applied magnetic field. Here, the trace of the Polyakov loop is largely insensitive to the magnetic background, which seems to have a weak deconfining effect. Lattice results show that a magnetic field does decrease the deconfinement temperature, but the effect is larger than that seen here.

## CHAPTER 6

### ELECTRIC FIELDS AT FINITE TEMPERATURE

*Some of the material in this chapter has been previously published [59]. This work was done in collaboration with and under the supervision of Dr. Michael Ogilvie.*

Pair production in an external field is a form of semiclassical tunneling with applications in many areas of physics [12, 92, 93, 7, 94, 95]. Here I present a complete first-principles calculation of the one-loop thermal correction to the pair production rate of charged scalars in a static electric field. The effect of pair production in a background electric field at zero temperature was derived first by Euler and Heisenberg [16] and subsequently rederived by Schwinger [4] using modern field-theoretic techniques. The physics of the pair production is simple: when the energy contained in an external electric field is large enough, it becomes energetically favorable to produce charged pairs which screen the external field. From a modern perspective, the presence of an external electric field over a large spatial region creates a metastable state, which decays by the nucleation of charged-particle pairs. In this way, it is similar to the false vacuum decay [96–98]. This similarity is most clearly seen in the worldline formalism, as shown in the calculation of the zero-temperature pair production rate by Affleck et al. [47]. The inclusion of thermal effects naturally increases the rate at which the metastable state decays [99].

Schwinger's expression for the decay rate is obtained from the imaginary part of the one-loop effective action of charged particles in a constant external electric field. For charged scalars, the one-loop decay rate at zero-temperature is

$$\Gamma = \frac{(eE)^2}{(2\pi)^3} \sum_{p=1}^{\infty} \frac{(-1)^{p+1}}{p^2} \exp\left[-\frac{m^2}{eE}\pi p\right] \quad (6.1)$$

with a similar result for fermions. The factor of  $1/e$  in the exponent signals that this is a nonperturbative result. These results have been extended in a number of ways [100–102, 26, 103, 54, 64, 104]. One obvious extension is to finite temperature and density. In the case of external *magnetic* fields, the properties of the thermal one-loop effective action are well-known [105, 106]. However, in the case of electric fields, there has been no clear consensus on the form or even the existence of one-loop thermal corrections to the zero-temperature decay rate [107, 18, 108–110, 34, 111]. Although the formal expression for the decay rate can be readily constructed using, say, Schwinger's proper time formulation, the analytic structure of the resulting formulae is quite intricate and leads to structural ambiguities [34]. It has been suggested that the one-loop thermal contribution to the decay rate may be zero, but there is no obvious symmetry principle that would lead to this conclusion. The worldline formalism has proven to be a very powerful tool in quantum field theory at zero temperature, capable of reproducing and extending Schwinger's result [47, 54, 64] as well as providing a compact, powerful framework for the calculation of gauge theory amplitudes [50, 51]. It will be shown that the worldline formalism can be used to calculate thermal corrections to Schwinger's one-loop result. To the best of my knowledge, this is the first time the worldline formalism has been used to calculate a nonperturbative finite-temperature effect in a four-dimensional gauge theory. Worldline methods have previously been used in a nonperturbative analysis of the phase diagram of the two-dimensional Gross-Neveu model [112].

I restrict the initial presentation to the simplest case of charged scalars in QED, and will return to the case of fermions in QED and QCD in chapter 7. The case of QCD is relevant, for instance, in phenomenological flux-tube models of quark-antiquark pair production during hadronization in heavy ion collisions [7, 8, 113].

## 6.1 THE WORLDLINE FORMALISM AT FINITE TEMPERATURE

For simplicity, initially we consider a theory with a charged scalar in a constant Minkowski-space electric field. The Lagrangian is given by

$$\mathcal{L} = (D_\mu \phi)^* (D_\mu \phi) + m^2 \phi^* \phi \quad (6.2)$$

with a covariant derivative  $D_\mu \equiv \partial_\mu + ieA_\mu$  where  $A_\mu$  provides the constant background electric field in Euclidean space. As in the zero temperature derivation, the effective action may be placed in the form [54],

$$S_{eff}^{(1)} = 2 \oint [dx] K_0 \left( m \sqrt{\int_0^1 du \dot{x}^2} \right) \exp \left[ -ie \int_0^1 du A \cdot \dot{x} \right], \quad (6.3)$$

where the path integral is taken over closed worldline paths. In the worldline formalism, nonzero temperature may be introduced via the replacement [114, 115]

$$\langle x | e^{-s(-D^2)} | x \rangle \rightarrow \sum_{n \in \mathbb{Z}} \langle x | e^{-s(-D^2)} | x + n\beta \hat{e}_4 \rangle \quad (6.4)$$

in the functional determinant, which corresponds to the boundary condition  $x_\mu(0) = x_\mu(1) + \delta_{\mu 4} n\beta$ .

The effective action is simplified by replacing the modified Bessel function with its asymptotic form for large argument,

$$S_{eff}^{(1)} \sim \sqrt{\frac{2\pi}{m}} \oint [dx] \left( \int_0^1 du \dot{x}^2 \right)^{-1/4} \exp \left[ - \left( m \sqrt{\int_0^1 du \dot{x}^2} + ie \int_0^1 du A \cdot \dot{x} \right) \right]. \quad (6.5)$$

This is equivalent to performing a saddle point approximation on the integral over  $s$ , with the saddle point given by

$$s_0^2 = \frac{m^2}{4} \int_0^1 du \dot{x}^2. \quad (6.6)$$

This is a good approximation if  $s_0 \gg 1$ , which at zero temperature corresponds to a weak field condition [54]. We may now evaluate the functional integral in steepest descents, thus reducing the problem to finding instanton solutions to the worldline action

$$S_{eff} = m \sqrt{\int_0^1 du \dot{x}^2} + ie \int_0^1 du A(x(u)) \cdot \dot{x}, \quad (6.7)$$

which, as before entails solving the following equations of motion:

$$\frac{1}{\sqrt{\int_0^1 du \dot{x}^2}} m \dot{x}_\mu = ie F_{\mu\nu} \dot{x}_\nu, \quad (6.8)$$

but now with the finite-temperature boundary conditions. Notice that the quantity in the square root is still a constant of the motion, as can be verified by contracting the above with  $\dot{x}_\mu$ .

We impose a constant (Minkowski-space) electric field by taking  $A_3 = -iEx_4$  with the other three components either zero or constant. Then the only non-zero components of  $F$  are  $F_{34} = -F_{43} = +iE$ . The general solution of the equations of motion (3.16) for  $x_\mu(u)$  is a circular orbit of radius  $R = m/eE$  centered about  $(\bar{x}_3, \bar{x}_4)$

$$x_3 = \frac{m}{eE} \cos\left(\frac{eaE}{m} u + \varphi\right) + \bar{x}_3 \quad (6.9)$$

$$x_4 = \frac{m}{eE} \sin\left(\frac{eaE}{m} u + \varphi\right) + \bar{x}_4 \quad (6.10)$$

where the parameter  $a = \sqrt{\int_0^1 du \dot{x}^2}$  is determined from the boundary conditions on the finite-temperature worldline path integral. Finite temperature worldline instantons are sections of the  $T = 0$  circle solutions whose endpoints are separated by  $n\beta$  in the time direction. In order

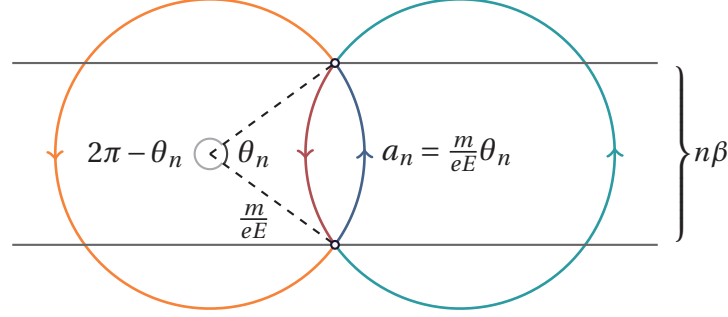


Figure 6.1: The four basic finite-temperature classical paths in the  $x_3 - x_4$  plane with a winding of  $\pm n$  in the timelike direction, shown as portions of zero-temperature circular paths. All four paths begin and end on the same two points, which are separated by  $n\beta$  in Euclidean time. From left to right, the paths are an antiparticle long path, an antiparticle short path, a particle short path and a particle long path. The radius  $R$  is  $m/eE$  and the length of the short arcs  $a_n$  is  $R\theta_n$ .

for such solutions to exist at all, the diameter of the  $T = 0$  solution must be greater than  $n\beta$ ,

$$2R = \frac{2m}{eE} > n\beta. \quad (6.11)$$

In other words, the maximum value of  $n$ ,  $n_{max}$  is given by

$$n_{max} = \left\lfloor \frac{2mT}{eE} \right\rfloor. \quad (6.12)$$

This implies that there are no one-loop thermal effects from worldline instantons for  $T < eE/2m$ , i.e., at sufficiently low temperatures [111].

For any value of  $n\beta$  for which solutions exist, there is a short path of central angle less than  $\pi$  corresponding to a particle trajectory and another corresponding to an antiparticle trajectory; both trajectories contribute to the free energy of the metastable phase. There are also two long paths of central angle greater than  $\pi$  which contribute to the decay rate. All four paths are shown in Fig. 6.1. From the geometry we see that the arc length of a short path  $R\theta_n$  is determined by  $R \sin(\theta_n/2) = n\beta/2$ . The arc length of a corresponding long path is  $R(2\pi - \theta_n)$ . Appending a short path of arc length  $R\theta_n$  to a corresponding long path of arc length  $R(2\pi - \theta_n)$  gives the  $T = 0$  circular solution found in Ref. [47].



Such solutions can be extended by adding on  $p$  windings. The actions of these solutions are given by

$$S_{np}^{(s)} = \frac{m^2}{2eE} [(\theta_n + 2\pi p) + \sin\theta_n] \quad (6.13)$$

$$S_{np}^{(l)} = \frac{m^2}{2eE} [(2\pi - \theta_n + 2\pi p) - \sin\theta_n], \quad (6.14)$$

where the superscripts ( $s$ ) and ( $l$ ) stand for *short* and *long* solutions, respectively. Note that

$$S_{np}^{(s)} = S_{n0}^{(s)} + S_{0p} \quad (6.15)$$

$$S_{np}^{(l)} = S_{n0}^{(l)} + S_{0p} \quad (6.16)$$

and that the two solutions become degenerate when  $\theta_n = \pi$ .

### 6.1.1 Fluctuation prefactors

The prefactors  $K_{np}^{(s)}$  and  $K_{np}^{(l)}$  are given in terms of the functional determinant of the second variation operator, which is the sum of a local and a nonlocal term [47]. For a solution centered at  $\bar{x}$ , we have

$$M_{\mu\nu} \equiv \left. \frac{\delta S_{eff}}{\delta x_\nu \delta x_\mu} \right|_{x_{cl}} = L_{\mu\nu} - \vartheta \frac{eE}{R^2} (x_\mu(u) - \bar{x}_\mu)(x_\nu(u') - \bar{x}_\nu) \quad (6.17)$$

where

$$L_{\mu\nu} = \left[ -\frac{eE}{\vartheta} \delta_{\mu\nu} \frac{d^2}{du^2} + ieF_{\mu\nu} \frac{d}{du} \right] \delta(u - u') \quad (6.18)$$

and  $\vartheta$  is the total angle spanned by the instanton solution, that is,  $\vartheta = 2\pi p + \theta_n$  for short paths and  $\vartheta = 2\pi(p + 1) - \theta_n$  for long paths. For fluctuations about zero temperature solutions, the eigenvalue problem for  $M_{\mu\nu}$  can be solved by inspection. For fluctuations about finite temperature solutions this is made difficult by the boundary conditions at the endpoints. Fortunately, the functional determinant may be computed without any explicit knowledge of the spectrum. The matrix determinant lemma [116] can be used to isolate the effect of the

nonlocal term,

$$\det'[M_{\mu\nu}] = \det'[L_{\mu\nu}] \left[ 1 - \vartheta \frac{eE}{R^2} \iint du du' (x(u) - \bar{x})_\mu (L^{-1})_{\mu\nu} (x(u') - \bar{x})_\nu \right] \quad (6.19)$$

and the local part of the functional determinant is computed using the method of Gel'fand and Yaglom [117, 118]. Consider the following set of initial value problems ( $\rho = 1, 2, 3, 4$ ):

$$L_{\mu\nu} \eta_\nu^{(\rho)} = 0 \quad (6.20)$$

$$\eta_\nu^{(\rho)}(0) = 0 \quad (6.21)$$

$$\dot{\eta}_\nu^{(\rho)}(0) = \delta_{\nu\rho}. \quad (6.22)$$

Up to a phase, the local prefactor can be written

$$(N \det'[L_{\mu\nu}])^{-1/2} = \frac{(eE)^2}{(2\pi\vartheta)^2} \sqrt{\frac{\det[\tilde{\eta}_\mu^{(\nu)}(1)]}{\det[\eta_\mu^{(\nu)}(1)]}} \quad (6.23)$$

where  $N$  is a normalization factor and  $\tilde{\eta}_\mu^{(\nu)}$  are the solutions of the corresponding *free* initial value problem, with  $\tilde{L}_{\mu\nu} = -\frac{eE}{\vartheta} \frac{d^2}{du^2} \delta_{\mu\nu}$ . It is then straightforward to show

$$(N \det'[L_{\mu\nu}])^{-1/2} = (-1)^p \frac{(eE)^2}{(2\pi\vartheta)^2} \sqrt{\frac{\vartheta^2}{2(1 - \cos \vartheta)}}. \quad (6.24)$$

As we will see in section 6.2.1, the overall phase  $e^{i2\pi p/2} = (-1)^p$  is related to the Morse index of the classical path. Note that this quantity is manifestly real, which means any imaginary contribution must come from the nonlocal part.

To compute the nonlocal part we find the Green's function directly, by solving the equation

$$L_{\mu\rho} G_{\rho\nu}(u - u') = \delta_{\mu\nu} \delta(u - u') \quad (6.25)$$

with Dirichlet boundary conditions. A lengthy but straightforward calculation gives, for the nontrivial components  $G_{33} = G_{44}$  and  $G_{43} = -G_{34}$ ,

$$G_{33} = \frac{1}{2eE} \left[ -\sin(\vartheta|u - u'|) + \sin(\vartheta u') + \sin(\vartheta u) - \frac{4 \sin(\vartheta u/2) \sin(\vartheta u'/2) \cos(\vartheta(u - u')/2)}{\tan(\vartheta/2)} \right] \quad (6.26)$$

$$G_{43} = \frac{1}{2eE} \left[ \text{sgn}(u - u')(\cos(\vartheta|u - u'|) - 1) + \cos(\vartheta u') - \cos(\vartheta u) - \frac{\sin(\vartheta(u - u')) + \sin(\vartheta u') - \sin(\vartheta u)}{\tan(\vartheta/2)} \right]. \quad (6.27)$$

The nonlocal part of the determinant can now be computed directly:

$$\left[ 1 - \vartheta \frac{eE}{R^2} \iint du du' x_\mu(u) G_{\mu\nu}(u - u') x_\nu(u') \right] = \frac{\vartheta}{2} \cot\left(\frac{\vartheta}{2}\right). \quad (6.28)$$

Note that for long paths  $\pi < \vartheta < 2\pi$  (modulo  $2\pi$ ), so the nonlocal part of the determinant is negative. Because of this, it is clear that it is the long paths that contribute to the imaginary part of the effective action.

The prefactor can now be assembled as before

$$\begin{aligned} & \left( \int d^4x \right) \frac{\sqrt{2\pi/m}}{\left[ \int_0^1 du \dot{x}^2 \right]^{1/4}} \left( \det' \left[ \frac{\delta S_{\text{eff}}}{\delta x_\mu \delta x_\nu} \Big|_{x_{cl}} \right] \right)^{-1/2} \\ & = V_3 \beta \frac{(eE)^2}{(2\pi)^{3/2} (nm\beta)^{1/2} \vartheta^2} \left[ 1 - \left( \frac{n\beta eE}{2m} \right)^2 \right]^{-1/4}. \end{aligned} \quad (6.29)$$

For long paths, an extra factor of  $\pm i/2$  should be included because the contribution to the imaginary part results from an integration over only one half of the Gaussian peak in the imaginary direction [63]. The sign depends on the way in which the analytic continuation is performed.

The functional determinant for the short paths is always positive, and the functional determinant for the long paths is always negative, in agreement with arguments given in section 6.2.1.

The sum of the short path contributions represents the free energy density of the metastable phase, and is given by

$$f = - \sum_{p=0}^{\infty} \sum_{n=1}^{n_{max}} 2K_{np}^{(s)} e^{-S_{np}^{(s)}} \quad (6.30)$$

where

$$K_{np}^{(s)} = \frac{(-1)^p (eE)^2}{(2\pi)^{3/2} (n\beta m)^{1/2}} \cdot \frac{\left[1 - \left(\frac{n\beta eE}{2m}\right)^2\right]^{-1/4}}{\left[2\pi p + 2 \sin^{-1}\left(\frac{n\beta eE}{2m}\right)\right]^2} \quad (6.31)$$

$$S_{np}^{(s)} = \frac{m^2}{2eE} \left[ 2\pi p + 2 \sin^{-1}\left(\frac{n\beta eE}{2m}\right) + \frac{n\beta eE}{m} \sqrt{1 - \left(\frac{n\beta eE}{2m}\right)^2} \right]. \quad (6.32)$$

In the limit  $E \rightarrow 0$ , equation (6.30) precisely reproduces the free energy of a free relativistic particle in the limit  $\beta m \gg 1$ . Compare the limiting form of equation (6.30) with the exact expression [68]

$$f = - \frac{m^2}{\pi^2 \beta^2} \sum_{n=1}^{\infty} \frac{1}{n^2} K_2(n\beta m). \quad (6.33)$$

As  $\beta \rightarrow \infty$  we have

$$f \sim - \sum_{n=1}^{\infty} 2 \frac{m^{3/2}}{(2\pi)^{3/2} (n\beta)^{5/2}} e^{-n\beta m} \quad (6.34)$$

which is the precise form of equation (6.30) as  $E \rightarrow 0$ . Figure 6.2 is a plot of the exact result for  $-f/m^4$ , as given by equation (6.33) versus  $T/m$ , along with the approximate form given by equation (6.34).

The long paths, on the other hand, give a thermal correction  $\Gamma_T$  to the zero-temperature decay rate  $\Gamma_0$ . Our final result for scalars is

$$\Gamma_T = 2 \text{Im} \left\{ \sum_{p=0}^{\infty} \sum_{n=1}^{n_{max}} 2K_{np}^{(l)} e^{-S_{np}^{(l)}} \right\} \quad (6.35)$$

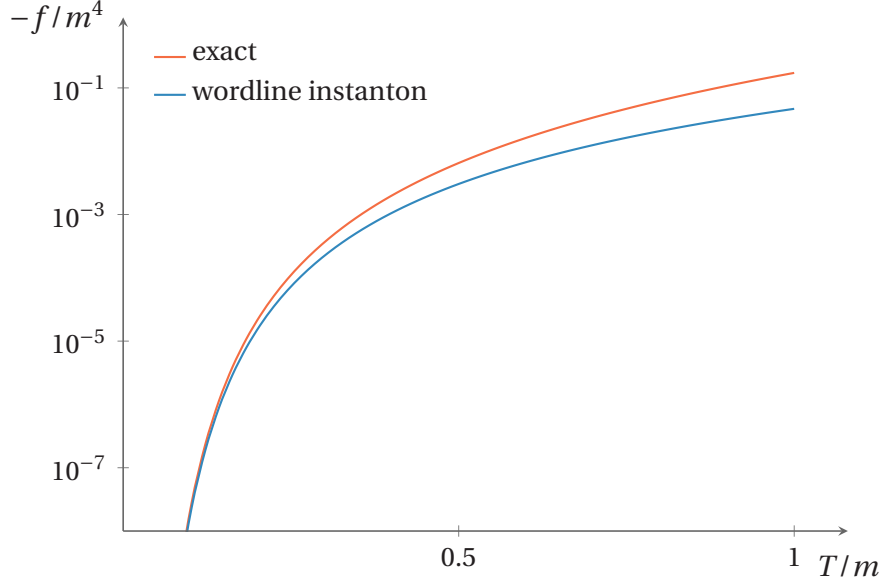


Figure 6.2: The worldline instanton expression for  $-f/m^4$  versus  $T/m$  compared with the exact expansion in the limit  $E \rightarrow 0$ .

where

$$K_{np}^{(l)} = \frac{i}{2} \cdot \frac{(-1)^p (eE)^2}{(2\pi)^{3/2} (n\beta m)^{1/2}} \cdot \frac{\left[1 - \left(\frac{n\beta eE}{2m}\right)^2\right]^{-1/4}}{\left[2\pi(p+1) - 2\sin^{-1}\left(\frac{n\beta eE}{2m}\right)\right]^2} \quad (6.36)$$

$$S_{np}^{(l)} = \frac{m^2}{2eE} \left[ 2\pi(p+1) - 2\sin^{-1}\left(\frac{n\beta eE}{2m}\right) - \frac{n\beta eE}{m} \sqrt{1 - \left(\frac{n\beta eE}{2m}\right)^2} \right]. \quad (6.37)$$

This concludes the derivation of our results for scalars in an external electric field.

## 6.2 DISCUSSION

In this section, I discuss some of the unusual features of our results, and their generalization to related problems. In Fig. 6.3, the total decay rate  $\Gamma = \Gamma_0 + \Gamma_T$  is plotted as a function of  $T/m$  for three values of  $eE/m^2$ . The leftmost part of each curve represents the contribution of  $\Gamma_0$  alone, which is independent of temperature. Each curve shows singularities, indicated by dotted lines, at  $T/m = neE/2m^2$ . Each singularity occurs at a threshold temperature, above which a new

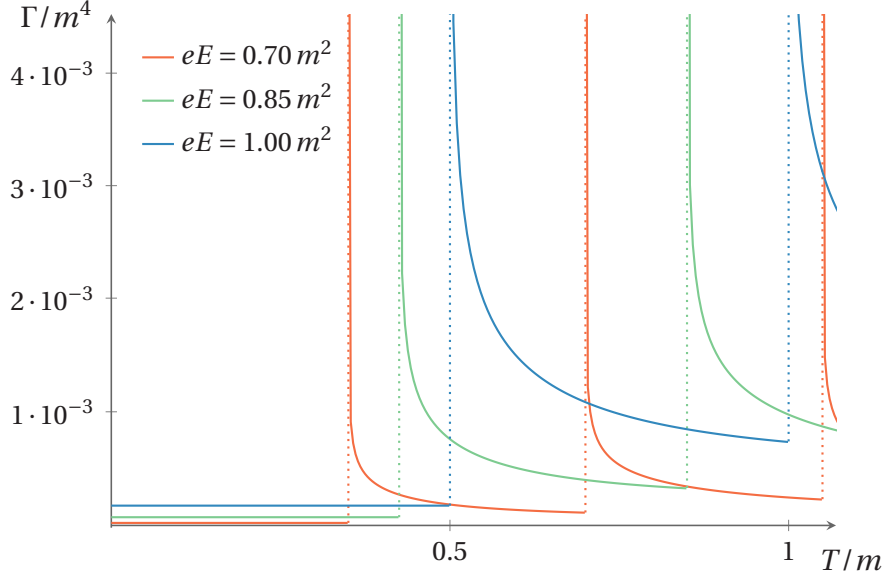


Figure 6.3: The total one-loop decay rate  $\Gamma = \Gamma_0 + \Gamma_T$  divided by  $m^4$  versus  $T/m$  for various values of  $eE/m^2$ . The dotted lines represent the singularities at  $T/m = neE/2m^2$ , which are rendered finite by effects not included at one loop. The leftmost part of each curve represents the contribution of  $\Gamma_0$  alone.

worldline instanton solution becomes possible. It can be shown that, wherever it is nonzero,  $\Gamma_T$  is always larger than  $\Gamma_0$ . By examining the reliable values of  $\Gamma/m^4$  to the left of each singularity, we see that the overall rise in the decay rate envelope appears to be linear in  $T$ .

The locations of the set of thresholds are controlled by the dimensionless parameter  $2mT/eE$ , and by the associated integer part  $n_{max}$ . Any finite temperature instanton must satisfy  $2R = 2m/eE > n\beta$ . If  $n_{max} = 0$ , i.e.  $T < eE/2m$ , there are no finite temperature instantons, and therefore no corrections to the zero-temperature decay rate. As  $T$  is increased, the threshold for a new solution is crossed whenever  $n_{max}$  increases by one. This has some similarity with the problem of vacuum decay at finite temperature. In the problem of the decay of the false vacuum, the Euclidean bounce solution in the thin wall approximation is a critical bubble of radius  $R_c$ , obtained from the competition between volume and surface tension contributions to the bounce action. At nonzero temperature, this solution is unmodified until  $2R_c > \beta$ , that is, until the bubble diameter exceeds the length of the compact direction [119, 120]. There are also

some similarities with the problem of one-loop stability of gauge fields at finite temperature in an external field, but the mechanism there is different and results from the competition between positive contributions to the energy eigenvalues from Matsubara frequencies with the negative contribution from the lowest Landau level [76].

### 6.2.1 Morse-theoretic analysis

One of the striking features of our result for the decay rate, associated with the behavior at thresholds, is the singular behavior of the decay rate  $\Gamma_T$ . This singularity is due to the factor

$$\left[1 - \left(\frac{n\beta eE}{2m}\right)^2\right]^{-1/4} \quad (6.38)$$

in eqns. (6.31) and (6.36) for the fluctuation prefactors  $K_{np}^{(s)}$  and  $K_{np}^{(l)}$ . The origin of the singularity can be understood at the classical level, however. In Figure 6.4, the action  $S$  is plotted for a family of arc-shaped paths spanning a total angle  $\theta$ , with  $n\beta m = 1$ , and endpoint separation fixed to  $n\beta\hat{e}_4$ . Classical solutions are only obtained at the extrema, where  $R = m/eE$ , and are given by  $S_{n0}^{(s)}$  and  $S_{n0}^{(l)}$ . We see that for  $eE/m^2 < 2$ , there is a local minimum corresponding to the short path, and a local maximum corresponding to the long path. The instability of the long path is obvious. At  $eE/m^2 = 2$ , the two extrema merge and  $n_{max}$  changes by one. The long and short paths are local maxima and minima of the action, respectively, along a given direction in functional space. Recall that  $n_{max}$  is the greatest integer less than  $2R/\beta = 2mT/eE$ . When  $2mT/eE$  is an integer, the long and short paths are degenerate, and both are arcs of angle  $\pi$  and arc length  $\pi R$ . If  $T$  is increased slightly, the degeneracy is lifted and a new maximum and minimum of the action exist. The singularity in  $K_{np}^{(s)}$  and  $K_{np}^{(l)}$  is associated with the degeneracy of the two solutions. This behavior is reminiscent of the behavior associated with the classical spinodal, where a local maximum and minimum merge and the quadratic approximation fails.

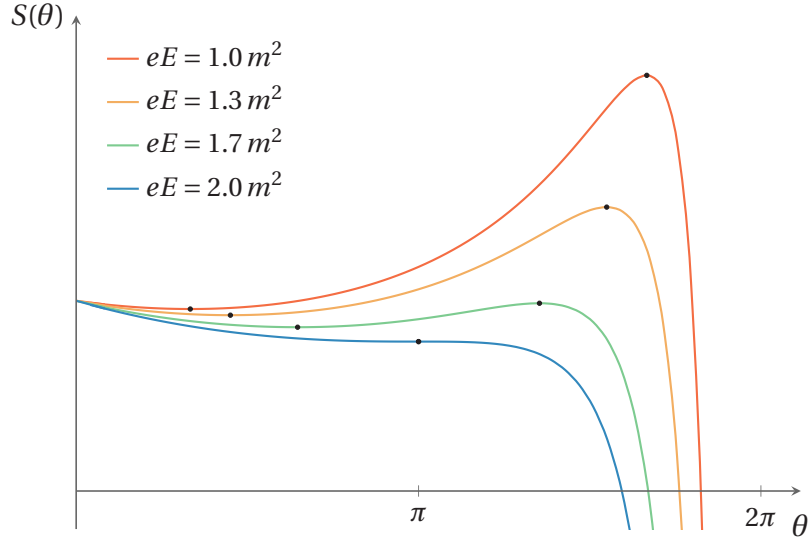


Figure 6.4: The action  $S$  for an arc solution as a function of  $\theta$  with  $n\beta m = 1$ . Only the extrema, indicated by dots, represent classical solutions, with the short path solution a local minimum and the long path solution a local maximum. The values of the action at the extrema are given by  $S_{n0}^{(s)}$  and  $S_{n0}^{(l)}$ , respectively. At  $eE/m^2 = 2$ , the two extrema merge.

This behavior is not restricted to the case of a constant, homogeneous electric field, but will occur generally for an inhomogeneous electric field when the temperature is nonzero and a zero-temperature instanton exists.

Morse theory provides a useful characterization of the eigenvalues of second variation operators about a functional extremum [121, 118]. The *caustic* is the envelope of trajectories obtained by fixing  $x_\mu(0)$  and varying  $\dot{x}_\mu(0)$ . A *focal point* of a classical path is defined as a contact point between the path and the caustic surface. The central point of Morse theory may be stated thus: the number of negative eigenvalues of the second variation operator about a given classical path equals the number of *focal points* strictly between its endpoints, where each focal point is counted with its multiplicity. This number is the *Morse index* of the path.

In the present case, all classical solutions are circles of constant radius  $R = m/eE$ . Therefore, the *caustic* is the union of a larger circle of radius  $2R$  with a single point at  $x_\mu(0)$ . A diagram



illustrating this caustic is in figure 6.5. Zero-temperature worldline instanton solutions of winding  $p$  (as well as our long paths of the same winding) contact the caustic  $2p + 1$  times, which establishes their imaginary contribution to the effective action. Short paths of winding  $p$  contact the caustic  $2p$  times, which nets a real contribution to the effective action. In either case, the  $2p$  negative eigenvalues associated with additional windings result in an overall factor of  $(-1)^p$  in the prefactor, as shown in equation (6.24). The appearance of such pairs of negative eigenvalues can be seen explicitly in the derivation of the functional determinant prefactor for zero-temperature solutions (see Appendix 6.4).

I emphasize that these features do not depend on the exact shape of the worldline instanton solution. Exact worldline instanton trajectories are known for several inhomogeneous field configurations [64]. Those orbits are no longer circles, but they are closed and periodic<sup>5</sup>, which is sufficient to establish that the striking qualitative features of our results—the singularities and thresholds, as well as the fact that short paths contribute to the free energy while long paths contribute the decay rate—are expected for inhomogeneous field configurations as well.

### 6.2.2 Higher-order effects

We have seen in previous sections that the singularities in the effective action result from the inadequacy of the Gaussian approximation at points in functional space where two critical points become degenerate. At such points, the quadratic coefficient in the Hessian operator vanishes, and higher-order terms are necessary for a correct computation of the effective action. The inclusion of such higher-order effects is difficult even at zero temperature. At finite temperature, higher-order effects will give rise to finite lifetimes for quasiparticle excitations in the thermal medium. These lifetimes may be calculated within the hard thermal loop (HTL) framework [122]. It is at least plausible that these finite lifetime effects smear out the threshold

---

<sup>5</sup>As, of course, they must [56, 57].

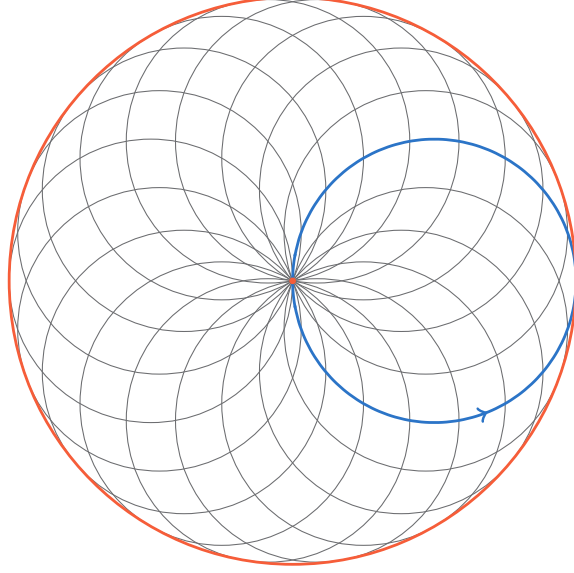


Figure 6.5: A set of trajectories formed by varying  $\dot{x}(0)$ . The envelope of such trajectories is the caustic, indicated in red. A representative path is in blue. As the path touches the caustic, the fluctuation operator about it acquires a negative eigenvalue.

singularities, rendering the decay rate finite. A complete calculation of this type is far beyond our grasp. However, the singularities can be eliminated heuristically by including the effect of a damping rate for the charged scalars. A damping rate for scalar QED can be obtained from a hard-thermal-loop calculation of the imaginary part of the scalar self energy. We include this effect by replacing  $m \rightarrow m - i\gamma$  in equation (6.38), where  $\gamma \sim 0.04 e^2 T$  is the scalar damping rate [123, 124]. This amounts to replacing the singular factor

$$\left[1 - \left(\frac{n\beta eE}{2m}\right)^2\right]^{-1/4} \rightarrow \left[\frac{1 - \left(\frac{n\beta eE}{2m}\right)^2}{\left(1 - \left(\frac{n\beta eE}{2m}\right)^2\right)^2 + \left(\frac{2\gamma}{m}\left(\frac{n\beta eE}{2m}\right)^2\right)^2}\right]^{1/4} \quad (6.39)$$

in equation (6.36).

In Fig. 6.6 the total decay rate  $\Gamma = \Gamma_0 + \Gamma_T$  with the modified threshold behavior is plotted as a function of  $T/m$  for the same three values of  $eE/m^2$  used in Fig. 6.3. As in that figure, the leftmost part of each curve represents the contribution of  $\Gamma_0$  alone, which is independent of temperature. Each curve shows local maxima at  $T/m = neE/2m^2$ . There is very little difference between

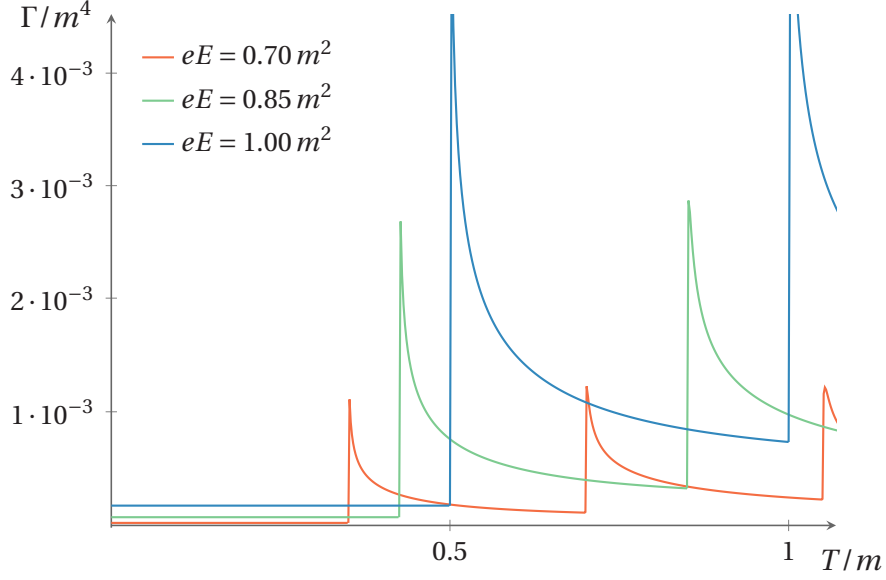


Figure 6.6: The total one-loop decay rate  $\Gamma = \Gamma_0 + \Gamma_T$  divided by  $m^4$  versus  $T/m$  for various values of  $eE/m^2$ , including HTL damping effects. The leftmost part of each curve represents the contribution of  $\Gamma_0$  alone.

the unmodified and modified decay rates, except in the close vicinity of a threshold. Other modifications of the vacuum decay rate using the HTL damping rate have been attempted. The results are not sensitive to the particular modification used, and the decay rate away from thresholds is virtually unchanged. This indicates that the thermal contribution to the pair production is substantially larger than the  $T = 0$  contribution once the first threshold is crossed.

### 6.3 CONCLUSIONS

I have presented a first-principles worldline instanton method for calculating the thermal contributions to Schwinger pair production in an electric field, and argued that many of their features carry over to the case of inhomogeneous fields as well. In section 6.5, I give a formal derivation of these results by applying a saddle-point approximation to the standard proper time representation of the effective potential for scalars in an external electric field.

The decay rate shows unphysical behavior at a series of thresholds, but this is an artifact of the Gaussian approximation to the functional integral; we have seen that this behavior is made physical by the phenomenological inclusion of hard thermal loop effects. Once the first threshold for thermal effects is crossed, the thermal contribution is larger than the  $T = 0$  contribution, rising as each successive threshold is crossed. This strongly indicates the potential importance of thermal effects in all such nonperturbative pair production processes. These results are extended to cases of more phenomenological interest, such as quarks in constant nonabelian electric fields, with Polyakov loop and finite density effects included, in the following chapter.

The worldline formalism is powerful but physically opaque. A simple physical understanding of these results, analogous to the many physically transparent derivations of the zero temperature decay rate, would also be highly desirable.

#### 6.4 APPENDIX: ZERO-TEMPERATURE FLUCTUATION PREFACTOR

We illustrate the use of the matrix determinant lemma by computing the prefactor for the zero temperature worldline solutions. Because the local part  $L_{\mu\nu}$  of the second variation operator (6.18) has zero modes associated with proper time translations and expansions/contractions of the zero temperature circle, it is noninvertible, which means the spectrum must be known and there is no benefit over the direct calculation. However, at finite temperature both zero modes are lifted and the method becomes much more convenient. The second variation of the action about the worldline instanton solution (assumed without loss of generality to be centered at the origin) is [47]

$$M_{p,\mu\nu} = eE \left[ \left( -\frac{\delta_{\mu\nu}}{2\pi p} \frac{\partial^2}{\partial u^2} + ieF_{\mu\nu} \frac{\partial}{\partial u} \right) \delta(u - u') - \frac{2\pi p}{R^2} x_\mu^p(u) x_\nu^p(u') \right]. \quad (6.40)$$

The determinant can be written as

$$\det'[M_{p,\mu\nu}] = \det'[L_{\mu\nu}](-2\pi p e E) \left( 1 - 2\pi p \frac{eE}{R^2} \iint du du' x_\mu^p(u) (L^{-1})'_{\mu\nu} x_\nu^p(u') \right) \quad (6.41)$$

$$L_{\mu\nu} = \left[ -\frac{eE}{2\pi p} \frac{d^2}{du^2} \delta_{\mu\nu} + ieF_{\mu\nu} \frac{d}{du} \right]. \quad (6.42)$$

As usual, the primed determinant and Green's function are computed with zero modes removed. The factor  $(-2\pi p e E)$  appears because, while changes of the radius of the instanton circle are associated with a zero mode of the local part, they do not correspond to a zero mode of the full second variation operator; the corresponding eigenvalue must be handled separately.

The determinant of the local part can be computed by taking the product of eigenvalues, as in Affleck et al. Ignoring the irrelevant transverse directions we have

$$\det'[L_{\mu\nu}] = \mathcal{N}^2 \prod_{\substack{q \neq 0 \\ q \neq p}} \left( 2\pi e E \left( \frac{q^2}{p} - q \right) \right)^2 \quad (6.43)$$

where  $\mathcal{N}$  is a normalization factor to be fixed by the identity

$$\oint [dx] \exp \left[ -\frac{m^2}{4s_0} \int_0^1 du \dot{x}^2 \right] = \mathcal{N} \left[ \det'(M_{p,\mu\nu}^{free}) \right]^{-1/2} = \frac{m^4}{(4\pi s_0)^2} \quad (6.44)$$

with  $M_{p,\mu\nu}^{free}$  defined as in equation (3.28). Therefore,

$$\det'[L_{\mu\nu}] = \left( \frac{4\pi s_0}{m^2} \right)^4 \frac{1}{(2\pi p e E)^2} \prod_{\substack{q \neq 0 \\ q \neq p}} \frac{\left( \frac{q^2}{p} - q \right)^2}{\left( \frac{q^2}{p} \right)^2} \quad (6.45)$$

$$= \left( \frac{4\pi^2 p}{eE} \right)^4 \frac{1}{(2\pi p e E)^2} \left[ \lim_{z \rightarrow 1} \frac{\sin(\pi p z)}{\pi p z (1-z)} \right]^2 \quad (6.46)$$

$$= \left[ \left( \frac{4\pi^2 p}{eE} \right)^2 \frac{(-1)^{p+1}}{2\pi p e E} \right]^2, \quad (6.47)$$

which clearly parallels the zero-temperature derivation (equations (3.30) through (3.32)). The second line comes from a standard identity [42].

We now proceed to the nonlocal part which, as we will see, is trivial. The Green's function  $(L^{-1})'_{\mu\nu}$  can be obtained from the spectral representation

$$(L^{-1})'_{\mu\nu} = \sum_{\substack{q \neq 0 \\ q \neq p}} \frac{1}{\lambda_q} \begin{pmatrix} \cos(2\pi q(u-u')) & -\sin(2\pi q(u-u')) \\ \sin(2\pi q(u-u')) & \cos(2\pi q(u-u')) \end{pmatrix} \quad (6.48)$$

and thus

$$\int_0^1 du \int_0^1 du' x_\mu(u) (L^{-1})'_{\mu\nu} x_\nu(u') = \sum_{\substack{q \neq 0 \\ q \neq p}} \frac{1}{\lambda_q} \left( \frac{\sin(\pi(p-q))}{\pi(p-q)} \right)^2 = 0. \quad (6.49)$$

The last remaining piece to be evaluated is the contribution of the zero mode associated with proper time translations  $x^\mu(u) \rightarrow x^\mu(u + \varphi/2\pi p)$ . As usual, one need only consider an infinitesimal translation

$$x^\mu(u + \varphi) \approx x^\mu(u) + \varphi \left. \frac{d}{d\varphi} x^\mu(u + \varphi/2\pi p) \right|_{\varphi=0} \quad (6.50)$$

and write the second term in terms of normalized eigenfunctions. Per this standard argument, a factor of

$$R \int_0^{2\pi} \frac{d\varphi}{\sqrt{2\pi}} = \sqrt{2\pi} \frac{m}{eE} \quad (6.51)$$

must be included in the functional integral.

Collecting everything, we obtain for the prefactor

$$(\int d^4x) \frac{\sqrt{2\pi/m}}{\left[ \int_0^1 du \dot{x}^2 \right]^{1/4}} (\det' [M_{p,\mu\nu}])^{-1/2} = \pm V_4 \frac{i}{2} \frac{(eE)^2}{(2\pi)^3 p^2} (-1)^{p+1} \quad (6.52)$$

in agreement with Schwinger's formula. The factor of 1/2 comes from integrating over only one half of the Gaussian peak in the imaginary direction, and the sign depends on the way in which the analytic continuation is performed.

## 6.5 APPENDIX: EQUIVALENCE WITH PROPER-TIME FORMALISM

The proper time expression for the one-loop finite temperature contribution to the effective action of a charged scalar is [34]

$$\mathcal{L}_{eff}^{1T} = -\frac{(eE)^2}{8\pi^2} \sum_{n=1}^{\infty} \int_0^{\infty} \frac{ds}{s^2} \csc(s) e^{-\frac{m^2 s}{eE} - \frac{eE(n\beta)^2}{4} \cot(s)}. \quad (6.53)$$

We wish to calculate a Gaussian approximation to this integral. The exponent has pairs of saddle points given implicitly by

$$\sin(s_0) = \frac{n\beta eE}{2m} \equiv \frac{n\beta}{2R} \quad (6.54)$$

provided the right side is smaller than 1, that is,  $n \leq n_{max}$  (see eq. (6.12)). For definiteness and simplicity  $s_0$  is taken to lie in the first quadrant, corresponding to our short path solutions. The second derivative of the exponent at the saddle point is

$$\begin{aligned} \left. \frac{\partial^2}{\partial s^2} \left( \frac{m^2}{eE} s + \frac{eE(n\beta)^2}{4} \cot(s) \right) \right|_{s_0} &= \frac{eE(n\beta)^2}{2} \cot(s_0) \csc^2(s_0) \\ &= \frac{4m^3}{(eE)^2 (n\beta)} \sqrt{1 - \left( \frac{n\beta}{2R} \right)^2}. \end{aligned} \quad (6.55)$$

The Gaussian approximation to the integral reads

$$\mathcal{L}_{(n)}^{1T} = -\frac{(eE)^2}{8\pi^2} \sum_{n=1}^{n_{max}} \frac{1}{s_0^2} \frac{2R}{n\beta} \left( \frac{2\pi(eE)^2 n\beta}{4m^3 \sqrt{1 - \left( \frac{n\beta}{2R} \right)^2}} \right)^{1/2} e^{-S(s_0)} \quad (6.56)$$

$$= -\frac{(eE)^2}{\sqrt{2\pi^3}} \sum_{n=1}^{n_{max}} \sum_{p=0}^{\infty} \frac{\left[ 1 - \left( \frac{n\beta eE}{2m} \right)^2 \right]^{-1/4}}{(nm\beta)^{1/2} \left( 2\pi p + 2 \sin^{-1} \left( \frac{n\beta eE}{2m} \right) \right)^2} e^{-S(s_0)} \quad (6.57)$$

where

$$S(s_0) = \frac{m^2}{2eE} \left[ 2\pi p + 2 \sin^{-1} \left( \frac{n\beta eE}{2m} \right) + \frac{n\beta eE}{m} \sqrt{1 - \left( \frac{n\beta eE}{2m} \right)^2} \right] \quad (6.58)$$

in complete agreement with equations (6.30) and (6.31).

# CHAPTER 7

## ELECTRIC FIELDS AT FINITE TEMPERATURE II

In the previous chapter, we obtained compact expressions representing the effects of a real space electric field in the thermodynamics of a complex scalar field. For applications, we may require some generalizations of these expressions, for instance, for the case of spinor particles moving in the presence of a nontrivial Polyakov loop. This brings these expressions into closer contact with the physical processes of particle production in flux tubes and the breaking of the color string. As in the zero temperature case, we could also make use of a better characterization of the momentum distribution of produced particles, so a finite-temperature generalization of Nikishov's virial representation [37], equation (2.70) of this text, is of great interest.

To keep the presentation as short and simple as possible, each generalization is presented as a separate development of the basic formalism. Combining them, if necessary, should present no difficulty.

### 7.1 PROPER-TIME FORMULA

We would like to obtain some insight on the proper-time expression (6.53). The derivation of Gies [34] parallels that of Schwinger [4], which was reproduced in section 2.5, taken together



with the image charge construction (6.4). The calculation is complex, with many steps; one wonders whether a simpler, more direct computation is possible. We address this in this section.

Our goal is to calculate the functional determinant of the Klein-Gordon operator for a charged scalar in the background of a Euclidean electric field  $\mathcal{E}$ , which is essentially a magnetic field in the 3d-plane,

$$D \equiv -\partial_{\perp}^2 + m^2 - \partial_4^2 + e^2 \mathcal{E}^2 x_4^2. \quad (7.1)$$

We will use the formalism of zeta function regularization. See for example the book of Ramond for an introduction [125]. Let the zeta function associated with  $D$  be defined as the analytic continuation of

$$\zeta_D(z) \equiv \sum_n a_n^{-z}, \quad (7.2)$$

where the  $a_n$  are the eigenvalues of  $d$ , to the complex  $z$  plane. Of course,  $D$  has a continuous spectrum, so the above sum is over both continuous and discrete indices. The utility of this construct stems from the formal observation

$$\left. \frac{d\zeta_D(z)}{dz} \right|_{z=0} = - \sum_n \log a_n e^{-z \log a_n} \Big|_{z=0} = - \log \left( \prod_n a_n \right), \quad (7.3)$$

thus it is natural to define

$$\det_{\zeta} D \equiv e^{-\zeta'_D(0)}. \quad (7.4)$$

Hereafter the subscript  $\zeta$  will be omitted, and it is understood that all functional determinants are defined in this way. Naturally, the one-loop effective action can be written in terms of this determinant,

$$S_{eff}^{(1)} = -\frac{1}{2} \log \det D = \zeta'_D(0). \quad (7.5)$$

Consider first the case of zero temperature. It can be shown that the zeta function can be written as

$$\zeta_D(z) = \frac{1}{\Gamma(z)} \int_0^{\infty} ds s^{z-1} \int d^4x K(x, x; s), \quad (7.6)$$

where the heat kernel  $K(x, y; s)$  satisfies

$$\frac{\partial K(x, y; s)}{\partial s} = -D_x K(x, y; s), \quad (7.7)$$

$$K(x, y; 0) = \delta^{(4)}(x - y). \quad (7.8)$$

The differential operator  $D$  has a free particle portion as well as a harmonic oscillator portion, with eigenvalues  $(2n + 1)\omega$ , where  $\omega = \sqrt{e^2 \mathcal{E}^2}$ , and orthonormal eigenfunctions

$$\psi_n(x_4) = \frac{1}{\sqrt{2^n n!}} \left(\frac{\omega}{\pi}\right)^{1/4} H_n(\omega^{1/2} x_4) e^{-\omega x_4^2/2}. \quad (7.9)$$

We can then use the spectral representation to decompose  $K$  as

$$K(x, y; s) = K_{\perp}(x, y; s) K_{\parallel}(x, y; s) \quad (7.10)$$

where

$$K_{\perp}(x, y; s) = \int \frac{d^2 p_{\perp}}{(2\pi)^2} e^{-s(p_{\perp}^2 + m^2) - i p_1(x_1 - y_1) - i p_2(x_2 - y_2)}, \quad (7.11)$$

$$K_{\parallel}(x, y; s) = \frac{eE}{2\pi} \left(\frac{\omega}{\pi}\right)^{1/2} \sum_{n=0}^{\infty} \frac{e^{-s(2n+1)\omega}}{2^n n!} H_n(\omega^{1/2} x_4) H_n(\omega^{1/2} y_4) e^{-\omega(x_4^2 + y_4^2)/2}. \quad (7.12)$$

The factor of  $eE/2\pi$  is the usual density of states due to the degeneracy of the Landau levels.

The sum can be done with the aid of Mehler's formula [126],

$$\sum_{n=0}^{\infty} \frac{(\rho/2)^n}{n!} H_n(x) H_n(y) e^{-(x^2 + y^2)/2} = \frac{1}{\sqrt{1 - \rho^2}} \exp\left[\frac{4\rho xy - (1 + \rho^2)(x^2 + y^2)}{2(1 - \rho^2)}\right] \quad (7.13)$$

giving

$$K_{\parallel}(x, y; s) = \sqrt{\frac{\omega}{2\pi \sinh(2\omega s)}} \exp\left[\frac{\omega xy}{\sinh(2\omega s)} - \omega \coth(2\omega s) \frac{x^2 + y^2}{2}\right]. \quad (7.14)$$

With this, it is straightforward to construct the zeta function. Setting  $x = y$  and integrating, we find

$$\int d^4x K_{\parallel}(x, x, s) = \frac{1}{\sqrt{2 \sinh(2\omega s)}} \frac{1}{\sqrt{\coth(2\omega s) - \frac{1}{\sinh(2\omega s)}}} \quad (7.15)$$

$$= \frac{1}{\sinh(\omega s)}. \quad (7.16)$$

Together with the free particle portion we obtain for the zeta function,

$$\zeta_D(z) = \frac{e\mathcal{E}(\int d^3x)}{2\pi\Gamma(z)} \int ds s^{z-1} \int \frac{d^2p_{\perp}}{(2\pi)^2} e^{-s(p_{\perp}^2+m^2)} \operatorname{csch}(e\mathcal{E}s). \quad (7.17)$$

As in the computation of the zero-temperature Euler–Heisenberg effective Lagrangian (2.56), the leading behavior of the hyperbolic cosecant is singular at  $s = 0$ . Once these are subtracted in the usual way, the finite part of the functional determinant is easily evaluated: only the term in which the derivative acts on the Gamma function contributes in the  $z \rightarrow 0$  limit. Then using the fact that

$$\left. \frac{d}{dz} \Gamma(z) \right|_{z=0} = - \left. \frac{\Gamma'(z)}{(\Gamma(z))^2} \right|_{z=0} = 1 \quad (7.18)$$

we obtain for the finite part of the effective Lagrangian

$$\mathcal{L}_{eff}^{(1)} = -\frac{e\mathcal{E}}{4\pi} \int_0^{\infty} \frac{ds}{s} \int \frac{d^2p_{\perp}}{(2\pi)^2} e^{-sm_{\perp}^2/e\mathcal{E}} \left( \operatorname{csch}(s) - \frac{1}{s} + \frac{s}{6} \right), \quad (7.19)$$

where  $m_{\perp}^2 \equiv m^2 + p_{\perp}^2$ . If the Gaussian integration over  $p_{\perp}$  is performed, this equation is recognized as the expression of Weisskopf for the effective Lagrangian describing scalars in a magnetic field (2.64). The corresponding expression for a Minkowski space electric field may be obtained with the replacements  $\mathcal{E} \rightarrow iE$ ,  $s \rightarrow is$ .

The calculation at finite temperature is analogous. In particular, the kernel (7.14) is the same. The compactness of the timelike direction manifests in the expression for the zeta function in

terms of the heat kernel,

$$\zeta_D^T(z) = \frac{1}{\Gamma(z)} \sum_{n \in Z} \int_0^\infty ds s^{z-1} \int d^3x K(x, x + n\beta\hat{e}_4; s). \quad (7.20)$$

Without any loss of generality we consider the symmetrized expression

$$\frac{eE}{2\pi} \sum_n \int dx_4 \exp \left[ \frac{\omega}{\sinh(2\omega s)} (x_4 - n\beta/2)(x_4 + n\beta/2) - \omega \coth(2\omega s) \frac{(x_4 - n\beta/2)^2 + (x_4 + n\beta/2)^2}{2} \right] \quad (7.21)$$

which can be rewritten as

$$\frac{eE}{2\pi} \sum_n \exp \left[ - \left( \frac{1}{\sinh(2\omega s)} + \coth(2\omega s) \right) \frac{n^2 \beta^2 \omega}{4} \right] \int dx_4 \exp \left[ \frac{\omega}{\sinh(2\omega s)} x_4^2 - \omega \coth(2\omega s) x_4^2 \right]. \quad (7.22)$$

The first factor is the finite temperature part, and the second is the zero temperature part previously calculated. Using the hyperbolic identity

$$\operatorname{csch}(2\omega s) + \coth(2\omega s) = \coth(\omega s) \quad (7.23)$$

we can write the resulting kernel as

$$K_{\parallel}^T(x, x; s) = \frac{e\mathcal{E}}{2\pi} \operatorname{csch}(e\mathcal{E}s) \sum_n e^{-\frac{n^2 \beta^2 e\mathcal{E}}{4} \coth(e\mathcal{E}s)}. \quad (7.24)$$

The free-particle portion is unchanged by the compactness of the timelike direction. Finally we can write the finite temperature portion of the effective Lagrangian

$$\mathcal{L}_{eff}^{1T} = -\frac{e\mathcal{E}}{4\pi} \sum_{n \neq 0} \int_0^\infty \frac{ds}{s} \int \frac{d^2 p_{\perp}}{(2\pi)^2} \operatorname{csch}(e\mathcal{E}s) e^{-m_{\perp}^2 s - \frac{e\mathcal{E}(n\beta)^2}{4} \coth(e\mathcal{E}s)}. \quad (7.25)$$

This, after performing the integration over transverse momenta  $p_{\perp}$  and rotating to a Minkowski space electric field  $\mathcal{E} \rightarrow iE$ ,  $s \rightarrow is$ , is (6.53).

Using the generating function for Laguerre polynomials  $L_k$ ,

$$\sum_{k=0}^{\infty} t^k L_k(z) = \frac{1}{1-t} \exp\left(-\frac{zt}{1-t}\right) \quad (7.26)$$

together with the identity

$$\coth s = 1 + \frac{2e^{-2s}}{1 - e^{-2s}}, \quad (7.27)$$

it is possible to find the alternate representation

$$\mathcal{L}_{\text{eff}}^{1T} = -\frac{(e\mathcal{E})^2}{2\pi} \sum_{n \neq 0} \int_0^{\infty} \frac{ds}{s} \int \frac{d^2 p_{\perp}}{(2\pi)^2} e^{-(1+m_{\perp}^2/e\mathcal{E})s - e\mathcal{E}(n\beta)^2/4} \sum_{k=0}^{\infty} e^{-2ks} L_k\left(\frac{(n\beta)^2 e\mathcal{E}}{2}\right). \quad (7.28)$$

## 7.2 CHEMICAL POTENTIAL AND NONABELIAN EFFECTS

Within the worldline formalism, it is straight forward to include the effects of a nonzero chemical as well as some special cases of nonabelian gauge field effects.

We begin by considering the case of a nonzero chemical potential  $\mu$ . If we temporarily identify the charge and particle number quantum numbers, the chemical potential can be usefully considered as a static component of the abelian field such that  $A_v \rightarrow A_v + \mu \delta_{v,0}$ . This changes the worldline action (3.15) to

$$\bar{S} = m \sqrt{\int_0^1 du \dot{x}^2} + i \int_0^1 du [eA(x(u)) + \mu \hat{e}_4] \cdot \dot{x}. \quad (7.29)$$

It follows that zero-temperature instantons, which are worldline paths with zero winding in the Euclidean time direction, have no  $\mu$  dependence. Finite-temperature instanton solutions begin and end at the same spatial coordinates, but have a net change in  $x_4$  of  $\pm n\beta$ . Particle paths will pick up an extra factor of  $n\beta\mu$  and antiparticle paths a factor of  $-n\beta\mu$ . Because our previous results include both particle and antiparticle paths with equal weighting, the effect of

$\mu$  is to add a factor of  $\cosh(n\beta\mu)$  to the prefactors  $K_{np}^{(s)}$  and  $K_{np}^{(l)}$ .

$$\Gamma_T = 2 \operatorname{Im} \left\{ \sum_{p=0}^{\infty} \sum_{n=1}^{n_{max}} K_{np}^{(l)} e^{-S_{np}^{(l)}} (e^{n\beta\mu} + e^{-n\beta\mu}) \right\} \quad (7.30)$$

There are two known classes of constant nonabelian gauge fields which give rise to constant electric fields: field configurations which generalize constant abelian electric fields, and field configurations where the matrix-valued gauge field  $F_{\mu\nu}$  is nonzero because one or more of the commutators  $[A_\mu, A_\nu] \neq 0$ . I will consider only the former case here. In addition to the effects of a constant electric field, I will also include the effects of a nontrivial Polyakov loop.

I will consider a limited class of nonabelian fields where, perhaps after a gauge transformation,  $A_4$  and  $E$  are nonzero and constant, and both lie in the maximal commuting subalgebra, or Cartan algebra, of the gauge group. We can then write the matrices  $E$  and  $P$  in a representation  $R$  as

$$E_{ab} = E_a \delta_{ab} \quad (7.31)$$

$$P_{ab} = e^{i\psi_a} \delta_{ab}. \quad (7.32)$$

If these eigenvalues are known in the fundamental representation, the case of principal interest, then eigenvalues of  $E$  and  $P$  can be constructed for any given larger other representation. All of our previous formulae can then be taken over to this extended case by the replacements

$$E \rightarrow E + E_a \quad (7.33)$$

$$\mu \rightarrow \mu + i\psi_a \quad (7.34)$$

with an overall summation over the index  $a$ . The case of production of a nonabelian particle pair in an abelian electric field can be written succinctly as

$$\Gamma_T = 2 \operatorname{Im} \left\{ \sum_{p=0}^{\infty} \sum_{n=1}^{n_{max}} K_{np}^{(l)} e^{-S_{np}^{(l)}} \left( e^{n\beta\mu} \operatorname{Tr}_R P^n + e^{-n\beta\mu} \operatorname{Tr}_R P^{-n} \right) \right\}. \quad (7.35)$$

This displays in a clear manner an important difference between particles carrying only abelian charge and those carrying nonabelian charge. In a region of the  $(\mu, T)$  plane where  $\text{Tr}_R P$  is small, that is to say, where the particles are confined, the thermal production rate is suppressed by the Polyakov loop. In a region where  $\text{Tr}_R P$  is close to its maximal value,  $\text{Tr}_R 1 \equiv d_R$ , there is very little suppression.

In the more general case where there is a nonabelian electric field, the decay rate is more complicated and probably best written as a sum:

$$\Gamma_T = 2 \text{Im} \left\{ \sum_{p=0}^{\infty} \sum_{n=1}^{n_{\max}} \sum_{a=1}^{d_R} K_{np}^{(l)}(E + E_a) e^{-S_{np}^{(l)}(E + E_a)} \left( e^{n\beta\mu + in\psi_a} + e^{-n\beta\mu - in\psi_a} \right) \right\}, \quad (7.36)$$

where I have explicitly denoted the dependence of  $K_{np}^{(l)}$  and  $S_{np}^{(l)}$  on  $E + E_a$ .

### 7.3 UNIFORM ASYMPTOTICS

Realizing that the results from the worldline formalism can be obtained from the proper-time formula (6.53) suggests an alternate way to handle the singularities in the effective action for scalars in an electric field. Consider an integral of the general form

$$I = \int_0^{\infty} ds g(s) e^{-f(s)}, \quad (7.37)$$

where  $f(s)$  is a reasonably well-behaved function with two saddle points  $s_1$  and  $s_2$ , that is, two (possibly complex) roots to the equation

$$f'(s) = 0. \quad (7.38)$$

Necessarily, the second derivatives at each saddle have different signs. I arbitrarily take  $s_1$  to be the positive one. If the saddles coalesce, the second derivatives go to zero and the standard

Gaussian approximation to the contribution of the saddle  $s_k$

$$I_k = g(s_k) \sqrt{\frac{2\pi}{f''(s_k)}} e^{-f(s_k)} \quad (7.39)$$

diverges. This is precisely the origin of the singular behavior in the prefactors (6.31) and (6.36).

From here I adopt the notation  $g_k \equiv g(s_k)$ ,  $f_k \equiv f(s_k)$ , etc.

There exist standard techniques for deriving asymptotic approximations to expressions of this type. The exposition below is based on the work of Miller [127], who, in turn, credited Carrier [128]. We require the integral representations of the Airy functions [129],

$$\text{Ai}(z) = \frac{1}{2\pi i} \int_{\infty e^{-i2\pi/3}}^{\infty e^{i2\pi/3}} ds e^{-\frac{1}{3}s^3 + sz} \quad (7.40)$$

$$i \text{Bi}(z) = \frac{1}{2\pi i} \int_{\infty}^{\infty e^{-i2\pi/3}} ds e^{-\frac{1}{3}s^3 + sz} + \frac{1}{2\pi i} \int_{\infty}^{\infty e^{i2\pi/3}} ds e^{-\frac{1}{3}s^3 + sz}, \quad (7.41)$$

where the integral limits indicate that the contours start and end at the point at infinity with the given arguments<sup>6</sup>. The shape of the contour is otherwise irrelevant.

If  $f(s)$  is expanded to third order about each saddle, and further assuming that the integral  $I$  is dominated by the contributions at the saddle points, we can write the approximate expression

$$I_k = g_k e^{-f_k} \int_{\infty e^{-i2\pi/3}}^{\infty} ds e^{-f_k'(s-s_k)^2/2 - f_k'''(s-s_k)^3/6}, \quad (7.42)$$

which can be placed in a form closer to the integral representations of the Airy functions by completing the cubic,

$$I_k = g_k \left| \frac{2}{f_k'''} \right|^{1/3} e^{-f_k + \frac{2}{3}x_k^3} \int_{\infty e^{-i2\pi/3}}^{\infty} ds e^{-\frac{1}{3}s^3 + sx_k}, \quad (7.43)$$

$$x_k \equiv -\left(\frac{f_k''}{2}\right) \left(\frac{2}{f_k'''}\right)^{2/3}.$$

---

<sup>6</sup> The arguments are given as multiples of  $\pi/3$  for definiteness only. In fact, it suffices that the contours begin and end in the wedge shaped regions where  $|e^{-s/3}| \rightarrow 0$  for large  $s$ .



The only remaining difference between this expression and the representations of the Airy functions (7.40) and (7.41) is the contour. This is easily handled: since the integrand is an entire function, the contour on this integral corresponds to the linear combination  $(\text{Ai}(x_k^2) - i \text{Bi}(x_k^2))/2$ . Finally we obtain

$$I_k = 2\pi g_k \left| \frac{2}{f_k'''} \right|^{1/3} e^{-f_k + \frac{2}{3}x_k^3} (i \text{Ai}(x_k^2) + \text{Bi}(x_k^2)). \quad (7.44)$$

As pointed out by Miller, there are spurious terms in this expression. Identifying them correctly requires some information about the problem. In the application to the proper-time formula (6.53), we have guidance from the worldline formalism, which tells us, for example, that

$$4\pi g_1 \left| \frac{2}{f_1'''} \right|^{1/3} e^{-f_1 + \frac{2}{3}x_1^3} i \text{Ai}(x_1^2) \quad (7.45)$$

is just a crude approximation to  $I_2$ , best left out altogether. We thus have

$$I_1 = 2\pi g_1 \left| \frac{2}{f_1'''} \right|^{1/3} e^{-f_1 + \frac{2}{3}x_1^3} \text{Bi}(x_1^2), \quad (7.46)$$

$$I_2 = 2\pi g_2 \left| \frac{2}{f_2'''} \right|^{1/3} e^{-f_2 + \frac{2}{3}x_2^3} (i \text{Ai}(x_2^2) + \text{Bi}(x_2^2)). \quad (7.47)$$

To carry out the computations we take

$$f(s) = \frac{m^2}{eE} s + \frac{(n\beta)^2 eE}{4} \cot s, \quad (7.48)$$

and may choose, for example,

$$g(s) = \frac{(eE)^2}{4\pi^2} \frac{1}{s^2} \cot s \quad (7.49)$$

for spinors, or

$$g(s) = \frac{(eE)^2}{8\pi^2} \frac{1}{s^2} \csc s \quad (7.50)$$

for scalars. The worldline formalism also lets us know that there is no contribution to the imaginary part of the effective action below the threshold at each value of  $n$ , because there the

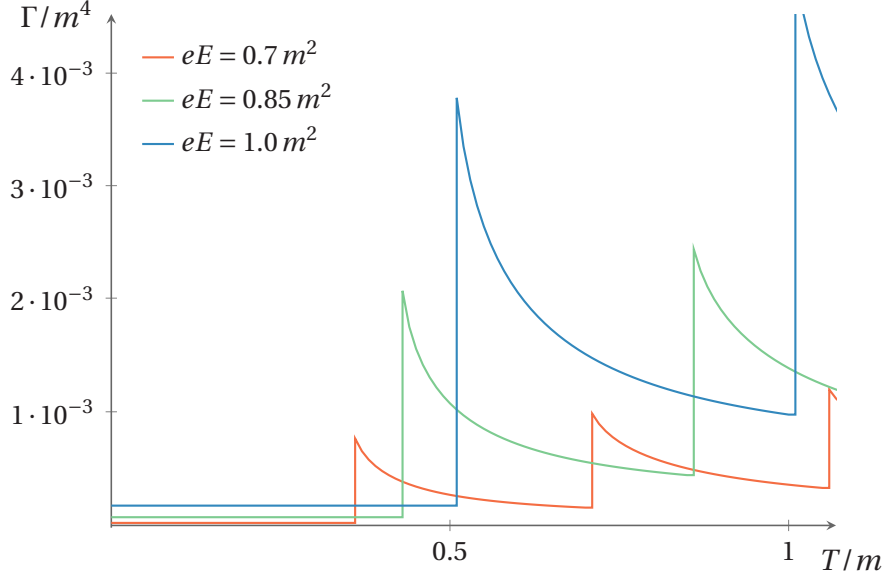


Figure 7.1: The total uniformized one-loop decay rate  $\Gamma = \Gamma_0 + \Gamma_T$  divided by  $m^4$  versus  $T/m$  for various values of  $eE/m^2$ . The leftmost part of each curve represents the contribution of  $\Gamma_0$  alone.

contributions to the effective action from the two complex worldline solutions form a complex conjugate pair.

The uniformized decay rate for scalars is presented in figure 7.1. Note the similarity with figure 6.6, which was obtained from a modified Gaussian approximation that incorporates a finite lifetime for the scalars, obtained from the hard thermal loop framework. The argument given here shows that this earlier construction is not needed: the scalar pair production rate is finite even without inclusion of a damping rate.

#### 7.4 VIRIAL REPRESENTATION

As in the case of pair production at zero temperature, for applications we require also the momentum distribution of created pairs. The procedure employed in 3.4 generalizes to the case of nonzero temperature in a straightforward manner, as the image charge construction (6.4)

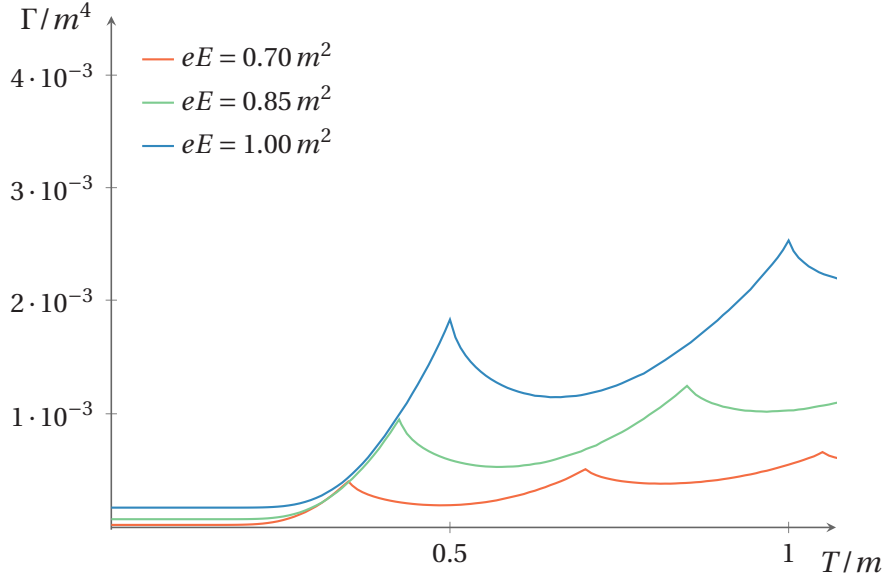


Figure 7.2: The total one-loop decay rate for scalars  $\Gamma = \Gamma_0 + \Gamma_T$  divided by  $m^4$  versus  $T/m$  for various values of  $eE/m^2$ , obtained by integrating the virial representation (equations (7.58) and (7.59)) over transverse momenta. Each curve reduces smoothly to the zero-temperature rate  $\Gamma_0$  for sufficiently small  $T$ .

does not affect the essence of the argument. Thus, one makes the substitution  $m \rightarrow m_\perp$ , where

$$m_\perp^2 = m^2 + p_\perp^2 \quad (7.51)$$

can be interpreted as the relativistic mass squared of the created particles. Then the steps leading to equations (6.31), (6.32), (6.36), and (6.37) are retraced, with the chief difference being the dimensionality of the path integral normalization factor (the first factor in equation (6.23)).

One important difference between the cases of zero and nonzero temperature is that, at zero temperature, the final expression, equation (2.70), can be integrated to recover the original Schwinger formula (2.67). In the finite temperature calculation, different sets of functional saddle points contribute to the decay rate depending on whether the transverse modes are integrated out. In particular, since the radius of the instanton solution corresponding to the

production of particles with transverse momentum  $p_\perp$  is given by

$$R_\perp = \frac{m_\perp}{eE} = \frac{1}{eE} \sqrt{m^2 + p_\perp^2}, \quad (7.52)$$

there are classical trajectories for all timelike windings  $n$ . Rather, there is now a minimum transverse momentum threshold for each  $n$ , which corresponds to the minimum instanton radius that permits a classical trajectory winding around the Euclidean time direction  $n$  times.

We thus require  $2R_\perp \geq n\beta$ , or

$$p_\perp \geq p_\perp^{min},$$

$$p_\perp^{min} \equiv m \operatorname{Re} \left[ \sqrt{\left( \frac{n\beta eE}{2m} \right)^2 - 1} \right]. \quad (7.53)$$

Therefore

$$\operatorname{Re} \mathcal{L}_T^{(1)} = \int \frac{d^2 p_\perp}{(2\pi)^2} \sum_{p=0}^{\infty} \sum_{n=1}^{\infty} 2K_{\perp,np}^{(s)} e^{-S_{\perp,np}^{(s)}} \quad (7.54)$$

$$i \operatorname{Im} \mathcal{L}_T^{(1)} = \int \frac{d^2 p_\perp}{(2\pi)^2} \sum_{p=0}^{\infty} \sum_{n=1}^{\infty} 2K_{\perp,np}^{(l)} e^{-S_{\perp,np}^{(l)}}. \quad (7.55)$$

The relevant instanton actions and prefactors are given by

$$K_{\perp,np}^{(s)} = \frac{(-1)^p (eE) \Theta(|p_\perp| - p_\perp^{min})}{(2\pi)^{1/2} (n\beta m_\perp)^{1/2}} \cdot \frac{\left[ 1 - \left( \frac{n\beta eE}{2m_\perp} \right)^2 \right]^{-1/4}}{\left[ 2\pi p + 2 \sin^{-1} \left( \frac{n\beta eE}{2m_\perp} \right) \right]} \quad (7.56)$$

$$S_{\perp,np}^{(s)} = \frac{m_\perp^2}{2eE} \left[ 2\pi p + 2 \sin^{-1} \left( \frac{n\beta eE}{2m_\perp} \right) + \frac{n\beta eE}{m_\perp} \sqrt{1 - \left( \frac{n\beta eE}{2m_\perp} \right)^2} \right], \quad (7.57)$$

$$K_{\perp,np}^{(l)} = \frac{i}{2} \cdot \frac{(-1)^p (eE) \Theta(|p_\perp| - p_\perp^{min})}{(2\pi)^{1/2} (n\beta m_\perp)^{1/2}} \cdot \frac{\left[ 1 - \left( \frac{n\beta eE}{2m_\perp} \right)^2 \right]^{-1/4}}{\left[ 2\pi(p+1) - 2 \sin^{-1} \left( \frac{n\beta eE}{2m_\perp} \right) \right]} \quad (7.58)$$

$$S_{\perp,np}^{(l)} = \frac{m_\perp^2}{2eE} \left[ 2\pi(p+1) - 2 \sin^{-1} \left( \frac{n\beta eE}{2m_\perp} \right) - \frac{n\beta eE}{m_\perp} \sqrt{1 - \left( \frac{n\beta eE}{2m_\perp} \right)^2} \right], \quad (7.59)$$

where

$$\Theta(x) = \begin{cases} 1 & x \geq 0 \\ 0 & x < 0 \end{cases} \quad (7.60)$$

is Heaviside's step function. The resulting total decay rate obtained from integrating these expressions over  $p_{\perp}$  is given in figure 7.2.

One might expect that this representation is dangerous because of the threshold singularities in the prefactors, which are present at all values of transverse momentum. It could seem that the use of a uniformization technique such as the one presented in section 7.3 would be paramount. However, the singularities are quite mild, and the results obtained here are largely insensitive to whether or not they have been removed.

## 7.5 THE THERMAL SCHWINGER PROCESS IN SPINOR QED

I discussed in section 3.3 how the worldline formalism can be extended to spinor electrodynamics. The worldline solutions remain identical apart from an overall factor of 1/2 in the effective action, and the path integral now carries a “spin factor” (3.36)

$$Sp[x, A] = \text{Tr} \mathcal{P} \exp \left[ \frac{i}{2} \sigma_{\mu\nu} \int_0^{\tau} ds F_{\mu\nu}(x(\tau)) \right] \quad (7.61)$$

where the symbol  $\mathcal{P}$  indicates path ordering of the exponential and the trace is the Dirac trace. For the special case of constant  $F_{\mu\nu}$  considered here, path ordering is unnecessary, and the spin factor is

$$Sp[x, A] = 4 \cos \left[ e \int_0^s d\tau E(x(\tau)) \right] \quad (7.62)$$

which reduces in the saddle-point approximation to

$$Sp[x, A] = 4 \cos(es_0 E). \quad (7.63)$$

At zero temperature the spin factor reduces to  $(-1)^p$  even for various inhomogenous field configurations. It has been conjectured that this is a general topological property of worldline instantons [54], which seems likely. The conjecture does not hold at finite temperature, however, because the solutions are not full circles. With the known values of  $s_0$  for short and long path solutions,

$$s_0^{(s)} = \frac{\theta_n + 2\pi p}{2eE}, \quad s_0^{(l)} = \frac{2\pi - \theta_n + 2\pi p}{2eE}, \quad (7.64)$$

we obtain

$$Sp[x, A] = \pm 4(-1)^p \sqrt{1 - \left(\frac{n\beta eE}{2m}\right)^2}, \quad (7.65)$$

where the plus sign is taken for short path solutions. Clearly, the spin factor cancels the singularities in the prefactors (6.31) and (6.36), which become zeros. The full prefactors are given by

$$K_{np}^{(s)} = \frac{2(-1)^n (eE)^2}{(2\pi)^{3/2} (n\beta m)^{1/2}} \cdot \frac{\left[1 - \left(\frac{n\beta eE}{2m}\right)^2\right]^{1/4}}{\left[2\pi p + 2 \sin^{-1}\left(\frac{n\beta eE}{2m}\right)\right]^2} \quad (7.66)$$

$$K_{np}^{(l)} = \frac{i}{2} \cdot \frac{2(-1)^n (eE)^2}{(2\pi)^{3/2} (n\beta m)^{1/2}} \cdot \frac{\left[1 - \left(\frac{n\beta eE}{2m}\right)^2\right]^{1/4}}{\left[2\pi(p+1) - 2 \sin^{-1}\left(\frac{n\beta eE}{2m}\right)\right]^2}. \quad (7.67)$$

Additionally, implementing fermions correctly at finite temperature requires antiperiodic boundary conditions on the Euclidean time direction. This is implemented easily as a factor of  $(-1)^n$  in the image charge construction (6.4). The long-path solution with the largest value of  $n$  has the smallest action, so the boundary conditions may cause the decay rate of the metastable state to become negative. This is surprising, but not unprecedented. An example is the spectrum of radiation produced by a Kerr black hole. It is well known that black holes formed from a collapsing body radiate with a thermal spectrum [93]. The spectrum of rotating black holes differs from the Schwarzschild case by the addition of a ‘‘chemical potential’’ term

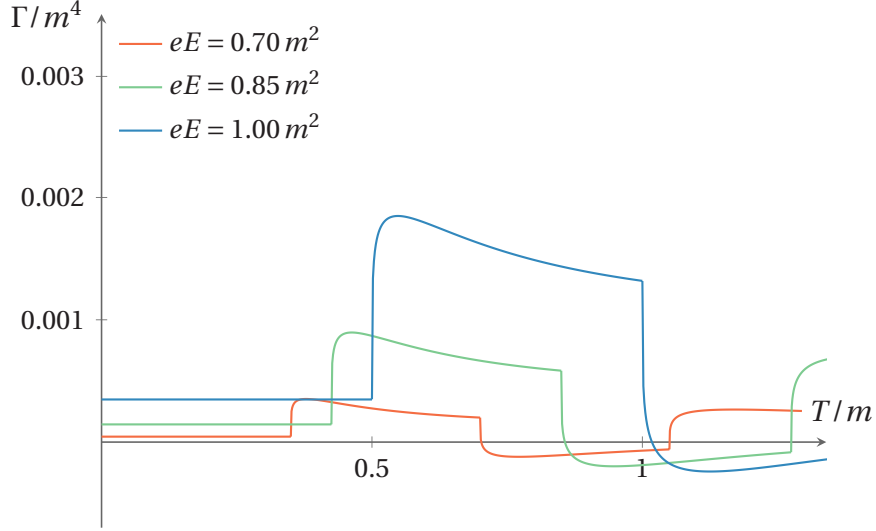


Figure 7.3: The total one-loop decay rate for spinors  $\Gamma = \Gamma_0 + \Gamma_T$  divided by  $m^4$  versus  $T/m$  for various values of  $eE/m^2$ . The leftmost part of each curve represents the contribution of  $\Gamma_0$  alone.

in the Planck factor [130]. For bosonic particles,

$$\rho(\omega, m) = \frac{1}{e^{2\pi\kappa^{-1}(\omega-r\Omega)} - 1}, \quad (7.68)$$

where  $\kappa$  is the surface gravity of the black hole,  $\Omega$  is the angular speed at the event horizon, and  $m$  is an azimuthal quantum number. When  $\omega < m\Omega$ , this factor becomes negative, and for sufficiently cold black holes, the overall luminosity may be negative. This is connected with the classical phenomenon of superradiance, which is in fact unrelated to Hawking radiation and is in place even for rotating stars.

The imaginary part of the effective action and its connection to the decay of metastable states has been thoroughly studied by Langer [96]; see also Zwerger [131] and Newman and Schulmann [132]. Probably the most natural interpretation for the present context is in a steady state sense: the physical situation is such that the metastable state is replenished continuously, and the decay rate represents a probability current exiting the metastable region. If the spatial region containing the electric has finite extent, a negative decay rate simply means that particles are removed from the region faster than they are produced via the Schwinger process. At finite

temperature, both the “forward” process, where particles are produced from the vacuum, as well as the “reverse” process, where real particles from the gas tunnel back into the void, are possible. Pauli blocking operates in both senses of the reaction, and may suppress either more strongly depending on the energy spectra inside and outside the metastable region. However, a detailed physical picture of this process is at present not available.

## 7.6 DISAGREEMENTS ON THERMAL SCHWINGER EFFECTS

There has been a long-standing lack of clarity on the issue of thermal corrections to Schwinger’s formula. There has been some disagreement between results computed in different methods, and some previously published derivations were later found to be incorrect [34]. In fact, prior to this work, to the best of our knowledge no correct expressions for the effective action in the presence of an electric field derived in the imaginary-time formalism had been derived. Some authors [18, 34], upon failing to derive the one-loop thermal correction from first principles, provided plausibility arguments that this correction should vanish. The same result was found through different methods [108], which seemed to bolster this conclusion.

Our conclusions differ from this previous apparent consensus, so the contradiction must be explained. In particular, I will explain why our conclusions differ from those of Hallin and Liljenberg [108], as their work is a complete derivation of pair production in a thermal medium using the elegant functional Schrödinger formalism. Their main conclusion is that, while the thermal medium enhances the production of particles for short times, as  $t \rightarrow \infty$  the enhancement disappears and the pair production rate reduces to the zero-temperature result of Schwinger [4]. In fact, I do not dispute this conclusion: their calculation represents how the presence of an electric field affects a density matrix which initially represents a thermal state. Clearly, in this type of situation two effects must happen: pair production via the Schwinger process, and ordinary acceleration of the particles in the gas. Because of this second effect,



over time the gas is no longer thermally distributed, and positive and negative charges become separated. Our formalism does not apply straightforwardly to this situation. As pointed out by Langer [96], the imaginary part of the effective action should be interpreted in a steady-state sense: the system is held in a given thermal state, which is continuously replenished, and the imaginary part of the effective action is related to a flux of particles exiting the metastable region. This set of assumptions, rather than those implemented in the work of Hallin and Liljenberg, seems to better represent the physical situation inside a flux tube. A flux tube is a comparatively small region, where chromoelectric fields are large, within the larger thermal medium of the quark gluon plasma. Degrees of freedom within the flux tube are free to exchange energy with the outside plasma, which may be thought of as a reservoir. In contrast, if one seeks a thermal correction to Schwinger's formula for use in a situation where electric fields are large throughout the extent of the plasma itself, the expressions of Hallin and Liljenberg may be more appropriate.

I discussed specifically the work of Hallin and Liljenberg, as there the difference between pair production in early and late time regimes is striking and clear. Similar remarks apply also to the work of Gavrilov and Gitman [133], and Kim, Lee, and Yoon [134].

Some recent papers have also considered instanton calculations for Schwinger pair production [135, 136]. Both sets of authors argue that a “lens” shaped trajectory, formed essentially by gluing together two of our short path solutions (see figure 6.1), is the relevant one for computing finite temperature corrections to pair production. Such lens-shaped solutions have been considered previously [6]: they represent the worldline trajectory of a charged particle in an electric field comprising both a constant component and a high frequency component. At either apex of the lens, the particle reflects from a sharp well-like potential, and the overall effect is to decrease the action of the solution, which corresponds to a dynamical enhancement of the Schwinger process by the intense high-frequency light. In a finite temperature system

containing only a constant electric field, there is no such wall potential, and the significance of such solutions becomes less clear.

#### ACKNOWLEDGEMENTS

I thank Gerald Dunne for helpful explanations, and for pointing me to the work of Miller [127].

## CHAPTER 8

### THE SIGN PROBLEM

*Some of the material in this chapter has been previously submitted for publication [137]. This work was done in collaboration with and under the supervision of Dr. Michael Ogilvie.*

In previous chapters I discussed the difficult problem of computing thermal corrections to Schwinger's pair production formula, and the long-standing lack of clarity surrounding the issue. A lattice computation of the thermal QED effective action in the presence of an electric field could have settled the disagreements in a fairly definitive way, and it seems a priori surprising that the problem remained unsolved for so long. Unfortunately, the simulation of electrodynamics in the presence of a constant electric background is made very difficult by the so-called *sign problem*.

Computational methods for reliably calculating a number of equilibrium quantities have been highly developed in lattice field theory and statistical physics. Where these techniques are applicable, they are often considered the standard against which other calculations should be compared. However, standard Monte Carlo methods require an identification between a classical probability distribution over configuration space and a representation of the partition function in terms of positive weights. Unfortunately, there are important systems which for which a representation of the partition function in terms of positive weights is *not* known,

which renders such methods inapplicable. This difficulty is known as the *sign problem* and is a significant obstacle in theoretical physics.

Two more examples of sign problems in lattice field theory are associated with QCD with non-zero chemical potential  $\mu$  [138, 139], and the  $i\phi^3$  field theory, which determines the critical indices of the Lee-Yang edge transition [140]. The sign problem in QCD with  $\mu \neq 0$  is particularly vexing because many interesting questions in particle physics, nuclear physics, and astrophysics depend on the properties of hadronic matter at nonzero baryon density. Lattice simulations have been enormously successful in elucidating the phase structure of QCD and related theories at finite temperature  $T$ , but a complete first-principles understanding of the QCD phase diagram in the  $\mu - T$  plane remains unrealized. The difficult problem of simulating QCD at nonzero  $\mu$  was clear decades ago [141], but a satisfactory algorithm has been elusive. There are several approaches to the sign problem of finite density QCD under active development, including methods based on duality [142], Lefschetz thimbles [143], and complex Langevin equations [144].

## 8.1 COMPUTATIONAL COMPLEXITY OF MONTE CARLO

The failure to develop a general solution to the sign problem led Troyer and Wiese to propose that the sign problem is **NP**-hard, which would strongly indicate that no general solution exists [145]. In this section I discuss their demonstration and argue that it fails.

The classes **P** and **NP**, as well as the concept of **NP**-hardness, are central to computational complexity theory. An introduction accessible to physicists can be found in Aaronson’s book [146]. The class **P** can be described informally as the set of yes-or-no questions that can be *efficiently* answered. “Efficiently” here means “in polynomial time”, which in turn means “in a number of steps bounded by a polynomial on the length of the string specifying the problem instance”.

For example, the question “is a given list ordered?” can be answered in time proportional to the length of the list, so it is in the class **P**. Just as informally, the computational class **NP** is defined as the set of yes-or-no questions such that an affirmative<sup>7</sup> answer can be efficiently *verified*. The name **NP** comes from an earlier, equivalent definition of this class and stands for “nondeterministic polynomial time”. Clearly, if a problem is in **P**, it is also in **NP**, but the converse is not known to be true; the question of whether  $\mathbf{P} = \mathbf{NP}$ ? is the single most important open problem in computer science. An example of a problem in **NP** which is not known to be in **P** is: given integers  $N$  and  $M$  with  $M < N$ , does  $N$  have a prime factor less than  $M$ ? There is no known algorithm for determining  $N$ ’s prime factors that runs in a time bounded by a polynomial in the number of digits, but, given a candidate list of prime factors, verifying that the answer is yes is simply a matter of multiplying the factors together to make sure they are indeed prime factors of  $N$ , and then checking if any of them are greater than  $M$ .

A problem in **NP** is said to be **NP**-hard if any problem in **NP** can be efficiently reduced to it. A *reduction* from problem  $P$  to problem  $Q$  is a map from instances of  $p$  of  $P$  to “equivalent” instances of  $q$  of  $Q$ , where “equivalent” means that the answer to  $p$  is “yes” if and only if the answer to  $q$  is also “yes”. If an efficient reduction from  $P$  to  $Q$  exists, an algorithm which solves  $Q$  efficiently also solves  $P$  efficiently. Thus, a problem which is **NP**-hard is, in a sense, “at least as hard as any problem in **NP**.” This description illustrates a common proof strategy for demonstrating that a problem  $Q$  is **NP**-hard: it suffices to exhibit a reduction from  $P$  to  $Q$ , with  $P$  a problem known to be **NP**-hard.

It is widely believed that  $\mathbf{P} \neq \mathbf{NP}$ , which means it is considered unlikely that an efficient algorithm for solving generic instances of problems in **NP** exists, and, in particular, at least some instances of **NP**-hard problems are expected to be intractable. Thus, the claim that the sign

---

<sup>7</sup> The word “affirmative” is important: the set of yes-or-no questions where a *negative* answer is efficiently verifiable is known as the class **co-NP**. The exact nature of the relationship between **NP** and **co-NP** is unknown, but it is widely believed that  $\mathbf{co-NP} \neq \mathbf{NP}$ .

problem is **NP**-hard carries serious consequences: if the problem is expected to be unsolvable in the general case, a proposed solution must be tightly reliant on specific properties of a given instance.

Troyer and Wiese’s demonstration is based on a reduction from the Ising spin glass, which has been known to be **NP**-hard for some time [147]. Specifically, the problem of determining the ground state energy of a system defined by the Hamiltonian

$$H = - \sum_{j,k} J_{jk} \sigma_j \sigma_k, \quad (8.1)$$

where the classical spins  $\sigma_j$  take on values  $\pm 1$ , and the couplings  $J_{jk}$  are either 0 or  $\pm J$ , is **NP**-hard. This problem can be recast as the yes-or-no question of determining whether the ground state energy is less than some constant  $E_0$ . This version of the problem is clearly in the complexity class **NP**: a proposed assignment of values to the classical spins  $\sigma_j$  immediately yields a value of the total energy of the system, which can be compared against the bound  $E_0$ . The discreteness of the energy levels implies that it suffices to consider the mean energy  $\langle E \rangle$  of the system at sufficiently low temperature. For  $\beta J \geq N \log 2 + \log(12N)$ , where  $N$  is the number of sites,  $\langle E \rangle < E_0 + J/2$  if the ground state energy is less than  $E_0$ , and  $\langle E \rangle > E_0 + J$  otherwise.

Given an instance of the Ising spin glass specified by the values of the couplings  $J_{jk}$ , the following quantum mechanical model is constructed,

$$\hat{H} = - \sum_{j,k} J_{jk} \sigma_j^x \sigma_k^x. \quad (8.2)$$

This Hamiltonian commutes with all spins  $\sigma_j^x$ , so they are each a good quantum number, and the spectrum is identical to that of the classical system. An alternate representation as a sum over “worldlines” is given in the Trotter–Suzuki formalism, which is analogous to the usual thermal field theory Matsubara formalism. An introduction in the context of quantum spin

glasses can be found in Chakrabarti and Das [148]. The partition function is written

$$Z = \text{Tr} \exp\left(\beta \sum_{j,k} J_{jk} \sigma_j^x \sigma_k^x\right) = \text{Tr} \left\{ \left[ \exp\left(\frac{\beta}{N_t} \sum_{j,k} J_{jk} \sigma_j^x \sigma_k^x\right) \right]^{N_t} \right\}. \quad (8.3)$$

In the general case where an external biasing field may be present, this identity is still valid in the limit as  $N_t \rightarrow \infty$ , as a consequence of the Trotter product formula. Inserting a complete set of eigenvalues of the  $\sigma_j^z$  and using the cyclic property of the trace we obtain

$$Z = \sum_{j,k} \prod_{j,k} \langle s_{j,0}^z s_{k,0}^z | e^{-\Delta\tau \hat{H}_{jk}} | s_{j,1}^z s_{k,1}^z \rangle \langle s_{j,1}^z s_{k,1}^z | e^{-\Delta\tau \hat{H}_{jk}} | s_{j,2}^z s_{k,2}^z \rangle \dots \quad (8.4)$$

$$\dots \times \langle s_{j,N_t-1}^z s_{k,N_t-1}^z | e^{-\Delta\tau \hat{H}_{jk}} | s_{j,0}^z s_{k,0}^z \rangle,$$

where  $\Delta\tau \equiv \beta/N_t$ ,  $\hat{H}_{jk} \equiv J_{jk} \sigma_j^x \sigma_k^x$ , and the sum is over classical spin configurations on the space of  $N_t$  copies of the original system. The problem then reduces to computing the matrix elements in this expression. Thus

$$\langle ++ | e^{-\Delta\tau \hat{H}_{jk}} | ++ \rangle = \langle -- | e^{-\Delta\tau \hat{H}_{jk}} | -- \rangle = \cosh(\Delta\tau J_{jk}) \quad (8.5)$$

$$\langle ++ | e^{-\Delta\tau \hat{H}_{jk}} | -- \rangle = \langle -- | e^{-\Delta\tau \hat{H}_{jk}} | ++ \rangle = \sinh(\Delta\tau J_{jk}) \quad (8.6)$$

$$\langle +- | e^{-\Delta\tau \hat{H}_{jk}} | -+ \rangle = \langle -+ | e^{-\Delta\tau \hat{H}_{jk}} | +- \rangle = \sinh(\Delta\tau J_{jk}), \quad (8.7)$$

with all other matrix elements vanishing.

The partition function is now represented as a sum over weights. If all the  $J_{jk} \geq 0$ , that is, in the case of purely ferromagnetic couplings, all weights are positive, and the loop algorithm permits an evaluation of thermal averages in polynomial time [149]. If there is at least one antiferromagnetic coupling  $J_{jk} < 0$ , some of the terms in the partition sum (8.4) are negative, and no efficient algorithm is known.

The authors of [145] then conclude that the sign problem is the *origin of the NP-hardness* of the quantum spin glass, and thus, that the sign problem itself should be regarded as **NP-hard**. This last step seems somewhat suspect, and should be examined carefully.

Implicit in our discussion is the notion of a *computational problem*, which can be thought of a mathematical object representing a set of well-defined questions that might be answered by a computer. The sign problem does not represent a set of well-defined questions, so it is *not* a computational problem. Rather, it is a *property* of certain *representations* of physical problems. Strictly speaking, a property cannot be **NP-hard**. For example, the well-known problem **CLIQUE** is **NP-hard** in general, but can be efficiently solved for planar graphs: it suffices to check subgraphs with 4 vertices or less, as a complete subgraph with 5 vertices or more always makes the supergraph nonplanar [150]. This does not establish that nonplanarity itself is **NP-hard**, merely that, *for the particular case of CLIQUE*, restricting oneself to planar instances makes the problem more tractable. Similarly, *in the specific case of the spin glass*, examples with no antiferromagnetic couplings are easier to solve.

That the sign problem is representation-specific bears emphasizing. Troyer and Wiese's demonstration rests upon the property that their representation of the quantum spin glass has a sign problem if and only if there is at least one antiferromagnetic coupling. It is easy to obtain a representation with just the opposite property, that is, which has a sign problem if and only if there is *no* antiferromagnetic coupling. The reduction is as follows. Given a spin glass defined by the classical Hamiltonian (8.1), we construct the quantum mechanical Hamiltonian

$$\hat{H} = - \sum_{j,k} J_{jk} \sigma_j^z \sigma_k^z \quad (8.8)$$

if there is at least one antiferromagnetic coupling, and

$$\hat{H} = - \sum_{j,k} J_{jk} \sigma_j^y \sigma_k^y \quad (8.9)$$



otherwise. The representation (8.8) is always a sum over positive weights, irrespective of the signs of the couplings, while (8.9) always has both positive and negative weights. It may seem undesirable that the reduction selected specifically for antiferromagnetic couplings. This kind of aesthetic consideration should not be dismissed if one is attempting to construct an elegant, parsimonious physical theory, but is ultimately irrelevant for computational complexity.

This example shows that the proof strategy employed in [145] is inadequate for characterizing the computational complexity challenges associated with sign problems. The authors assert in footnote 4, “Note that the conclusions drawn in this Letter are independent of the representation”. What can indeed be concluded independently of representation is that computing thermal averages in quantum spin glasses is **NP**-hard. On the other hand, the statements concerning the sign problem are specific to the choice of representation of quantum spin glasses. Since a representation of the quantum spin glass solely in terms of positive weights is immediate, clearly the hardness cannot be due to the sign problem, and is best attributable to the (representation-independent) nonconvexity of the energy landscape.

The authors define a *solution to the sign problem* as “an algorithm of polynomial complexity to evaluate the thermal average  $\langle A \rangle$ ”. This definition clearly demands too much: even for the classical spin glass, straightforwardly representable in terms of positive weights, such an algorithm does not exist unless **P** = **NP**. That the simulation may become trapped in local minima of the free energy and thus fail to compute the thermal average accurately is not a failure of the simulation. A physical system described by the same Hamiltonian would also be expected to become trapped in local minima, and relax to thermal equilibrium only after an exponential amount of time. If it were otherwise, a strategy for solving **NP**-hard problems efficiently would be to build in the laboratory a system described by the Hamiltonian (8.2), cool it down, and physically measure the spins at each site. Such a strategy is unlikely to work unless quantum computers can solve **NP**-hard problems in polynomial time, which is considered

unlikely<sup>8</sup> [151]. The strategy has since been attempted at D-Wave Systems. Whether it results in any speedup at all over classical algorithms is a matter of contention [152]; an *exponential* speedup seems extremely implausible, especially in a realistic material that a physicist may wish to study using Monte Carlo simulation. In summary, the **NP**-hardness of the quantum spin glass is a statement about the physical system itself, not its simulation. The physicist's task is not to find thermal averages quickly, but rather to ensure that the simulation accurately captures the physics of the system, including the exponential time to equilibrium.

Any system described by a self-adjoint Hamiltonian has real energy eigenvalues, and thus a representation of the partition function as a sum over positive weights *always* exists. The difficulty lies in finding such a representation without having to solve the problem completely. Analogous situations have been encountered previously in computer science. One example is the complexity of Nash equilibria: it can be proven that a mixed Nash equilibrium always exists [153], but actually *finding* one can be very difficult. This difficulty has been characterized in various ways. The problem of finding a Nash equilibrium was demonstrated to be complete for the class **PPAD** [154], which is weaker evidence of intractability than **NP**-hardness. It has also been shown that determining whether a *second* Nash equilibrium exists is **NP**-hard [155]. Similar approaches may be promising for correctly characterizing the hardness of sign problems.

## 8.2 DUALITY TRANSFORMATION

The three systems mentioned in the introduction—electrodynamics with an electric background,  $i\phi^3$  field theory, and QCD at finite density—have a form of  $PT$  symmetry [156–159, 73]. This symmetry was initially found in the study of generalizations of the  $ix^3$  quantum-mechanical Hamiltonian, where  $P : x \rightarrow -x$  and  $T : i \rightarrow -i$ . A large class of scalar lattice field theories with sign problems have Lagrangians satisfying  $L^*(\phi) = L(-\phi)$ , a form of  $PT$  symmetry.

---

<sup>8</sup>This point was in fact mentioned in the penultimate paragraph of [145].

This symmetry can be found in both continuum and lattice models; it implies that any eigenvalue of the Hamiltonian or transfer matrix is either real or part of a complex conjugate pair. If all the eigenvalues are real, the Hamiltonian or transfer matrix can be made Hermitian by a similarity transformation [160].

I will present a procedure for finding dual forms of the partition function  $Z$  for a large class of such  $PT$ -symmetric scalar field theories; a duality transformation yields representations with real local actions which are easily simulated by standard lattice field theory methods in any number of dimensions. This class includes models in the  $i\phi^3$  universality class as well as charged scalar fields with nonzero chemical potential. Models in this class exhibit a rich set of possible behaviors. Because their transfer matrices are non-Hermitian, they may have complex eigenvalues. This leads to damped oscillations of correlation functions, a behavior well-known in the context of improved actions [161]. This represents a loss of spectral positivity, but is seen in many physical systems, *e.g.* liquids. In some cases, spatially modulated phases occur [162].

Our starting point is a lattice model with a single real scalar field  $\chi$  and a Euclidean lattice action of the form

$$S(\chi) = \sum_x \left[ \frac{1}{2} (\partial_\mu \chi(x))^2 + V(\chi(x)) \right] \quad (8.10)$$

where the sum is over all lattice sites  $x$ , and  $\partial_\mu \chi(x) \equiv \chi(x + \hat{\mu}) - \chi(x)$ . The potential  $V$  is taken to satisfy the  $PT$  symmetry condition  $V(-\chi) = V(\chi)^*$ . Because of this condition, the Fourier transform  $\tilde{w}(\tilde{\chi})$  of  $w(\chi) \equiv \exp[-V(\chi)]$  with respect to  $\chi$  is real. If  $\tilde{w}(\tilde{\chi})$  is everywhere positive, we say that the *dual positivity condition* is satisfied and define a real function  $\tilde{V}(\tilde{\chi}) = -\log(\tilde{w}(\tilde{\chi}))$ .

The partition function is

$$Z[h] = \int \prod_x d\chi(x) \exp \left[ -S(\chi(x)) + \sum_x i h(x) \chi(x) \right] \quad (8.11)$$

where  $h(x)$  is an arbitrary source. We rewrite  $Z$  as

$$Z = \int \prod_x d\pi_\mu d\tilde{\chi} d\chi \exp \left\{ - \sum_x \left[ \frac{1}{2} \pi_\mu^2 + i \pi_\mu \partial_\mu \chi + \tilde{V}(\tilde{\chi}) + i \chi (\tilde{\chi} + h) \right] \right\} \quad (8.12)$$

where the spacetime dependency of the fields  $\phi(x)$ ,  $\chi(x)$  and source  $h(x)$  has been suppressed. After a lattice integration by parts, the integral over  $\chi$  yields

$$Z = \int \prod_x d\pi_\mu \exp \left\{ - \sum_x \left[ \frac{1}{2} \pi_\mu^2 + \tilde{V}(\partial \cdot \pi - h) \right] \right\}. \quad (8.13)$$

This represents a dual form of the partition function where the field  $\pi$  and the action are both real, similar to dual forms for models with fields defined on compact manifolds. Thus, when the dual positivity condition is satisfied, the partition function has a manifestly positive form and the sign problem is solved. In the more general case where the dual positivity condition does not hold, the same procedure reduces the problem of simulating a complex action to the simulation of a system with a true sign problem where all weights are real. In the former case, the strategy for simulation of the model is clear: one simulates the new action

$$\tilde{S}[\pi_\mu] = \sum_x \left[ \frac{1}{2} \pi_\mu^2(x) + \tilde{V}(\partial \cdot \pi(x)) \right] \quad (8.14)$$

using standard methods. There is a clear extension to the case of more than one  $PT$ -symmetric scalar field. Correlation functions of the original field  $\chi$  may be obtained in the usual way by differentiation with respect to  $h(x)$ . In particular, non-coincident correlation functions of  $\chi$  are obtained in the new representation using the field  $i\tilde{V}'(\partial \cdot \pi(x))$ . Although the field  $\chi$  is real, note that the expectation value of  $\chi$  is either zero or purely imaginary, as a consequence of the complex weights in the original form of  $Z$ . A real expectation value for  $\chi$  would violate  $PT$  symmetry.

Conditions on functions  $w$  which satisfy the dual positivity condition can be obtained from Bochner's theorem, which states that a function  $\tilde{w}(k)$  on a locally compact abelian group

is positive if and only if  $w(x)$  is positive-definite, that is, the matrix  $w(x_j - x_k)$  has positive eigenvalues for any choice of the set  $\{x_j\}$ . This theorem is easily understood from the formula

$$\int dx \psi^*(x) w(x) \psi(x) = \int \frac{dk}{2\pi} \frac{dq}{2\pi} \tilde{\psi}^*(k) \tilde{w}(k-q) \tilde{\psi}(q). \quad (8.15)$$

The simplest of the constraints imposed by Bochner's theorem is  $V(x) + V(-x) > 2V(0)$ . This constraint excludes the double-well potential and other potentials that lead to conventional spontaneous symmetry breaking at tree level. This is consistent with  $PT$  symmetry which demands that  $\langle \chi \rangle^* = -\langle \chi \rangle$ , i.e., that  $\langle \phi \rangle$  be purely imaginary. This limitation does not seem fundamental, because this constraint does not appear in other duality-based treatments of complex actions [163].

In the general case, it may be simplest to take the form of the dual potential  $\tilde{V}$  as given, and determine the parameters of  $V$  from it. In general,  $V$  will then contain nonrenormalizable interactions. Such interactions correspond to irrelevant operators in the continuum limit. They do not affect, for example, critical indices, which depend only on the universality class. If one parametrizes  $V$  as a polynomial in  $\phi$ ,  $V = \sum_n g_n \phi^n / n!$ , then the coefficients  $g_n$  are naturally obtained from the generating functional of the zero-dimensional dual theory defined by

$$g_n \equiv \left. \frac{\partial^n V}{\partial \chi^n} \right|_{\chi=0} = -(i)^n \langle \tilde{\chi}^n \rangle_c, \quad (8.16)$$

the cumulant of the dual variable  $\tilde{\chi}$  averaged with weight  $\tilde{w}(\tilde{\chi})$ . The mass parameter of  $V$  is given by  $g_2 = \langle \tilde{\chi}^2 \rangle_c = \langle \tilde{\chi}^2 \rangle - \langle \tilde{\chi} \rangle^2$  and is therefore always positive. It follows that in the dual theory the case  $g_2 = 0$  can only be obtained by a limiting process, and the region with  $g_2 < 0$  is not directly accessible. Note that  $g_2$  is the bare parameter, defined at the scale of a lattice spacing. For a generic dual potential  $\tilde{V}$ , the coupling  $g_3$  is nonzero and imaginary, so critical behavior is naturally in the  $i\phi^3$  universality class. An indirect approach to the case  $g_2 < 0$  is discussed in section 8.3.4.

### 8.3 APPLICATION TO COUPLED MODELS

It is very interesting to consider the coupling of  $PT$ -symmetric fields to normal fields [164]. We write the action as

$$S(\phi) = \sum_x \left[ \frac{1}{2} (\partial_\mu \phi(x))^2 + \frac{1}{2} (\partial_\mu \chi(x))^2 + V(\phi(x), \chi(x)) \right] \quad (8.17)$$

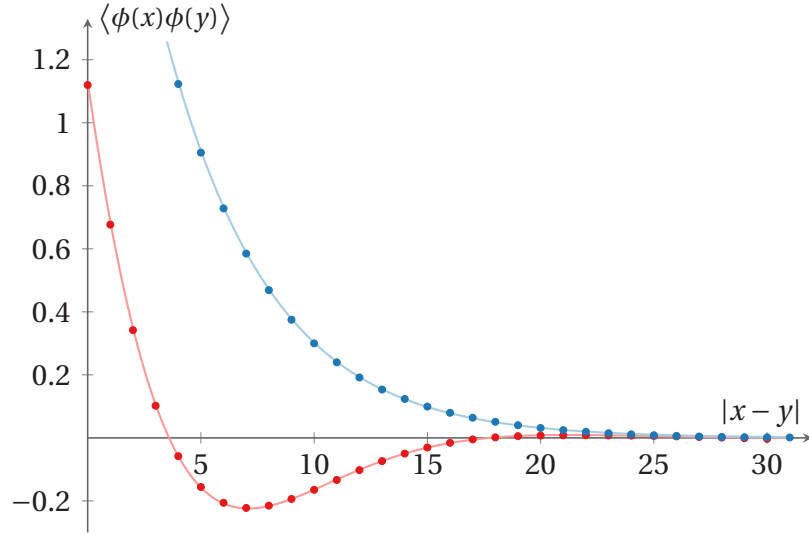
where the potential obeys the condition  $V(\phi(x), \chi(x))^* = V(\phi(x), -\chi(x))$ . Following similar steps applied to  $\chi$  as those given above, we arrive at a dual action of the form

$$\tilde{S} = \sum_x \left[ \frac{1}{2} (\partial_\mu \phi(x))^2 + \frac{1}{2} \pi_\mu^2(x) + \tilde{V}(\phi(x), \partial \cdot \pi(x) - h(x)) \right]. \quad (8.18)$$

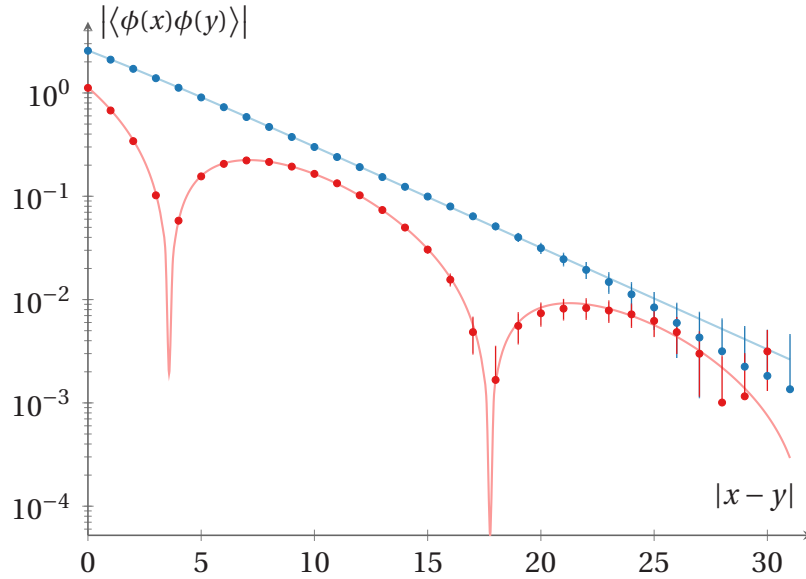
As in the case of a single field, expectation values involving  $\chi$  can be obtained from  $i\partial\tilde{V}'(\phi, \partial \cdot \pi) / \partial(\partial \cdot \pi)$ .

In this class of models  $\phi$  and  $\chi$  play roles similar to the real and imaginary parts of the Polyakov loop,  $P_R$  and  $P_I$ , in QCD at finite temperature  $T$  and chemical potential  $\mu$ . The Polyakov loop  $P = P_R + iP_I$  is associated with the free energy required to insert a very heavy quark into the system via  $\langle P \rangle = \exp(-F_Q/T)$ ;  $\langle P^* \rangle$  is related to the free energy  $F_{\bar{Q}}$  for insertion of a heavy antiquark. When  $\mu = 0$ ,  $P_R$  develops a real expected value and  $\langle P_I \rangle = 0$  such that  $F_Q = F_{\bar{Q}}$ . When  $\mu \neq 0$ , QCD has a sign problem, and a variety of techniques show that  $P_I$  acquires an imaginary expectation value [165, 166, 73, 159, 167]. This implies that  $\langle P \rangle \neq \langle P^* \rangle$  and  $F_Q \neq F_{\bar{Q}}$ . Both phenomenological models [159, 73] as well as simplified lattice models of QCD at nonzero density [167] show that correlation functions may exhibit damped oscillatory behavior for some range of parameters.

As a demonstration of the technique and the variety of results which may be obtained, I consider three different models. In all three models,  $S$  is quadratic in  $\chi$  so that both  $V$  and  $\tilde{V}$  are known analytically.



(a)



(b)

Figure 8.1: Propagator  $\langle \phi(x)\phi(y) \rangle$  as a function of  $|x-y|$  for the  $d = 1$  ICQ model on a lattice with 256 sites. In both curves,  $m_\phi^2 = 0.001$  and  $g = 0.1$ . The upper (blue) curves correspond to  $m_\chi^2 = 0.250$ , while the lower (red) curves have  $m_\chi^2 = 0.002$ . The solid lines represent the analytical form of the continuum result. The figure above, 8.1a, shows the propagator plotted on a linear scale, and the one below, 8.1b, shows the absolute value of the propagator plotted on a logarithmic scale. In the upper graph, the errors bars on all points are smaller than the points themselves. In the lower graph, error bars which intersect zero are not drawn.

### 8.3.1 ICQ model

Our first model is exactly solvable but displays nontrivial behavior. This imaginary-coupled quadratic (ICQ) model has a potential  $V$  of the form

$$V(\phi, \chi) = \frac{1}{2}m_\phi^2\phi^2 + \frac{1}{2}m_\chi^2\chi^2 - ig\phi\chi. \quad (8.19)$$

The last term in  $V$  makes the weight  $w$  complex. The eigenvalues of the mass matrix are given by  $(m_\phi^2 + m_\chi^2 \pm \sqrt{(m_\phi^2 - m_\chi^2)^2 - 4g^2})/2$ , so there are either two real masses or a complex conjugate pair, as required by the  $PT$  symmetry of the model. A quantum mechanical model of this form was considered in [164, 168]. The dual potential takes the form

$$\tilde{V}(\phi, \partial \cdot \pi) = \frac{1}{2}m_\phi^2\phi^2 + \frac{1}{2m_\chi^2}(\partial \cdot \pi - g\phi)^2. \quad (8.20)$$

Figure 8.1 shows simulation results for the one-dimensional ICQ model in the two different regions, on a lattice of size  $N = 256$ : the difference in behavior is striking between the upper curve where there are two real masses, and the lower curve where there is a complex conjugate mass pair. Similar results were obtained in two-dimensional simulations. The lines represent the analytical form of the continuum result for the propagators, and the error bars on the points are smaller than the points themselves. The nonmonotonicity of the lower curve makes the violation of spectral positivity obvious; in fact the lower curve is a damped sinusoid. The analytical result for the upper curve shows that it is the *difference* of two decaying exponentials, and therefore also violates spectral positivity. It is interesting to note that with the definition  $\psi = (\partial \cdot \pi - g\phi)/m_\chi^2$ , the equations of motion obtained from  $\tilde{S}$  can be reduced to a set of real linear equations for  $\phi$  and  $\psi$ . These equations may be derived from a Lagrangian of the form

$$\frac{1}{2}(\partial\phi)^2 + \frac{1}{2}m_\phi^2\phi^2 - \frac{1}{2}(\partial\psi)^2 - \frac{1}{2}m_\chi^2\psi^2 - g\phi\psi, \quad (8.21)$$

but this Lagrangian is not suitable for lattice simulation due to the negative quadratic terms.



### 8.3.2 ICY model

A second interesting model is the imaginary-coupled scalar Yukawa (ICY) model, where the potential has the form

$$V(\phi, \chi) = \frac{1}{2} m_\phi^2 \phi^2 + \frac{1}{2} m_\chi^2 \chi^2 - i g \chi \phi^2. \quad (8.22)$$

This in turn leads to a dual potential

$$\tilde{V}(\phi, \partial \cdot \pi) = \frac{1}{2} m_\phi^2 \phi^2 + \frac{1}{2 m_\chi^2} (\partial \cdot \pi - g \phi^2)^2. \quad (8.23)$$

Figure 8.2 shows the typical behavior of the propagator  $\langle \phi(x) \phi(y) \rangle$  as a function of  $|x - y|$  for the  $d = 2$  ICY model. An extensive search indicated no signs for a region of parameter space with complex conjugate mass pairs, but we were unable to rule out violations of spectral positivity of the type seen in the ICQ model when both masses are real. It seems possible that this is a model where masses are always real. This is consistent with the large- $m_\chi$  limit: After the rescaling  $\pi_\mu \rightarrow m_\chi \pi_\mu$  and the definition  $\lambda = g^2 / m_\chi^2$  we can take the limit  $m_\chi \rightarrow \infty$  to obtain a potential  $\lambda \phi^4 / 2$ . This is a bosonic form of a familiar argument for fermions: the  $i g \chi \phi^2$  interaction is repulsive and in the large  $m_\chi$  limit becomes a repulsive four-boson interaction [169].

### 8.3.3 ICDW model and spatially modulated phases

Our third example also generalizes the first, but in a different way: we define

$$V(\phi, \chi) = U(\phi) + \frac{1}{2} m_\chi^2 \chi^2 - i g \chi \phi, \quad (8.24)$$

which leads to

$$\tilde{V}(\phi, \partial \cdot \pi) = U(\phi) + \frac{1}{2 m_\chi^2} (\partial \cdot \pi - g \phi)^2. \quad (8.25)$$

The potential  $U$  can be chosen to give a first-order or second-order transition as a function of its parameters when  $g = 0$ . I will consider here the specific case of the imaginary-coupled

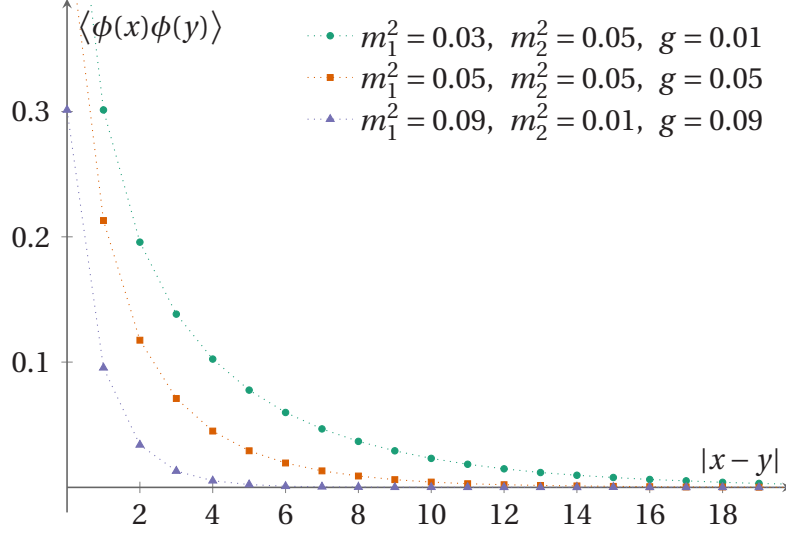


Figure 8.2: Typical results for the propagator  $\langle \phi(x)\phi(y) \rangle$  as a function of  $|x - y|$  for the  $d = 2$  ICY model for three different parameter sets on a  $64^2$  lattice.

double well (ICDW) model, where the potential has the form  $U(\phi) = \lambda(\phi^2 - v^2)^2$ . Because the field  $\chi$  enters quadratically, it may be integrated out, yielding an effective action of the form

$$S = \sum_x \left[ \frac{1}{2} (\partial_\mu \phi(x))^2 + U(\phi) \right] + \frac{g^2}{2} \sum_{x,y} \phi(x) \Delta(x-y) \phi(x) \quad (8.26)$$

where  $\Delta(x)$  is a free Euclidean propagator with mass  $m_\chi$ , i.e., a Yukawa potential. This additional term in the action acts to suppress spontaneous symmetry breaking. Models of this type have been used to model a wide variety of physical systems and are known to produce spatially modulated phases [170–173]. In this class of models the complex form of the action intermediates between a real local form and a real quasilocal form.

If the lowest-energy state is a constant solution  $\phi_0$ , it may be found by minimizing  $U(\phi) + g^2 \phi^2 / 2m_\chi^2$  with respect to  $\phi$ . Linearizing the equation of motion around  $\phi_0$ , the inverse propagator is found to be

$$p^2 + U''(\phi_0) + \frac{g^2}{p^2 + m_\chi^2} \quad (8.27)$$

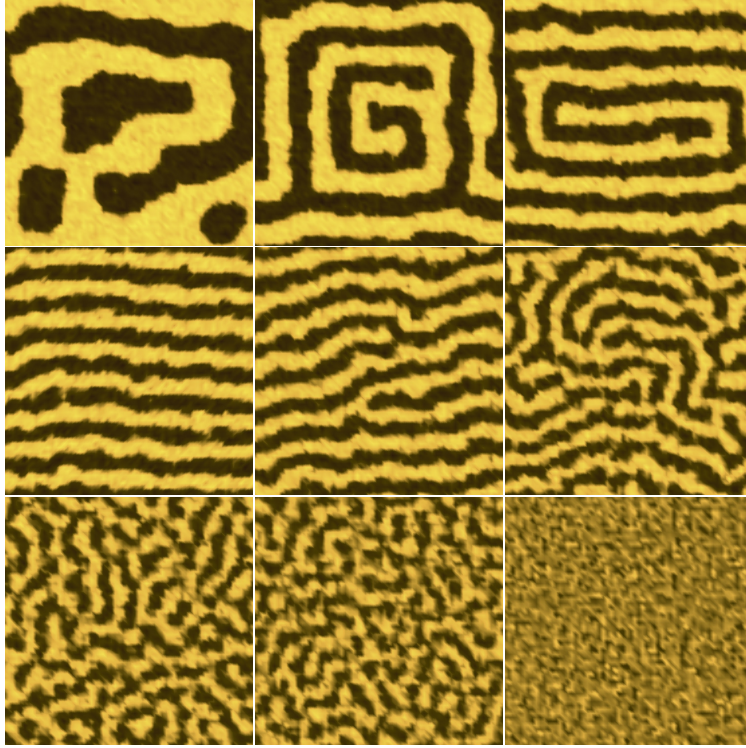


Figure 8.3: Configuration snapshots of  $\phi$  in the two-dimensional ICDW model on a  $64^2$  lattice for several values of  $g$ . From left to right, top to bottom:  $g = 0.8, 0.9, 1.0, 1.1, 1.2, 1.3, 1.4, 1.5$  and  $2.5$ . The other parameters are  $m_\chi^2 = 0.5$ ,  $\lambda = 0.1$  and  $\nu = 3$ .

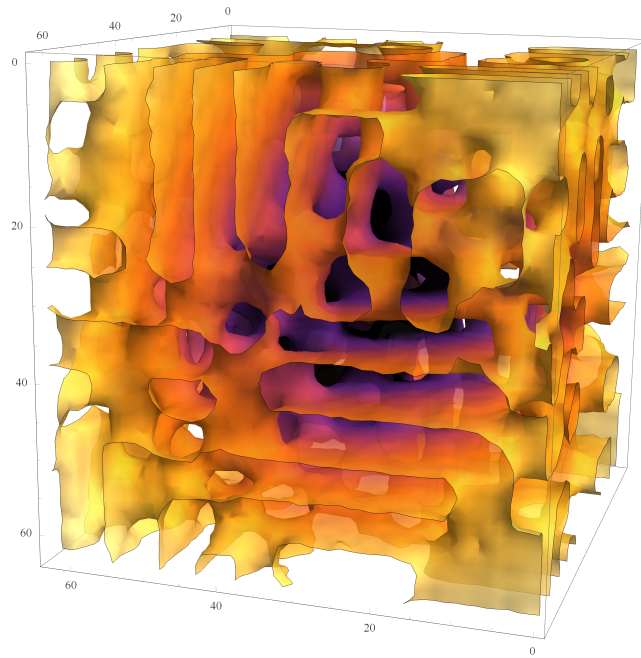
which has a minimum away from zero when  $g > m_\chi^2$ , given by

$$p_{min}^2 = g - m_\chi^2. \quad (8.28)$$

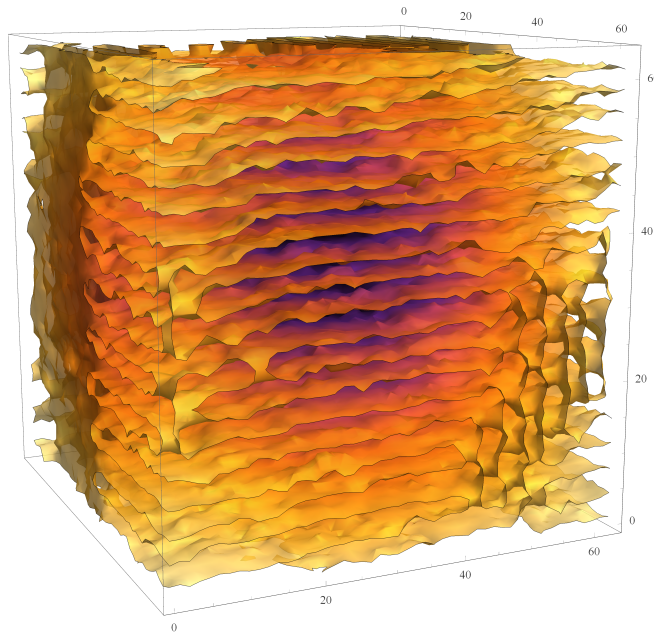
For this value of  $p^2$ , the inverse propagator has the value  $2g - m_\chi^2 + U''(\phi_0)$ . As long as this quantity is positive, the constant solution is stable to fluctuations at  $p^2 = p_{min}^2$ . On the other hand, if the two conditions

$$U''(\phi_0) + \frac{g^2}{m_\chi^2} > 0 \quad (8.29)$$

$$2g - m_\chi^2 + U''(\phi_0) < 0 \quad (8.30)$$



(a)  $g = 1.0$



(b)  $g = 1.4$

Figure 8.4: Configuration snapshots of  $\phi$  in the three-dimensional ICDW model on a  $64^3$  lattice for two values of  $g$ . The other parameters are  $m_\chi^2 = 0.5$ ,  $\lambda = 0.1$  and  $\nu = 3$ . The surfaces represent the domain walls between  $\phi > 0$  and  $\phi < 0$  regions. The color has no meaning and is meant only to guide the eye.

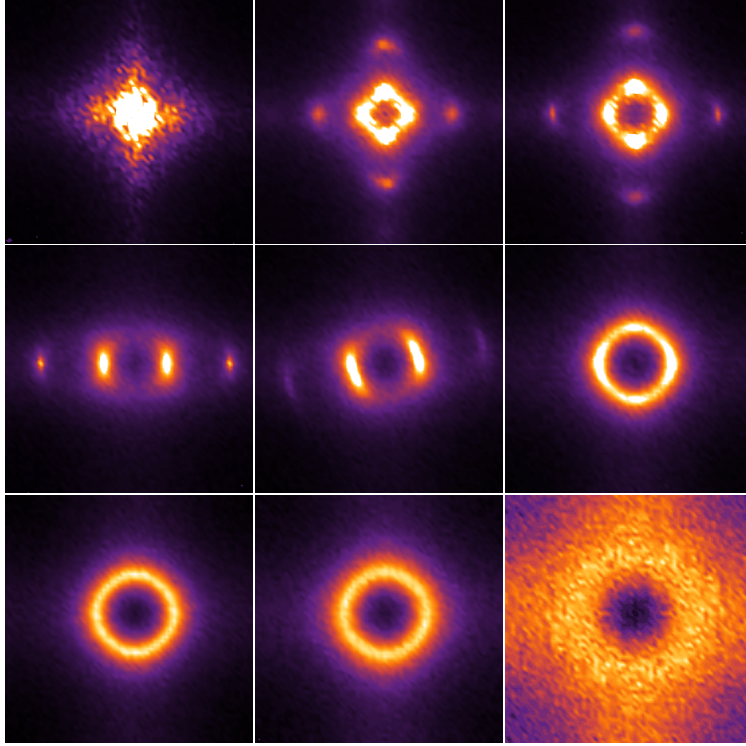


Figure 8.5: The Fourier transform  $\tilde{\phi}(k)$  in the  $d = 2$  ICDW model on a  $64^2$  lattice for several values of  $g$ , averaged over 200 Monte Carlo steps. From left to right, top to bottom:  $g = 0.8, 0.9, 1.0, 1.1, 1.2, 1.3, 1.4, 1.5$  and  $2.5$ . The other parameters are  $m_\chi^2 = 0.5$ ,  $\lambda = 0.1$  and  $\nu = 3$ .

are simultaneously satisfied, then  $\phi_0$  will be unstable to modulated behavior with wavenumber  $p_{min}$ . For  $U(\phi)$  a double well, this instability leads to a region where spatially modulated behavior occurs in lattice simulations of the dual form of the theory, as shown in the configuration snapshots for  $d = 2$  in figure 8.3. Light and dark portions represent positive and negative values of  $\phi$ , respectively. The length scale of the modulations decreases as  $g$  increases and the system moves toward restoration of the broken symmetry. Figure 8.5 shows that the mean spectral weight is concentrated on a ring at a specific wavenumber  $p_{min}$ , which increases with increasing  $g$ . For  $g = 0.9, 1.0, 1.0, 1.1, 1.2$ , it is also possible to see distinct peaks at higher wavenumber. These peaks are harmonics occurring at three times the fundamental frequency determined by  $p_{min}$ , and correspond to the fact that the value of the field is approximately constant within each discrete phase. Similar behavior is seen for  $d = 1$  and  $d = 3$ .

### 8.3.4 The $i\phi^3$ theory

The formalism for two coupled fields gives us an interesting construction of a model in the  $i\phi^3$  universality class. We write the action as

$$S(\phi) = \sum_x \left[ \frac{1}{2} (\partial_\mu \phi(x))^2 + \frac{1}{2} (\partial_\mu \chi(x))^2 + U(\phi) + \frac{1}{2} m_\chi^2 \chi^2 - i g \chi \phi \right], \quad (8.31)$$

with the potential  $U$  in the form

$$U(\phi) = \sum_{n=2}^N g_n \frac{\phi^n}{n!}, \quad (8.32)$$

with real couplings  $g_n$ . We can designate  $g_2$  as  $m_\phi^2$ , but its sign is unrestricted. If we take the mass  $m_\phi$  to be heavy compared to, e.g.  $m_\chi^2$  and  $g$ , each  $\phi$  vertex will generate a vertex in an low-energy effective action for  $\chi$  of the form  $g_n (-i g \chi)^n / n! M^n$ . The only restriction is that  $N$  must be even with  $g_N > 0$  [140].

## 8.4 THE BOSE GAS AT FINITE DENSITY

In the problem of a complex scalar field in the presence of a chemical potential  $\mu$ , the sign problem is associated with the kinetic term, rather than the potential term, so naively it might appear that the formalism presented here is inapplicable. Fortunately, the naive expectation is incorrect. Consider the contribution to the action due to the timelike links, given by

$$K_0 = (e^\mu \Psi'^* - \Psi^*) (e^{-\mu} \Psi' - \Psi) + \frac{1}{2} m^2 (\Psi'^* \Psi' + \Psi^* \Psi), \quad (8.33)$$

where one half of each mass term was allotted to each vertex. This gives the correct mass contribution when integrated over all links. We write the real and imaginary parts as  $\Psi = (\phi + i\chi)/\sqrt{2}$ , thus

$$\begin{aligned}
K_0 &= \frac{1}{2} \begin{pmatrix} \phi' \\ \phi \end{pmatrix}^\top A \begin{pmatrix} \phi' \\ \phi \end{pmatrix} + \frac{1}{2} \begin{pmatrix} \chi' \\ \chi \end{pmatrix}^\top A \begin{pmatrix} \chi' \\ \chi \end{pmatrix} + B^\top \begin{pmatrix} \chi' \\ \chi \end{pmatrix}; \\
A &\equiv (1 + \frac{1}{2}m^2 - \sigma_1 \cosh \mu), \quad B \equiv \begin{pmatrix} \phi' \\ \phi \end{pmatrix} \sigma_2 \sinh \mu.
\end{aligned} \tag{8.34}$$

Here,  $\sigma_k$  are the Pauli matrices. The key step is to write

$$\frac{1}{2} \begin{pmatrix} \chi' \\ \chi \end{pmatrix}^\top A \begin{pmatrix} \chi' \\ \chi \end{pmatrix} = \frac{1}{2} \begin{pmatrix} \chi' \\ \chi \end{pmatrix}^\top \left( 1 + \frac{m^2}{2} - \cosh \mu \right) \begin{pmatrix} \chi' \\ \chi \end{pmatrix} + \frac{1}{2} \cosh \mu \begin{pmatrix} \chi' \\ \chi \end{pmatrix}^\top \begin{pmatrix} 1 & -1 \\ -1 & 1 \end{pmatrix} \begin{pmatrix} \chi' \\ \chi \end{pmatrix}. \tag{8.35}$$

The term in the second line has the standard form of a kinetic term, only rescaled by a factor  $\cosh \mu$ , and can be dualized without difficulty. The first term on the right-hand side is diagonal, and thus contributes to the potential  $V(\chi)$ . The potential energy at each site  $x$  is obtained by adding the contributions of both links with  $x$  as the endpoint. Therefore, the potential  $V$  reads

$$\begin{aligned}
V(\chi(x)) &= \frac{1}{2} M^2 (\chi(x))^2 - i g \chi(x) [\phi(x + \hat{e}_4) - \phi(x - \hat{e}_4)]; \\
M^2 &\equiv 2(1 + \frac{1}{2}m^2 - \cosh \mu), \quad g \equiv \sinh \mu.
\end{aligned} \tag{8.36}$$

The continuum form of this result is

$$V(\chi) = \frac{m^2 - \mu^2}{2} \chi^2 - 2i\mu \chi \dot{\phi} \tag{8.37}$$

where  $\dot{\phi} \equiv \partial_4 \phi$ . Clearly, this reduces to the correct limiting form when  $\mu \rightarrow 0$ . It is now easy to dualize the action, which gives

$$\tilde{S} = \frac{1}{2} \cosh \mu (\partial_4 \phi) + \frac{1}{2} (\nabla \phi)^2 + \frac{1}{2} M^2 \phi^2 + \frac{1}{2} \pi_\mu^2 + \tilde{V}(\phi, \pi_\mu) \tag{8.38}$$

$$\tilde{V}(\phi, \pi_\mu) = \frac{1}{2M^2} \left( \cosh \mu (\partial_4 \pi_4) + \nabla \cdot \vec{\pi} - \sinh \mu [\phi(x + \hat{e}_4) - \phi(x - \hat{e}_4)] \right)^2. \tag{8.39}$$

It has now become clear why the naive belief (that a sign problem in the hopping term defeats the method) is wrong: only one of the components of the complex field is dualized, and the



action can be written in such a way that the imaginary hopping parameter is attached to the component left intact by the dual transformation.

The same construction is also applicable to the case of electric fields. Recall figure 2.1: the semiclassical spectrum of a particle in the presence of an electric field is identical to that of a particle subject to a spatially varying chemical potential. Since nothing in this derivation is contingent on the constancy of  $\mu$ , it carries over immediately.

Presenting the results of this method will be the subject of future work.

## 8.5 CONCLUSIONS

For scalar field theories with sign problems satisfying the dual positivity condition, the methods developed here enable straightforward simulation with a real local action. Relatively simple models show complicated behaviors that do not occur in conventional field theories, such as complex conjugate mass eigenstates and spatially modulated phases. These models and our simulation method provide a benchmark against which other simulation methods and analytical techniques can be tested. This method allows for simulation of models in the  $i\phi^3$  universality class as well as field theories with a nonzero chemical potential, or in the presence of electric fields.



## REFERENCES

- [1] Lev Davidovich Landau and E. M. Lifshits. *Quantum Mechanics*, volume v.3 of *Course of Theoretical Physics*. Butterworth-Heinemann, Oxford, 1991. ISBN 9780750635394.
- [2] Michael C. Ogilvie. Phases of Gauge Theories. *J.Phys.*, A45:483001, 2012. doi: 10.1088/1751-8113/45/48/483001.
- [3] Barry R. Holstein. Strong field pair production. *Am. J. Phys.*, 67:499–507, 1999. doi: 10.1119/1.19313.
- [4] Julian S. Schwinger. On gauge invariance and vacuum polarization. *Phys. Rev.*, 82: 664–679, 1951. doi: 10.1103/PhysRev.82.664.
- [5] Gerald V. Dunne. New Strong-Field QED Effects at ELI: Nonperturbative Vacuum Pair Production. *Eur. Phys. J.*, D55:327–340, 2009. doi: 10.1140/epjd/e2009-00022-0.
- [6] Ralf Schutzhold, Holger Gies, and Gerald Dunne. Dynamically assisted Schwinger mechanism. *Phys. Rev. Lett.*, 101:130404, 2008. doi: 10.1103/PhysRevLett.101.130404.
- [7] A. Casher, H. Neuberger, and S. Nussinov. Chromoelectric Flux Tube Model of Particle Production. *Phys. Rev.*, D20:179–188, 1979. doi: 10.1103/PhysRevD.20.179.
- [8] Bo Andersson, G. Gustafson, G. Ingelman, and T. Sjostrand. Parton Fragmentation and String Dynamics. *Phys. Rept.*, 97:31–145, 1983. doi: 10.1016/0370-1573(83)90080-7.
- [9] Simon Hands. The Phase diagram of QCD. *Contemp. Phys.*, 42:209–225, 2001. doi: 10.1080/00107510110063843.
- [10] V. Skokov, A. Yu. Illarionov, and V. Toneev. Estimate of the magnetic field strength in heavy-ion collisions. *Int. J. Mod. Phys.*, A24:5925–5932, 2009. doi: 10.1142/S0217751X09047570.
- [11] T. Ando, Y. Matsumoto, and Y. Uemura. Theory of Hall Effect in a Two-Dimensional Electron System. *Journal of the Physical Society of Japan*, 39:279, August 1975. doi: 10.1143/JPSJ.39.279.
- [12] Leonard Parker. Quantized fields and particle creation in expanding universes. 1. *Phys. Rev.*, 183:1057–1068, 1969. doi: 10.1103/PhysRev.183.1057.

- [13] T. Vachaspati. Magnetic fields from cosmological phase transitions. *Phys. Lett.*, B265: 258–261, 1991. doi: 10.1016/0370-2693(91)90051-Q.
- [14] Robert C. Duncan and Christopher Thompson. Formation of very strongly magnetized neutron stars - implications for gamma-ray bursts. *Astrophys. J.*, 392:L9, 1992. doi: 10.1086/186413.
- [15] R. P. Mignani, V. Testa, D. Gonzalez Caniulef, R. Taverna, R. Turolla, S. Zane, and K. Wu. Evidence for vacuum birefringence from the first optical-polarimetry measurement of the isolated neutron star RX J1856.5–3754. *Mon. Not. Roy. Astron. Soc.*, 465(1):492–500, 2017. doi: 10.1093/mnras/stw2798.
- [16] W. Heisenberg and H. Euler. Consequences of Dirac’s theory of positrons. *Z. Phys.*, 98: 714–732, 1936. doi: 10.1007/BF01343663.
- [17] Igor A. Shovkovy. Magnetic Catalysis: A Review. *Lect. Notes Phys.*, 871:13–49, 2013. doi: 10.1007/978-3-642-37305-3\_2.
- [18] Per Elmfors and Bo-Sture Skagerstam. Electromagnetic fields in a thermal background. *Phys. Lett.*, B348:141–148, 1995. doi: 10.1016/0370-2693(95)00124-4. [Erratum: *Phys. Lett.* B376,330(1996)].
- [19] O. Klein. Die Reflexion von Elektronen an einem Potentialsprung nach der relativistischen Dynamik von Dirac. *Z. Phys.*, 53:157, 1929. doi: 10.1007/BF01339716.
- [20] A Calogheracos and Norman Dombey. History and physics of the Klein paradox. *Contemp. Phys.*, 40:313–321, 1999. doi: 10.1080/001075199181387.
- [21] Fritz Sauter. Über das Verhalten eines Elektrons im homogenen elektrischen Feld nach der relativistischen Theorie Diracs. *Z. Phys.*, 69:742–764, 1931. doi: 10.1007/BF01339461.
- [22] Morad Aaboud et al. Evidence for light-by-light scattering in heavy-ion collisions with the ATLAS detector at the LHC. *Nature Phys.*, 13(9):852–858, 2017. doi: 10.1038/nphys4208.
- [23] David Tong. Lectures on the Quantum Hall Effect. 2016.
- [24] P. A. M. Dirac. A Theory of Electrons and Protons. *Proc. Roy. Soc. Lond.*, A126:360, 1930. doi: 10.1098/rspa.1930.0013.
- [25] F. Hund. Materieerzeugung im anschaulichen und im gequantelten wellenbild der materie. *Zeitschrift für Physik*, 117(1):1–17, Jan 1941. ISSN 0044-3328. doi: 10.1007/BF01337403.
- [26] Gerald V. Dunne. *Heisenberg-Euler effective Lagrangians: Basics and extensions*. 2004.
- [27] V. Weisskopf. The electrodynamics of the vacuum based on the quantum theory of the electron. *Kong. Dan. Vid. Sel. Mat. Fys. Med.*, 14N6:1–39, 1936.

- [28] Sidney R. Coleman and Erick J. Weinberg. Radiative Corrections as the Origin of Spontaneous Symmetry Breaking. *Phys. Rev.*, D7:1888–1910, 1973. doi: 10.1103/PhysRevD.7.1888.
- [29] L. S. Brown. *Quantum field theory*. Cambridge University Press, 1994. ISBN 9780521469463.
- [30] A. Zee. *Quantum field theory in a nutshell*. 2003. ISBN 0691140340, 9780691140346.
- [31] M. Srednicki. *Quantum field theory*. Cambridge University Press, 2007. ISBN 9780521864497, 9780511267208.
- [32] W. H. Furry. A Symmetry Theorem in the Positron Theory. *Phys. Rev.*, 51:125–129, 1937. doi: 10.1103/PhysRev.51.125.
- [33] A. Kuznetsov and N. Mikheev. Electroweak processes in external electromagnetic fields. *Springer Tracts Mod. Phys.*, 197:1–120, 2004. doi: 10.1007/b97444.
- [34] Holger Gies. QED effective action at finite temperature. *Phys. Rev.*, D60:105002, 1999. doi: 10.1103/PhysRevD.60.105002.
- [35] Ulrich D. Jentschura, Holger Gies, Sree Ram Valluri, Darrell R. Lamm, and Ernst Joachim Weniger. QED effective action revisited. *Can. J. Phys.*, 80:267–284, 2002. doi: 10.1139/p01-139.
- [36] W. Dittrich and H. Gies. *Probing the Quantum Vacuum: Perturbative Effective Action Approach in Quantum Electrodynamics and its Application*. Springer Tracts in Modern Physics. Springer Berlin Heidelberg, 2003. ISBN 9783540455851.
- [37] A. I. Nikishov. Pair production by a constant external field. *Zh. Eksp. Teor. Fiz.*, 57: 1210–1216, 1969.
- [38] S. L. Lebedev and V. I. Ritus. VIRIAL REPRESENTATION OF THE IMAGINARY PART OF THE LAGRANGE FUNCTION OF THE ELECTROMAGNETIC FIELD. *Sov. Phys. JETP*, 59: 237–244, 1984. [*Zh. Eksp. Teor. Fiz.*86,408(1984)].
- [39] Gerald V. Dunne and Christian Schubert. Two loop Euler-Heisenberg QED pair production rate. *Nucl. Phys.*, B564:591–604, 2000. doi: 10.1016/S0550-3213(99)00641-0.
- [40] G.H. Hardy. *Divergent Series*. AMS Chelsea Publishing Series. American Mathematical Society, 2000. ISBN 9780821826492.
- [41] J. C. Le Guillou and Jean Zinn-Justin, editors. *Large order behavior of perturbation theory*. 1990.
- [42] Izrail Solomonovich Gradshteyn, Iosif Moiseevich Ryzhik, Alan Jeffrey, Daniel Zwillinger, and Inc. Scripta Technica. *Table of integrals, series, and products*. Elsevier, Amsterdam, Boston, Paris, et al., 2007. ISBN 0-12-373637-4.

- [43] S. Chadha and P. Olesen. On Borel Singularities in Quantum Field Theory. *Phys. Lett.*, 72B:87–90, 1977. doi: 10.1016/0370-2693(77)90069-7.
- [44] C. Itzykson and J. B. Zuber. *Quantum Field Theory*. International Series In Pure and Applied Physics. McGraw-Hill, New York, 1980. ISBN 9780486445687, 0486445682.
- [45] Z. Bialynicka-Birula and I. Bialynicki-Birula. Nonlinear effects in Quantum Electrodynamics. Photon propagation and photon splitting in an external field. *Phys. Rev.*, D2: 2341–2345, 1970. doi: 10.1103/PhysRevD.2.2341.
- [46] Paul Papatzacos and Kjell Mork. Delbruck Scattering. *Phys. Rept.*, 21:81–118, 1975. doi: 10.1016/0370-1573(75)90048-4.
- [47] Ian K. Affleck, Orlando Alvarez, and Nicholas S. Manton. Pair Production at Strong Coupling in Weak External Fields. *Nucl. Phys.*, B197:509, 1982. doi: 10.1016/0550-3213(82)90455-2.
- [48] R. P. Feynman. Mathematical formulation of the quantum theory of electromagnetic interaction. *Phys. Rev.*, 80:440–457, 1950. doi: 10.1103/PhysRev.80.440.
- [49] Richard P. Feynman. An Operator calculus having applications in quantum electrodynamics. *Phys. Rev.*, 84:108–128, 1951. doi: 10.1103/PhysRev.84.108.
- [50] Zvi Bern and David A. Kosower. The Computation of loop amplitudes in gauge theories. *Nucl. Phys.*, B379:451–561, 1992. doi: 10.1016/0550-3213(92)90134-W.
- [51] Matthew J. Strassler. Field theory without Feynman diagrams: One loop effective actions. *Nucl. Phys.*, B385:145–184, 1992. doi: 10.1016/0550-3213(92)90098-V.
- [52] Christian Schubert. Perturbative quantum field theory in the string inspired formalism. *Phys. Rept.*, 355:73–234, 2001. doi: 10.1016/S0370-1573(01)00013-8.
- [53] Zvi Bern, Lance J. Dixon, and David A. Kosower. Progress in one loop QCD computations. *Ann. Rev. Nucl. Part. Sci.*, 46:109–148, 1996. doi: 10.1146/annurev.nucl.46.1.109.
- [54] Gerald V. Dunne and Christian Schubert. Worldline instantons and pair production in inhomogeneous fields. *Phys. Rev.*, D72:105004, 2005. doi: 10.1103/PhysRevD.72.105004.
- [55] Richard P. Feynman and Albert R. Hibbs. *Quantum Mechanics and Path Integrals: Emended Edition (Dover Books on Physics)*. Dover Publications, emended ed. edition, July 2010. ISBN 0486477223.
- [56] M. C. Gutzwiller. Periodic orbits and classical quantization conditions. *J. Math. Phys.*, 12:343–358, 1971. doi: 10.1063/1.1665596.
- [57] Robert G. Littlejohn. Semiclassical Structure of Trace Formulas. *J. Math. Phys.*, 31: 2952–2977, 1990. doi: 10.1063/1.528949.

- [58] Milton Abramowitz and Irene A. Stegun. *Handbook of Mathematical Functions with Formulas, Graphs, and Mathematical Tables*. Dover, New York, ninth dover printing, tenth gpo printing edition, 1964.
- [59] Leandro Medina and Michael C. Ogilvie. Schwinger Pair Production at Finite Temperature. *Phys. Rev.*, D95(5):056006, 2017. doi: 10.1103/PhysRevD.95.056006.
- [60] Sidney R. Coleman. Quantum Tunneling and Negative Eigenvalues. *Nucl. Phys.*, B298: 178, 1988. doi: 10.1016/0550-3213(88)90308-2.
- [61] J. Q. Liang and H. J. W. Muller-Kirsten. Nonvacuum bounces and quantum tunneling at finite energy. *Phys. Rev.*, D50:6519–6530, 1994. doi: 10.1103/PhysRevD.50.6519.
- [62] Lorenzo Battarra, George Lavrelashvili, and Jean-Luc Lehners. Negative Modes of Oscillating Instantons. *Phys. Rev.*, D86:124001, 2012. doi: 10.1103/PhysRevD.86.124001.
- [63] Sidney R. Coleman. The Uses of Instantons. *Subnucl.Ser.*, 15:805, 1979.
- [64] Gerald V. Dunne, Qing-hai Wang, Holger Gies, and Christian Schubert. Worldline instantons. II. The Fluctuation prefactor. *Phys. Rev.*, D73:065028, 2006. doi: 10.1103/PhysRevD.73.065028.
- [65] J. I. Kapusta and Charles Gale. *Finite-temperature field theory: Principles and applications*. Cambridge University Press, 2011. ISBN 9780521173223, 9780521820820, 9780511222801.
- [66] Claude W. Bernard. Feynman Rules for Gauge Theories at Finite Temperature. *Phys. Rev.*, D9:3312, 1974. doi: 10.1103/PhysRevD.9.3312.
- [67] P.M. Chaikin and T.C. Lubensky. *Principles of Condensed Matter Physics*. Cambridge University Press, 1995. ISBN 9781139648615.
- [68] Peter N. Meisinger and Michael C. Ogilvie. Complete high temperature expansions for one loop finite temperature effects. *Phys. Rev.*, D65:056013, 2002. doi: 10.1103/PhysRevD.65.056013.
- [69] Steven Weinberg. *The Quantum theory of fields. Vol. 1: Foundations*. Cambridge University Press, 2005. ISBN 9780521670531, 9780511252044.
- [70] Mithat Unsal. Abelian duality, confinement, and chiral symmetry breaking in QCD(adj). *Phys. Rev. Lett.*, 100:032005, 2008. doi: 10.1103/PhysRevLett.100.032005.
- [71] Erich Poppitz and Mithat Unsal. Conformality or confinement (II): One-flavor CFTs and mixed-representation QCD. *JHEP*, 12:011, 2009. doi: 10.1088/1126-6708/2009/12/011.
- [72] P. N. Meisinger, T. R. Miller, and M. C. Ogilvie. Phenomenological equations of state for the quark gluon plasma. D65:034009, 2002. doi: 10.1103/PhysRevD.65.034009.

- [73] Hiromichi Nishimura, Michael C. Ogilvie, and Kamal Pangaeni. Complex Saddle Points and Disorder Lines in QCD at finite temperature and density. *Phys. Rev.*, D91(5):054004, 2015. doi: 10.1103/PhysRevD.91.054004.
- [74] G.S. Bali, F. Bruckmann, G. Endrodi, F. Gruber, and A. Schaefer. Magnetic field-induced gluonic (inverse) catalysis and pressure (an)isotropy in QCD. 1304:130, 2013. doi: 10.1007/JHEP04(2013)130.
- [75] T Banks and A Casher. Chiral symmetry breaking in confining theories. B169:103–125, 1980.
- [76] P. N. Meisinger and M. C. Ogilvie. The finite temperature SU(2) Savvidy model with a nontrivial Polyakov loop. D66:105006, 2002. doi: 10.1103/PhysRevD.66.105006.
- [77] M. M. Anousirian. Index Theory and the Axial Current Anomaly in Two-Dimensions. *Phys. Lett.*, 70B:301–305, 1977. doi: 10.1016/0370-2693(77)90663-3.
- [78] Joe E. Kiskis. Fermions in a Pseudoparticle Field. *Phys. Rev.*, D15:2329, 1977. doi: 10.1103/PhysRevD.15.2329.
- [79] N. K. Nielsen and Bert Schroer. Axial Anomaly and Atiyah-Singer Theorem. *Nucl. Phys.*, B127:493–508, 1977. doi: 10.1016/0550-3213(77)90453-9.
- [80] Márcio Ferreira, Pedro Costa, Débora P. Menezes, Constança Providência, and Norberto Scoccola. Deconfinement and chiral restoration within the SU(3) Polyakov–Nambu–Jona-Lasinio and entangled Polyakov–Nambu–Jona-Lasinio models in an external magnetic field. *Phys. Rev.*, D89(1):016002, 2014. doi: 10.1103/PhysRevD.89.016002, 10.1103/PhysRevD.89.019902. [Addendum: *Phys. Rev.* D89, no. 1, 019902(2014)].
- [81] Alejandro Ayala, M. Loewe, and R. Zamora. Inverse magnetic catalysis in the linear sigma model with quarks. *Phys. Rev.*, D91(1):016002, 2015. doi: 10.1103/PhysRevD.91.016002.
- [82] Niklas Mueller and Jan M. Pawłowski. Magnetic catalysis and inverse magnetic catalysis in QCD. *Phys. Rev.*, D91(11):116010, 2015. doi: 10.1103/PhysRevD.91.116010.
- [83] Umut Gürsoy, Ioannis Iatrakis, Matti Järvinen, and Govert Nijs. Inverse Magnetic Catalysis from improved Holographic QCD in the Veneziano limit. *JHEP*, 03:053, 2017. doi: 10.1007/JHEP03(2017)053.
- [84] Diego M. Rodrigues, Eduardo Folco Capossoli, and Henrique Boschi-Filho. (Inverse) Magnetic Catalysis in (2+1)-Dimensional Gauge Theories from Holographic Models. 2017.
- [85] S. P. Klevansky. The Nambu-Jona-Lasinio model of quantum chromodynamics. *Rev. Mod. Phys.*, 64:649–708, 1992. doi: 10.1103/RevModPhys.64.649.



- [86] Tetsuo Hatsuda and Teiji Kunihiro. QCD phenomenology based on a chiral effective Lagrangian. *Phys. Rept.*, 247:221–367, 1994. doi: 10.1016/0370-1573(94)90022-1.
- [87] Kenji Fukushima. Chiral effective model with the Polyakov loop. *Phys. Lett.*, B591: 277–284, 2004. doi: 10.1016/j.physletb.2004.04.027.
- [88] Hiromichi Nishimura and Michael C. Ogilvie. A PNJL Model for Adjoint Fermions with Periodic Boundary Conditions. *Phys. Rev.*, D81:014018, 2010. doi: 10.1103/PhysRevD.81.014018.
- [89] Raoul Gatto and Marco Ruggieri. Deconfinement and Chiral Symmetry Restoration in a Strong Magnetic Background. *Phys. Rev.*, D83:034016, 2011. doi: 10.1103/PhysRevD.83.034016.
- [90] Kenji Fukushima, Marco Ruggieri, and Raoul Gatto. Chiral magnetic effect in the PNJL model. *Phys. Rev.*, D81:114031, 2010. doi: 10.1103/PhysRevD.81.114031.
- [91] Raoul Gatto and Marco Ruggieri. Quark Matter in a Strong Magnetic Background. *Lect. Notes Phys.*, 871:87–119, 2013. doi: 10.1007/978-3-642-37305-3\_4.
- [92] Ya. B. Zeldovich and Alexei A. Starobinsky. Particle production and vacuum polarization in an anisotropic gravitational field. *Sov. Phys. JETP*, 34:1159–1166, 1972. [*Zh. Eksp. Teor. Fiz.*61,2161(1971)].
- [93] S. W. Hawking. Black hole explosions. *Nature*, 248:30–31, 1974. doi: 10.1038/248030a0.
- [94] A. Ringwald. Fundamental physics at an x-ray free electron laser. In *Electromagnetic probes of fundamental physics. Proceedings, Workshop, Erice, Italy, October 16-21, 2001*, pages 63–74, 2001.
- [95] Dmitri Kharzeev and Kirill Tuchin. From color glass condensate to quark gluon plasma through the event horizon. *Nucl. Phys.*, A753:316–334, 2005. doi: 10.1016/j.nuclphysa.2005.03.001.
- [96] J. S. Langer. Theory of the condensation point. *Annals Phys.*, 41:108–157, 1967. doi: 10.1016/0003-4916(67)90200-X. [*Annals Phys.*281,941(2000)].
- [97] Sidney R. Coleman. The Fate of the False Vacuum. 1. Semiclassical Theory. *Phys. Rev.*, D15: 2929–2936, 1977. doi: 10.1103/PhysRevD.15.2929,10.1103/PhysRevD.16.1248. [Erratum: *Phys. Rev.*D16,1248(1977)].
- [98] Curtis G. Callan, Jr. and Sidney R. Coleman. The Fate of the False Vacuum. 2. First Quantum Corrections. *Phys. Rev.*, D16:1762–1768, 1977. doi: 10.1103/PhysRevD.16.1762.
- [99] Ian Affleck. Quantum Statistical Metastability. *Phys. Rev. Lett.*, 46:388, 1981. doi: 10.1103/PhysRevLett.46.388.

- [100] E. Brezin and C. Itzykson. Pair production in vacuum by an alternating field. *Phys. Rev.*, D2:1191–1199, 1970. doi: 10.1103/PhysRevD.2.1191.
- [101] V. S. Popov and M. S. Marinov. E+ e- pair production in variable electric field. *Yad. Fiz.*, 16:809–822, 1972.
- [102] M. S. Marinov and V. S. Popov. Electron-Positron Pair Creation from Vacuum Induced by Variable Electric Field. *Fortsch. Phys.*, 25:373–400, 1977. doi: 10.1002/prop.19770250111.
- [103] Holger Gies and Klaus Klingmuller. Pair production in inhomogeneous fields. *Phys. Rev.*, D72:065001, 2005. doi: 10.1103/PhysRevD.72.065001.
- [104] Gerald V. Dunne. The Heisenberg-Euler Effective Action: 75 years on. *Int. J. Mod. Phys.*, A27:1260004, 2012. doi: 10.1142/S2010194512007222,10.1142/S0217751X12600044. [Int. J. Mod. Phys. Conf. Ser.14,42(2012)].
- [105] Walter Dittrich. EFFECTIVE LAGRANGIANS AT FINITE TEMPERATURE. *Phys. Rev.*, D19: 2385, 1979. doi: 10.1103/PhysRevD.19.2385.
- [106] Per Elmfors, David Persson, and Bo-Sture Skagerstam. QED effective action at finite temperature and density. *Phys. Rev. Lett.*, 71:480–483, 1993. doi: 10.1103/PhysRevLett.71.480.
- [107] M. Loewe and J. C. Rojas. Thermal effects and the effective action of quantum electrodynamics. *Phys. Rev.*, D46:2689–2694, 1992. doi: 10.1103/PhysRevD.46.2689.
- [108] Joakim Hallin and Per Liljenberg. Fermionic and bosonic pair creation in an external electric field at finite temperature using the functional Schrodinger representation. *Phys. Rev.*, D52:1150–1164, 1995. doi: 10.1103/PhysRevD.52.1150.
- [109] A. K. Ganguly, J. C. Parikh, and P. K. Kaw. Thermal tunneling of q anti-q pairs in A-A collisions. *Phys. Rev.*, C51:2091–2094, 1995. doi: 10.1103/PhysRevC.51.2091.
- [110] Avijit Kumar Ganguly. Comment on fermionic and bosonic pair creation in an external electric field at finite temperature. 1998.
- [111] Holger Gies. QED effective action at finite temperature: Two loop dominance. *Phys. Rev.*, D61:085021, 2000. doi: 10.1103/PhysRevD.61.085021.
- [112] Gerald Dunne, Holger Gies, Klaus Klingmuller, and Kurt Langfeld. Worldline Monte Carlo for fermion models at large N(f). *JHEP*, 08:010, 2009. doi: 10.1088/1126-6708/2009/08/010.
- [113] S. A. Bass et al. Microscopic models for ultrarelativistic heavy ion collisions. *Prog. Part. Nucl. Phys.*, 41:255–369, 1998. doi: 10.1016/S0146-6410(98)00058-1. [Prog. Part. Nucl. Phys.41,225(1998)].



- [114] D. G. C. McKeon and A. Rebhan. Thermal Green's functions from quantum mechanical path integrals. *Phys. Rev.*, D47:5487–5493, 1993. doi: 10.1103/PhysRevD.47.5487.
- [115] Igor A. Shovkovy. One loop finite temperature effective potential in QED in the worldline approach. *Phys. Lett.*, B441:313–318, 1998. doi: 10.1016/S0370-2693(98)01202-7.
- [116] James Joseph Sylvester. On the relation between the minor determinants of linearly equivalent quadratic functions. *Philosophical Magazine*, 1:295–305, 1851.
- [117] I. M. Gelfand and A. M. Yaglom. Integration in functional spaces and it applications in quantum physics. *J. Math. Phys.*, 1:48, 1960. doi: 10.1063/1.1703636.
- [118] S. Levit and U. Smilansky. A New Approach to Gaussian Path Integrals and the Evaluation of the Semiclassical Propagator. *Annals Phys.*, 103:198, 1977. doi: 10.1016/0003-4916(77)90269-X.
- [119] Andrei D. Linde. Decay of the False Vacuum at Finite Temperature. *Nucl. Phys.*, B216:421, 1983. doi: 10.1016/0550-3213(83)90293-6,10.1016/0550-3213(83)90072-X. [Erratum: Nucl. Phys.B223,544(1983)].
- [120] Jaume Garriga. Instantons for vacuum decay at finite temperature in the thin wall limit. *Phys. Rev.*, D49:5497–5506, 1994. doi: 10.1103/PhysRevD.49.5497.
- [121] M. Morse. *The Calculus of Variations in the Large*. Number v. 18 in American Mathematical Society. American mathematical society, 1934. ISBN 9780821810187.
- [122] Eric Braaten and Robert D. Pisarski. Calculation of the quark damping rate in hot QCD. *Phys. Rev.*, D46:1829–1834, 1992. doi: 10.1103/PhysRevD.46.1829.
- [123] Markus H. Thoma and Christoph T. Traxler. Damping rate of a scalar particle in hot scalar QED. *Phys. Lett.*, B378:233–237, 1996. doi: 10.1016/0370-2693(96)00380-2.
- [124] Abdessamad Abada and K. Bouakaz. Infrared behavior of the dispersion relations in high-temperature scalar QED. *JHEP*, 01:161, 2006. doi: 10.1088/1126-6708/2006/01/161.
- [125] Pierre Ramond. FIELD THEORY. A MODERN PRIMER. *Front. Phys.*, 51:1–397, 1981. [Front. Phys.74,1(1989)].
- [126] A. Erdélyi. *Higher Transcendental Functions*. Number v. 2 in Higher Transcendental Functions. R. E. Krieger Publishing Company, 1981. ISBN 9780898740691.
- [127] William H. Miller. Classical s matrix: Numerical application to inelastic collisions. *The Journal of Chemical Physics*, 53(9):3578–3587, 1970. doi: 10.1063/1.1674535.
- [128] George F. Carrier. Gravity waves on water of variable depth. *Journal of Fluid Mechanics*, 24(4):641–659, 1966. doi: 10.1017/S0022112066000892.

- [129] A. Erdélyi. *Higher Transcendental Functions*. Number v. 1 in Higher Transcendental Functions. R. E. Krieger Publishing Company, 1981. ISBN 9780898740691.
- [130] N. D. Birrell and P. C. W. Davies. *Quantum Fields in Curved Space*. Cambridge Monographs on Mathematical Physics. Cambridge Univ. Press, Cambridge, UK, 1984. ISBN 0521278589, 9780521278584, 9780521278584. doi: 10.1017/CBO9780511622632.
- [131] W Zwerger. Dynamical interpretation of a classical complex free energy. *Journal of Physics A: Mathematical and General*, 18(11):2079, 1985.
- [132] C. M. Newman and L. S. Schulman. Complex free energies and metastable lifetimes. *Journal of Statistical Physics*, 23(2):131–148, Aug 1980. ISSN 1572-9613. doi: 10.1007/BF01012588.
- [133] S. P. Gavrilov, D. M. Gitman, and J. L. Tomazelli. Density matrix of a quantum field in a particle-creating background. *Nucl. Phys.*, B795:645–677, 2008. doi: 10.1016/j.nuclphysb.2007.11.029.
- [134] Sang Pyo Kim, Hyun Kyu Lee, and Yongsung Yoon. Schwinger Pair Production at Finite Temperature in QED. *Phys. Rev.*, D79:045024, 2009. doi: 10.1103/PhysRevD.79.045024.
- [135] Adam R. Brown. Schwinger pair production at nonzero temperatures or in compact directions. 2015.
- [136] Oliver Gould and Arttu Rajantie. Thermal Schwinger pair production at arbitrary coupling. *Phys. Rev.*, D96(7):076002, 2017. doi: 10.1103/PhysRevD.96.076002.
- [137] Leandro Medina and Michael C. Ogilvie. Simulation of Scalar Field Theories with Complex Actions. 2017.
- [138] Philippe de Forcrand. Simulating QCD at finite density. *PoS*, LAT2009:010, 2009.
- [139] Gert Aarts. Introductory lectures on lattice QCD at nonzero baryon number. *J. Phys. Conf. Ser.*, 706(2):022004, 2016. doi: 10.1088/1742-6596/706/2/022004.
- [140] M. E. Fisher. Yang-Lee Edge Singularity and  $\phi^3$  Field Theory. *Phys. Rev. Lett.*, 40:1610–1613, 1978. doi: 10.1103/PhysRevLett.40.1610.
- [141] Simon Hands, John B. Kogut, Maria-Paola Lombardo, and Susan E. Morrison. Symmetries and spectrum of SU(2) lattice gauge theory at finite chemical potential. *Nucl. Phys.*, B558:327–346, 1999. doi: 10.1016/S0550-3213(99)00364-8.
- [142] Christof Gattringer and Kurt Langfeld. Approaches to the sign problem in lattice field theory. *Int. J. Mod. Phys.*, A31(22):1643007, 2016. doi: 10.1142/S0217751X16430077.
- [143] Marco Cristoforetti, Francesco Di Renzo, and Luigi Scorzato. New approach to the sign problem in quantum field theories: High density QCD on a Lefschetz thimble. *Phys. Rev.*, D86:074506, 2012. doi: 10.1103/PhysRevD.86.074506.

- [144] Erhard Seiler. Status of Complex Langevin. In *35th International Symposium on Lattice Field Theory (Lattice 2017) Granada, Spain, June 18-24, 2017*, 2017.
- [145] Matthias Troyer and Uwe-Jens Wiese. Computational complexity and fundamental limitations to fermionic quantum Monte Carlo simulations. *Phys. Rev. Lett.*, 94:170201, 2005. doi: 10.1103/PhysRevLett.94.170201.
- [146] Scott Aaronson. *Quantum Computing Since Democritus*. Cambridge University Press, New York, NY, USA, 2013. ISBN 0521199565, 9780521199568.
- [147] F Barahona. On the computational complexity of ising spin glass models. *Journal of Physics A: Mathematical and General*, 15(10):3241, 1982.
- [148] A. Das and B.K. Chakrabarti. *Quantum Annealing and Related Optimization Methods*. Lecture Notes in Physics. Springer Berlin Heidelberg, 2005. ISBN 9783540279877.
- [149] H. G. Evertz. The Loop algorithm. *Adv. Phys.*, 52:1, 2003. doi: 10.1080/0001873021000049195.
- [150] Casimir Kuratowski. Sur le problème des courbes gauches en topologie. *Fundamenta Mathematicae*, 15(1):271–283, 1930.
- [151] Charles H. Bennett, Ethan Bernstein, Gilles Brassard, and Umesh Vazirani. Strengths and weaknesses of quantum computing. *Submitted to: SIAM J. Sci. Statist. Comput.*, 1996.
- [152] Troels F. Rønnow, Zhihui Wang, Joshua Job, Sergio Boixo, Sergei V. Isakov, David Wecker, John M. Martinis, Daniel A. Lidar, and Matthias Troyer. Defining and detecting quantum speedup. *Science*, 345(6195):420–424, 2014. ISSN 0036-8075. doi: 10.1126/science.1252319.
- [153] J.F. Nash. Non-cooperative games. *Annals of Mathematics*, 54(2):286–295, 1951.
- [154] Xi Chen, Xiaotie Deng, and Shang-Hua Teng. Settling the complexity of computing two-player nash equilibria. *CoRR*, abs/0704.1678, 2007.
- [155] Vincent Conitzer and Tuomas Sandholm. Complexity results about nash equilibria. *CoRR*, cs.GT/0205074, 2002.
- [156] Carl M. Bender and Stefan Boettcher. Real spectra in nonHermitian Hamiltonians having PT symmetry. *Phys. Rev. Lett.*, 80:5243–5246, 1998. doi: 10.1103/PhysRevLett.80.5243.
- [157] Claude W. Bernard and Van M. Savage. Numerical simulations of PT symmetric quantum field theories. *Phys. Rev.*, D64:085010, 2001. doi: 10.1103/PhysRevD.64.085010.
- [158] Carl M. Bender. Making sense of non-Hermitian Hamiltonians. *Rept. Prog. Phys.*, 70:947, 2007. doi: 10.1088/0034-4885/70/6/R03.

- [159] Hiromichi Nishimura, Michael C. Ogilvie, and Kamal Pangeni. Complex saddle points in QCD at finite temperature and density. *Phys. Rev.*, D90(4):045039, 2014. doi: 10.1103/PhysRevD.90.045039.
- [160] Ali Mostafazadeh. Exact PT symmetry is equivalent to Hermiticity. *J. Phys.*, A36:7081–7092, 2003. doi: 10.1088/0305-4470/36/25/312.
- [161] M. Luscher and P. Weisz. Definition and General Properties of the Transfer Matrix in Continuum Limit Improved Lattice Gauge Theories. *Nucl. Phys.*, B240:349–361, 1984. doi: 10.1016/0550-3213(84)90270-0.
- [162] Peter N. Meisinger and Michael C. Ogilvie. PT Symmetry in Classical and Quantum Statistical Mechanics. *Phil. Trans. Roy. Soc. Lond.*, A371:20120058, 2013. doi: 10.1098/rsta.2012.0058.
- [163] Christof Gattringer and Thomas Kloiber. Lattice study of the Silver Blaze phenomenon for a charged scalar  $\phi^4$  field. *Nucl. Phys.*, B869:56–73, 2013. doi: 10.1016/j.nuclphysb.2012.12.005.
- [164] Carl M. Bender and Hugh F. Jones. Interactions of Hermitian and non-Hermitian Hamiltonians. *J. Phys.*, A41:244006, 2008. doi: 10.1088/1751-8113/41/24/244006.
- [165] Thomas A. DeGrand and Carleton E. DeTar. Phase Structure of QCD at High Temperature With Massive Quarks and Finite Quark Density: A  $Z(3)$  Paradigm. *Nucl. Phys.*, B225:590, 1983. doi: 10.1016/0550-3213(83)90536-9.
- [166] Simon Hands, Timothy J. Hollowood, and Joyce C. Myers. QCD with Chemical Potential in a Small Hyperspherical Box. *JHEP*, 07:086, 2010. doi: 10.1007/JHEP07(2010)086.
- [167] Oscar Akerlund, Philippe de Forcrand, and Tobias Rindlisbacher. Oscillating propagators in heavy-dense QCD. *JHEP*, 10:055, 2016. doi: 10.1007/JHEP10(2016)055.
- [168] Carl M. Bender, Alexander Felski, Nima Hassanpour, S. P. Klevansky, and Alireza Beygi. Analytic structure of eigenvalues of coupled quantum systems. *Phys. Scripta*, 92(1):015201, 2017. doi: 10.1088/0031-8949/92/1/015201.
- [169] David J. Gross and Andre Neveu. Dynamical Symmetry Breaking in Asymptotically Free Field Theories. *Phys. Rev.*, D10:3235, 1974. doi: 10.1103/PhysRevD.10.3235.
- [170] Michael Seul and David Andelman. Domain shapes and patterns: The phenomenology of modulated phases. *Science*, 267(5197):476–483, 1995. ISSN 0036-8075. doi: 10.1126/science.267.5197.476.
- [171] Zohar Nussinov, Joseph Rudnick, Steven A. Kivelson, and L. N. Chayes. Avoided critical behavior in  $O(n)$  systems. *Phys. Rev. Lett.*, 83:472–475, Jul 1999. doi: 10.1103/PhysRevLett.83.472.

- [172] C. B. Muratov. Theory of domain patterns in systems with long-range interactions of coulomb type. *Phys. Rev. E*, 66:066108, Dec 2002. doi: 10.1103/PhysRevE.66.066108.
- [173] C. Ortix, J. Lorenzana, and C. di Castro. Coulomb-Frustrated Phase Separation Phase Diagram in Systems with Short-Range Negative Compressibility. *Physical Review Letters*, 100(24):246402, June 2008. doi: 10.1103/PhysRevLett.100.246402.

# APPENDIX

## A.1 REPRESENTATIONS OF THE HURWITZ ZETA FUNCTION

The Hurwitz zeta function can be written with aid of the Gamma function as [129]

$$\zeta_{\text{H}}(s; z) = \sum_{n=0}^{\infty} \frac{1}{(n+z)^s} = \sum_{n=0}^{\infty} \frac{1}{\Gamma(s)} \int_0^{\infty} dt t^{s-1} e^{-(n+z)t} \quad (\text{A.1})$$

which reduces the sum to a geometric series,

$$\zeta_{\text{H}}(s; z) = \frac{1}{\Gamma(s)} \int_0^{\infty} dt t^{s-1} e^{-zt} \frac{1}{1-e^{-t}} \quad (\text{A.2})$$

$$= \frac{1}{2\Gamma(s)} \int_0^{\infty} dt t^{s-1} e^{-zt} \left( 1 + \coth\left(\frac{t}{2}\right) \right) \quad (\text{A.3})$$

$$= \frac{z^{-s}}{2} + \frac{2^{s-1}}{\Gamma(s)} \int_0^{\infty} dt t^{s-1} e^{-2zt} \coth t. \quad (\text{A.4})$$

We seek the analytic continuation of the Hurwitz zeta function in the vicinity of  $s = -1$ , which is relevant for the effective Lagrangian of Heisenberg and Euler discussed in Chapter 2. We must thus subtract off the leading behavior of the hyperbolic cotangent, and add it back in, obtaining

$$\zeta_{\text{H}}(s; z) = \frac{z^{-s}}{2} + \frac{z^{-(s-1)}}{s-1} + s \frac{z^{-(s+1)}}{12} + \frac{2^{s-1}}{\Gamma(s)} \int_0^{\infty} dt t^{s-1} e^{-2zt} \left( \coth t - \frac{1}{t} - \frac{t}{3} \right). \quad (\text{A.5})$$

Differentiating with respect to  $s$  and setting  $s = -1$  we obtain

$$\zeta'_{\text{H}}(-1; z) = \frac{1}{12} - \frac{z^2}{4} - \left( \frac{z}{2} - \frac{z^2}{2} - \frac{1}{12} \right) \log z - \frac{1}{4} \int_0^{\infty} \frac{dt}{t^2} e^{-2zt} \left( \coth t - \frac{1}{t} - \frac{t}{3} \right). \quad (\text{A.6})$$

which, with the identification

$$\zeta_{\text{H}}(-1; z) = \frac{z}{2} - \frac{z^2}{2} - \frac{1}{12}, \quad (\text{A.7})$$

is equation (2.58).

## A.2 PROOF OF MEHLER'S FORMULA

Below we sketch the demonstration of identity (7.13). The reader interested in Mehler's kernel may refer to Erdélyi [126].

If the harmonic oscillator ground-state wavefunction is represented as

$$e^{-x^2} = \frac{1}{\sqrt{\pi}} \int_{-\infty}^{\infty} da e^{-a^2+2iax}, \quad (\text{A.8})$$

application of Rodrigues' formula leads to the following integral representation of the Hermite polynomials:

$$H_n(x) = e^{x^2} \left( \frac{d}{dx} \right)^n \frac{1}{\sqrt{\pi}} \int_{-\infty}^{\infty} da e^{-a^2+2iax} = \frac{1}{\sqrt{\pi}} \int_{-\infty}^{\infty} da (-2ia)^n e^{(a-ix)^2}. \quad (\text{A.9})$$

This is inserted into the left hand side of Mehler's formula, giving

$$\sum_{n=0}^{\infty} \frac{(\rho/2)^n}{n!} H_n(x) H_n(y) e^{-(x^2+y^2)/2} \quad (\text{A.10})$$

$$= \frac{1}{\pi} \sum_{n=0}^{\infty} \frac{(\rho/2)^n}{n!} \iint da db (-2ia)^n (-2ib)^n e^{-(a-ix)^2 - (b-iy)^2} \quad (\text{A.11})$$

$$= \frac{1}{\pi} \iint da db e^{-(a-ix)^2 - (b-iy)^2 - 2\rho ab} \quad (\text{A.11})$$

$$= \frac{1}{\sqrt{\pi}} \int da e^{-(1-\rho^2)a^2 + x^2 + 2ia(x-\rho y)} \quad (\text{A.12})$$

$$= \frac{1}{\sqrt{1-\rho^2}} \exp \left[ x^2 - \frac{(x-\rho y)^2}{1-\rho^2} \right] \quad (\text{A.13})$$

$$= \frac{1}{\sqrt{1-\rho^2}} \exp \left[ \frac{4\rho xy - (1+\rho^2)(x^2+y^2)}{2(1-\rho^2)} \right], \quad (\text{A.14})$$

the desired result.